To the Graduate Council:

I am submitting herewith a thesis written by Rajesh Ramamurthy entitled " Crystallization Studies of Propylene Copolymer Fractions." I have examined the final copy of this thesis for form and content and recommend that it be accepted in partial fulfillment of the requirements for the degree of Master of Science, with a major in Polymer Engineering.

Paul J. Phillips, Major Professor

We have read this thesis and
recommended its acceptance:

Roberto S. Benson

Joe E. Sprunell

Accepted for the Council:

Associate Vice Chancellor and
Dean of the Graduate School

Crystallization Studies of Propylene Copolymer Fractions

A Thesis

Presented for the

Master of Science

Degree

The University of Tennessee, Knoxville

Rajesh Ramamurthy

May 1996

Abstract

The aim of this work was to study the effect of comonomer content and tacticity on the crystallization behavior of propylene copolymer fractions. Initially two random copolymers of propylene and ethylene with similar molecular weight, but different ethylene (comonomer) content, were fractionated successively in a soxhlet apparatus with solvents of increasing solvent power. These fractions varied in comonomer content and tacticity. The thermal properties from DSC, the morphologial studies from light microscopy, polymorphism from WAXD and the linear growth rates from hot stage microscope were determined. The comonomer content had a significant effect on the thermal, structural and morphological properties of the copolymer. The total impurity content of the copolymers was determined by calculating the defects caused by the effects of tacticity and comonomer. The equilibrium thermodynamic properties of these fractions were determined using different extrapolation techniques. The total defect content obeyed the Flory's total exclusion model. The effect of comonomer content on the regimes of crystallization for these fractions was also evaluated.

Acknowledgments

I wish like to thank my major professor, Dr. Paul J. Phillips for his support, patience and guidance through out the course of this project. Sincere thanks are also due to Dr. Roberto S. Benson and Dr. Joe E. Spruiell for their continued interest and efforts.

I am grateful to the inspiration and support given by Khaled Mezghani, Daryl Grummitt, Stein Schreiber, fellow students and the staff of Material Science and Engineering. Special thanks to Dr. Edward S. Clark for all the updates he provided in the field of polymers.

I am indebted to my parents, sister and brother for their continued support all through my education. Last but not the least I would like to thank all my friends (KNN) who never failed in helping me during the course of this work.

Table of Contents

Chapter

1. Introduction 1

2. Review of Theoretical Background and Literature. . 3

2.1 Polymer Crystallization. 3

Conditions for the formation of chain folding. . 5

2.2 Crystallization Theories. 9

Growth Theories. 12

Nucleation Theories 14

Modifications of LH theory. . . . 21

2.3 Thermal Behavior of Polypropylenes. . . . 22

2.4 Structure and Properties of Polypropylenes. . . 27

Chain conformation of Isotactic Polypropylene. 31

Crystal Structure of Polypropylene. . . 32

2.5 Theories of Fractionation 34

Fractionation of Copolymers. . . . 36

Fractionation by Solubility. . . . 36

3 Experimental. 41

3.1 Materials. 41

3.2 Fractionation. 41

3.3 Sample Preparation. 44

3.4 Differential Scanning Calorimetry. . . . 45

3.5 Polarized Light Microscopy. 45

3.6 Wide Angle X-ray Diffraction. 46

3.7 Fourier Transform Infrared Spectroscopy. . . 47

3.8 Nuclear Magnetic Resonance. 47

4 Results. 49

4.1 Fractionation. 49

4.2 Calculation of % ethylene content from IR. . . 54

4.3 Determination of Isotacticity from NMR and FTIR. . 57

4.4 Thermal Properties. 70

Melting From DSC. 70

Crystallization From DSC. . . . 70

Glass Transition. 74

4.5 X-Ray Diffraction studies. 74

4.6 Copolymer Morphology. 85

4.7 Crystallinity. 106

4.8 Latent Heat of Fusion. 106

5 Discussion. 109

5.1 Fractionation. 109

5.2 Equilibrium Melting Temperature. . . . 114

5.3 Gamma Phase in Fractions. 117

5.4 Crystallization. 120

Linear Growth Rates. 120

Secondary Nucleation Analysis. . . . 122

6. Conclusions. 136

Recommendations. 138

Reference. 140

Vita. 146

List of Figures

Figures Page

2.1 List of some Polymers that exhibit chain folding. . . 6

2.2 Lamellar structure in melt crystallized polyethylene. . 8

2.3 The "crystalline model": 11

2.4 Schematic of the factors that affect crystal growth. . 13

2.5 A simple nucleation model for long chains. . . . 17

2.6 Growth on the surface of the lamellae, viewed looking onto the fold plane, showing two different types of growth. 17

2.7 Regime I, II and III 19

2.8 Inclusion and Exclusion models. 24

2.9 Conformation and configuration of polypropylene. . . 29

2.10 Conformation of isotactic chain of PP in the crystal state. . 31

2.11 Possible orientations of chain axes in the crystal packing of iPP. 35

2.12 Classification of fractionation. 37

3.1 Soxhlet extraction setupfor solution fractionation. . . 43

4.1 Fractionation of 3% ethylene containing copolymer. . . 51

4.2 Fractionation of 5% ethylene containing copolymer. . . 52

4.3 FTIR analysis of 5% copolymer fraction. . . . 55

4.4 FTIR analysis of 3% copolymer fraction. . . . 56

4.5 Calibration for the determination of comonomer content in propylene copolymers. 58

4.6 Weight % ethylene present in each fraction . . . 59

4.7 NMR spectrum of low tacticity iPP sample with 91% HI isotacticity. 60

4.8 NMR spectrum of high tacticity iPP sample with 99% HI isotacticity. 61

4.9 NMR spectrum (methyl region) of low tacticity iPP sample with 91% heptane insoluble isotacticity. 62

4.10 NMR spectra (methyl region) of high tacticity iPP sample with 99% heptane insoluble isotacticity. 63

4.11 Calibration for the determination of % isotacticity. . . 66

4.12 Isotacticities for the fractions as a function of wt % ethylene content 68

4.13 Isotacticities for the fractions as a function of mole % ethylene content 69

4.14 DSC melting scans for the 3% copolymer fractions when melted dynamically at 10°/min 70

4.15 DSC melting scans for the 5% copolymer fractions when melted dynamically at 10°/min. 71

4.16 Depression in melting of fractions with increase in defect 75

4.17 The effect of defect on the crystallizability of the fractions. . 76

4.18 DSC crystallization curves for the 3% copolymer fractions dynamically when cooled at 10°/min. 77

4.19 DSC crystallization scans for the 5% copolymer fractions when cooled dynamically at 10°/min. 78

4.20 DSC exotherms for glass transition determination of the unfractionated 5% sample at a heating rate of 10°/min. . . 79

4.21 DSC exotherms for glass transition determination of the 2.2% fraction sample at a heating rate of 10°/min. 80

4.22 DSC exotherms for glass transition determination of the 3.7% fraction sample at a heating rate of 10°/min. 81

4.23 DSC exotherms for glass transition determination the 10% fraction sample at a heating rate of 10°/min. 82

4.24 Comonomer content as a function of glass transition for fractions 84

4.25 WAXD studies of fractions crystallized at 90°C isothermally. 87

4.26 WAXD studies of fractions crystallized at 100°C isothermally. 88

4.27 WAXD studies of fractions crystallized at 110°C isothermally. 89

4.28 Gamma content as a function of temperature for the fractions. 90

4.29 WAXD studies of unfractionated 5% propylene copolymer crystallized at various temperatures. 91

4.30 WAXD studies of unfractionated 3% propylene copolymer crystallized at various temperatures. 92

4.31 WAXD studies of fractionated 2.2% (ethylene) propylene copolymer crystallized at various temperatures. 93

4.32 WAXD studies of fractionated 3.7% (ethylene) propylene copolymer crystallized at various temperatures. 94

4.33 WAXD studies of fractionated 5% (ethylene) propylene copolymer crystallized at various temperatures. 95

4.34 WAXD studies of fractionated 10% (ethylene) propylene copolymer crystallized at various temperatures. 96

4.35 Crystalline morphology of 1% fraction at ; supercooling =60 (top) and (bottom) supercooling=52. (20 mag). 98

4.36 Crystalline morphology of 1% fraction at a supercooling =50 (20 mag). 99

4.37 Crystalline morphology of 2.2% fraction at ; (top) supercooling =54 and (bottom) supercooling=50. (20 mag). . . . 100

4.38 Crystalline morphology of 2.2% fraction at a (supercooling =50) showing sheaf like morphology 101

4.39 Crystalline morphology of 3.7% fraction at high supercooling, axialitic morphology. 102

4.40 Crystalline morphology of 2.2% fraction at low supercooling, axialitic morphology. 103

4.41 Crystalline morphology of 10% fraction at ; (top) supercooling =60 and showing prolific branching supercooling=50 (bottom). (20 mag) 104

4.42 Crystalline morphology of 2.2% fraction at ; supercooling = 37 (20 mag). 105

4.43 Latent heat of fusion of copolymer fractions calculated based on the crystallinity determinations from WAXD 107

5.1 Effect of fractionation on comonomer content and stereoregularity. 112

5.2 Effect of impurities on the melting of copolymer fractions. . 113

5.3 Equilibrium melting of unfractionated copolymers obtained from DSC. 115

5.4 Equilibrium melting of fractionated copolymers from Hoffman-Weeks plots 116

5.5 Comparison of Florys predicted T_m^o to experimental T_m^o. . 118

5.6 Effect of tacticity on the T_m^o of homopolymer compared with the total defect content in the copolymer fraction.. . . . 119

5.7 Growth rates as a function of crystallization temperature.for fractions of varying ethylene contents. 121

5.8 Growth rates vs. crystallization temperatureof copolymers. 123

5.9 Regime transitions in fractions of prpylene copolymers. . 124

5.10 Effect of T_g and T_{mo} on the regimes of u3% copolymer fraction. 126

5.11 Effect of T_g and T_{mo} on the regimes of u5% copolymer fraction 127

5.12 Effect of T_g and T_{mo} on the regimes of 1% copolymer fraction. 128

5.13 Effect of T_g and T_{mo} on the regimes of 2.2% copolymer fraction 129

5.14 Effect of T_g and T_{mo} on the regimes of 3.7% copolymer fraction 130

5.15 Effect of T_g and T_{mo} on the regimes of 5% copolymer fraction 131

5.16 Effect of T_g and T_{mo} on the regimes of 10% copolymer fraction 132

List of Tables

Table		Page
4.1	Fractionation of 3% propylene copolymer. . . .	52
4.2	Fractionation of 5% propylene copolymer. . . .	53
4.3	Spectral assignment for iPP.	64
4.4	Tacticity and % ethylene content calculated from FTIR and NMR.	67
4.5	Melting and Crystallization data for copolymer fractions. .	73
4.6	Glass transition temperatures of the fractions . . .	83
4.7	Gamma content (index) for the fractions at various supercoolings	86
5.1	Crystal growth kinetic data.	134

1 INTRODUCTION

Polypropylene has grown into a very important commercial thermoplastic, due to growth of new emerging catalyst technologies and its specific properties. Recently there have been unprecedented developments in homogeneous catalyst technologies, which has led to successful engineering of specific molecular characteristics in polyolefins.

Polypropylene, due to its crystallinity, is preferred in many applications where high strength/stiffness ratio is required. Filled polypropylenes have proved successful in engineering applications and are now a major competitor for resins like ABS. Polypropylene's high melting point gives products having attractive properties over a wide range of temperatures. The need for more amorphous olefins is always present for low temperature applications, where weldability/sealability at a lower temperature is possible. Copolymerization proved to be a very good answer for this, since the products could satisfy the required criteria. Both saturated ethylene propylene rubber/toughened polypropylene and unsaturated EPDM became very popular, while the former was more stable to oxidation. Another major reason for adding small amounts of comonomer in the polymerization of propylene was to increase the rate of polymerization. Small amounts of ethylene comonomer (5%) can increase the rate of polymerization of propylene by 35% in the presence of $TiCl_3/AlEt_3$ catalysts. (Sar van der ven 1990)

Synthesis of different structures of propylene copolymers random, alternating or block, depends on the combination of the Ziegler-Natta catalyst

components. The r_1r_2 (product of the monomer reactivity ratios) indicates the expected comonomer distribution along the chain. The addition of the comonomer in the random case is such that the monomers are present in the chain at a constant concentration. Copolymer chains are expected not only to differ in their molecular weight and tacticity, as in the case of the homopolymer, but also in the comonomer distribution. This comonomer distribution can be either *intermolecular*, where there is a difference in the comonomer content in each polymer chain, or they can be *intramolecular* based on differences in comonomer distribution over the chain (sequence distribution).

Characterization of the comonomer content, molecular and structural features of the polymer is vital in understanding crystallization, thermal and morphological properties. Mezghani and Phillips (1995) recently have studied the effect of comonomer on the structure and thermal properties of unfractionated propylene copolymers. As a continuation of this work, in order to study the copolymers with narrower comonomer contents, successive solvent extraction has been carried out for two propylene copolymers with different ethylene contents. Thus the focus of this research is to learn more about the crystallization, melting, growth rate and morphology for the set of propylene copolymer fractions which have been obtained. Though there is literature on comonomer sequencing, polymorphism, fractionation, melting and crystallization of propylene-ethylene copolymers, studies using narrow fractions cannot be found. The purpose of this research is an attempt to throw some light on this problem.

2 REVIEW OF THEORETICAL BACKGROUND AND LITERATURE

2.1 Polymer Crystallization

The long chain nature of macromolecules gives rise to a complicated growth mechanism. Thus crystallization of polymers is one of the most challenging fields in the area of polymers. It is based on the traditional science of long molecules and the growth of simple crystals. Over the years many fruitful theories have been proposed from all fields of science and the quest for a better prediction with experimental evidence of the crystallization of these complex molecules still continues.

Crystal structure was first determined from the discovery that simple crystalline materials diffract X-rays (Van Laue and Bragg 1911-1912). When extended to polymers such studies indicated the existence of ordered regions (*crystalline*) and randomly ordered regions (*amorphous*) regions. The longest dimension in a polycrystalline material was found to be 50 - 500Å which is a small fraction of the extended polymer molecule. This led to the development of the fringed micelle model, (Herman 1930) which represented the polymer chain as wandering successively through random regions and through bundles of ordered regions (*micelle*).

Since X-ray scattering and birefringence gave only secondary evidence, polarized microscopy was used to study morphological details up to a 10μ level. Evidence of spherulites came from these observations, which were

detected earlier by geophysicists in crystalline minerals. Spherulites cited were at least two orders of magnitude larger than the fringed micelle model (20 nm). The molecular chains prefer to be tangential to the spherulites rather than along the radial direction, which could not be satisfied by the fringed micelle model. Although the fringed micelle model failed in this case, it is used in explaining the oriented structure of drawn fibers, the structure of polyvinyl chloride and may be the structure of high octene content homogeneous polyethylene's.

The introduction of the modern electron microscope in 1957, coinciding with the discovery of linear stereo-regular polyolefins, led to the citation of the first sub microscopic polymer crystals of polyethylene (Keller 1957, Till 1957, Fischer 1957, Jacodine 1955).

The foundation stone for modern understanding of polymer crystallization was laid by the twin discoveries of polymer lamellae and the concept of chain folding. The fringed micelle model which existed earlier explained that one molecule participates in more than one crystallite, this accounted for the interpretation of the mechanical properties based on inter crystalline linkages. A questionable feature of the fringed micelle model was drastically high free energy and strain accumulations at the interface. (Hoffman and Lauritzen 1961). Kinetically nucleation controlled chain growth with chain folds was found to be more favorable since the excess free energy expected in the fringed micelle model was considerably larger than the fold surface free energies. Till then the lamellar nature and chain folding were not considered in the explanation of the structure of polymers.

Storks (1938) suggested chain folding in trans., 1-4 poly (isoprene), but this went unrecognized due to lack of advanced electron microscopes. On his studies on polyethylene's in dilute solutions, Keller (1957) showed the nature of polymer single crystals, led by Jaccodine (1955) and supported by the independent research of Till on polyethylene (1957), and Fischer (1957). Based on electron diffraction experiments, Bunn (1939) proved that the polymer chain axis was perpendicular to the flat faces of the crystal (the thickness was 110-140Å compared to 2000Å long molecular chain). This urged Keller to predict that the upper and lower faces of the crystal were comprised of chain folds. Soon it was suggested that many polymers exhibited chain folding (Fig 2.1).

Conditions for the formation of chain folding

- Polymers have to be structurally regular so that they can be easily crystallized. Atactic polystyrene cannot be crystallized since it lacks stereo regularity.
- The chain length should be long enough to recover the excess free energy caused due to folds. n-Paraffin's containing 16-90 carbon atoms cannot chain fold while polyethylene with 124 C-atoms if quench crystallized forms a fold.(Keller et al. 1971)
- Chain flexibility of the polymer is an important aspect, thus polymers like polyethylene terephthalate, in spite of their stiff phenyl rings are thought to fold because of the presence of flexible -O-CH_2-CH_2-O while poly (p-phenylenes) which have limited chain mobility due to adjacent phenyl rings cannot chain fold.

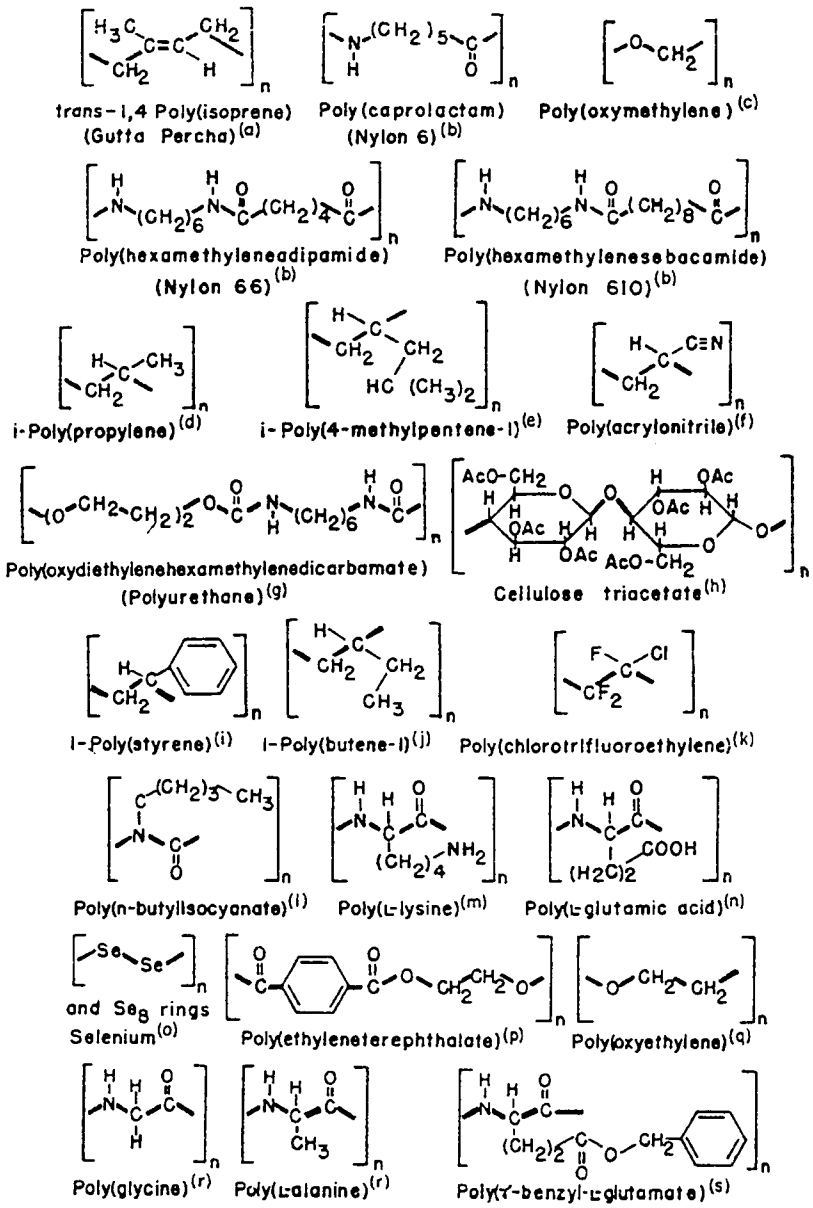


Fig. 2.1 List of some Polymers that exhibit chain folding

Since majority of the polymers are melt processed, study of crystal growth from polymer melts became the main area of interest. The quest was to see if similar lamellar nature prevailed in the melt state. The earliest observations of spherulites from the melt were reported by Bunn and Alcock (1945) based on their birefringence experiments. Detailed studies on morphology was done by Keith and Padden (1959), Price (1959) and Keller (1959). The first evidence of lamellar nature in the melt crystallized polymer was reported by Fischer (1957) in which he showed that the spherulite consisted of chain folded lamellae radiating from the central point (Fig 2.2). Crystallizable polymers crystallize as axialites or spherulites depending on their isothermal growth temperature. Polymer texture studies suggested the possibility that molecular chains are perpendicular to the flat faces of the lamellae.(Palmer and Cobbold, 1964; Keller and Sawada. 1964; Hock. 1965)

The concept of the tightly folded chain in melt grown polymers has been a controversial topic for decades. Flory (1962) completely disagreed with this concept and proposed the '*switchboard*' model. The experiments attempting to support irregularly folded chains have been reported with regard to molecular weight and crystallization conditions (Mandelkern 1976; Fatou and Mandelkern 1965; Mandelkern 1971; Mandelkern *et al.* 1972). The presence of tie molecules due to a chain re-entering into another crystal could well explain the elastic nature of polymers, and led to the proposal of the interzonal model by Mandelkern (1974)

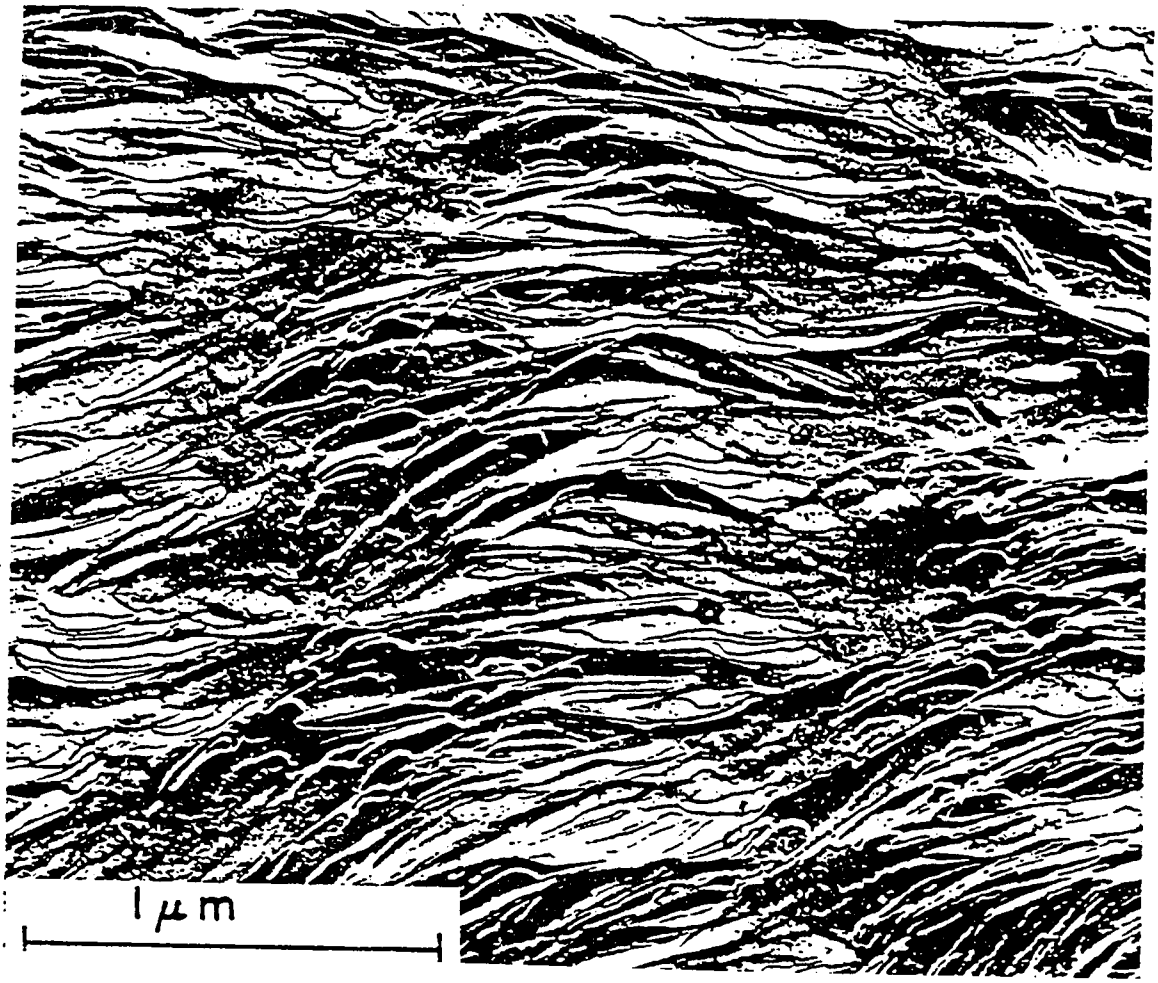


Fig. 2.2 Lamellar structure in melt crystallized polyethylene. Electron micrograph of replica from melt crystallized thin film showing lamellae ~150 Å thick, growth is from left to right. (Padden 1959)

Elastic neutron scattering experiments led to the conclusion that a polymer is its own theta solvent, as formerly suggested by Flory (1953). Neutron scattering has aided in understanding the difference in crystallization between the solution grown and melt grown crystals. Understanding of melt grown crystals is based on the assumption that scattering from deuterated polyethylene had a different coherent scattering than from its hydrogenated counterpart. This led to the conclusion that the exact molecular trajectory is difficult to predict since the interpretation of data from the neutron scattering totally dependeds on the modeling of the scattering data. The presence of total adjacent re-entry which could be a simple crystalline model would be impossible in semicrystalline polymers grown from the melt. Similarly due to a lack of explanation of the excess surface densities in the non adjacent re-entry model, its total presence was ruled out. These possibilities have been reviewed by Phillips (1990), where he states that the molecular trajectory of a polymer which results from highly supercooled system, is that of a psuedorandom coil which requires some adjacent re-entry, non adjacent re-entry and the reminder of the surface largely comprising of tie molecules and cilia.

2.2 Crystallization Theories

The structure of polymer crystals and its growth has been reviewed by Keller (1968), Wunderlich (1976), Bassett (1981), Dosiere (1989), Phillips (1990,1992) and recently by Goldbeck-Wood (1992).

The earliest description of crystallization was due to Newton (1730), while the first quantitative theory of crystallization was after Gibbs (1878) based on his thermodynamics. He was able to give a good explanation of the nucleation and growth step based on his theory of thermodynamics. these were based on the concepts of small molecule crystallization. It was understood that chain folding and imperfect crystallization led to metastable crystals, which may be understood on the basis of kinetics. Complicated kinetic theories based on chain folding were soon suggested (Price, Hoffman 1959) and this lead to various competing approaches. The most widely used one is based on nucleation model (Hoffman and Lauritzen), which has been widely examined and modified based on experimental correlation. Other approaches based on surface roughening by Sadler, molecular nucleation by Wunderlich and multipath model by Point are worth mentioning.

In order to understand the crystal growth in a very simple manner the *crystalline model* (Fig. 2.3) was proposed, which when compared to the real crystal which had no dislocations, entanglements or other defects. This model is based on the idea that adjacent reentry predominates and takes into account cilia and loops as correction factors. It is still very popular to use the idea of predominantly adjacent re-entry after strongly favored experiments (Mansfield. 1983; Sadler, 1982; Spells. and Sadler., 1984; Sadler 1984) but it is still very important not to forget the possibility of non-adjacent re-entry and the random model (Disc. Faraday Soc., 1979).

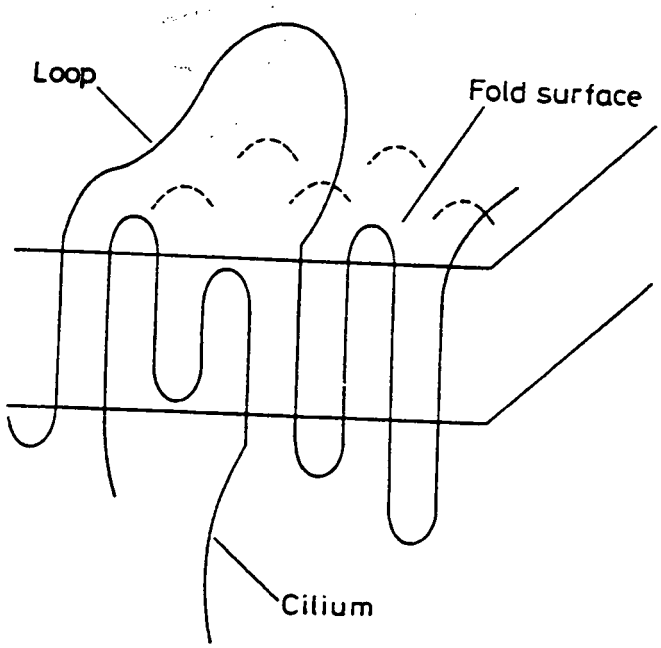


Fig 2.3 The "crystalline model": a single crystal in which molecules transverse the lamella perpendicular to the fold surface. Cilia are formed at the end of the molecules outside the crystalline core The folds are predominantly adjacent and the loop sizes may vary.

Growth Theories

Growth theories can be broadly classified into equilibrium and kinetic. The equilibrium theory could explain the lamellar thickening of the polymer, but it failed to account for inclusion of inherent chain folding, this led to the popularity of the kinetic model. Most of the morphological interpretations of polymers are based on the kinetic rather than equilibrium factors, since it is assumed that the preferred thickness of the crystal is the one which maximizes the growth rate. Any crystal, given enough time, can equilibrate but in order to achieve this, energy barriers have to be overcome.

The kinetic theory is based on the principle that growth rate depends on the thickness of the crystal, thus the growth fronts can have a range of thickness. In order for crystallization to proceed there should be some driving force or motivation, related to supercooling. The higher the super cooling the greater the drive to crystallize, but if this is the only criterion then the crystal with an infinite thickness would have the fastest growth rate. It is thus necessary to over come the barrier term which opposes crystal growth. A schematic of this phenomenon is given below in Fig.(2.4). Apart from the nucleation theory Sadler suggested a multi-path model based on entropy effects, this was totally based on computer simulations and was primarily qualitative (although based on concepts well established in crystallization of atom or small molecules) (Sadler 1983).

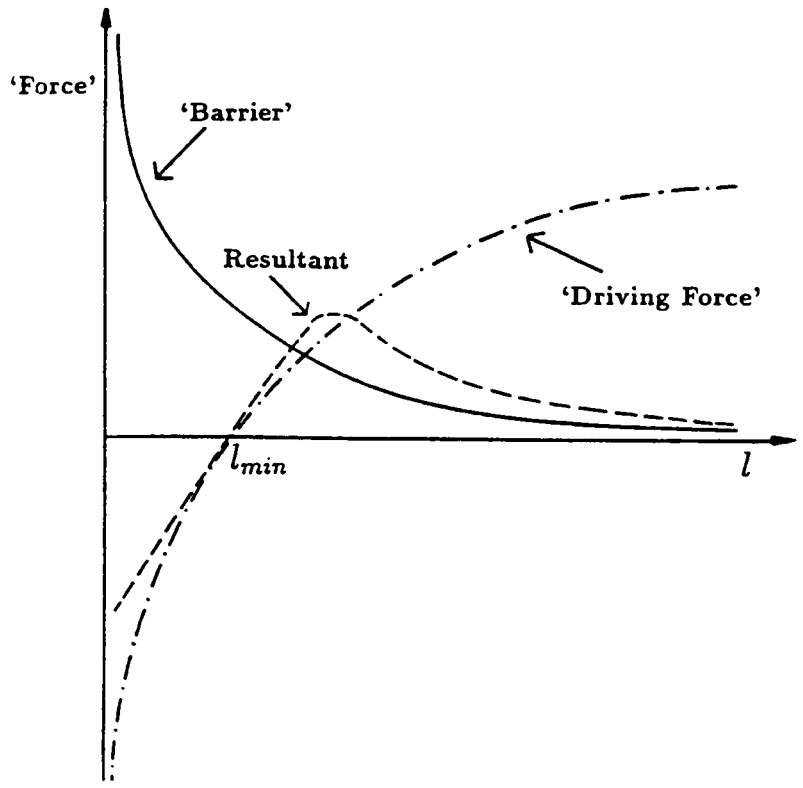


Fig 2.4 Schematic of the factors that affect crystal growth

Nucleation Theories

The kinetic theories use nucleation as the barrier to primary growth, this is based on the nucleation behavior of small molecules.

Growth of small molecules

The growth studies of small molecules have been popular for the last six decades (Jackson 1974; Stranski 1928; Papaptrou 1936). The rate determining step is generally the factor which hinders growth the most. These processes have been categorized based on their dynamics for interface control, which is prominent in vapor and solution grown crystals, and diffusion control which is prominent in melt grown crystals. Interface controlled dynamics, particularly nucleation control, has been the primary way of describing polymer crystal growth. This was based on the argument that the growth rate and the lamellar thickening of the polymer from the melt behave in a similar manner to solution grown counterparts. It is only recently that diffusion theories have been used for melt grown polymers (Keith and Padden 1986; 1987)

Polymers

Nucleation is described as the formation of a critical nucleus. This is directly related to the supercooling, for steady growth in all directions. This approach is difficult to adopt directly in macromolecules due to the complications involved in chain folding and the presence of lamellae.

Lauritzen and Hoffman (Hoffman and Lauritzen 1961) were able to prove that the nucleation theories can also be extended to macromolecules.

Simple nucleation model for long chains

A single nucleus of length, l, deposits on a flat surface creating an increase in excess surface free energy and a decrease in bulk free energy. The stems are all assumed to possess the same length and are laid subsequently adjacent to each other so that they spread laterally. The addition of each stem results in an increase of the surface free energy due to the fold surface and a decrease of the bulk free energy, which is related to l. If $l<l_{min}$ at a given supercooling there is an increase in bulk free energy but this is small compared to the energy lost during the formation of the fold. If $l>l_{min}$, there is a decrease in the free energy and this leads to growth in each direction at a rate g. Hence the spreading rate g increases with l and is a function of both supercooling and lamellar thickness. The similarity between the conventional nucleation and the nucleation of polymers is that there is a barrier which has to be overcome by spontaneous fluctuation in order to deposit the first nucleus. The size of the initial stem has to be larger than the critical size in order for growth to occur. The major difference from that of simple molecules is that stable growth can occur only laterally and is considered as one dimensional (Sadler 1987). Recently a model has been proposed by Hikosaka (Hikosaka 1990; Hikosaka *et al.* 1991,1982,1984) called the sliding diffusion model in which a possibility of growth in all the directions has been considered. This process may not be a nucleation process, since, the free energy barrier to be overcome increases with the thickness of the first stem only and not with the ones to follow thereby ruling out the purpose of the

critical nucleus (Sadler 1987). The growth rate of a nucleation controlled face can be explained in terms of the rate of deposition and the rate of lateral growth. In the first instance, if g is large the nucleus, having formed, spreads rapidly to cover the substrate before another nucleation event can take place. The rate of nucleation in this instance is iL, where L is the substrate width, and the growth rate is given by

$$G_m = biL \tag{2.1}$$

where b is the thickness of the stem and m represents the mononucleation regime. This is also called the regime I. Imperfections in the crystal length prohibit the spreading of the steps and considerably reduce L. The average distance between imperfections is called the persistence length L_p. This correction in the equation. (2.1) gives rise to

$$G_m = biL_p \tag{2.1a}$$

This is termed as regime I growth and is illustrated in *Fig* 2.5 and 2.6.

Linear growth rates can be defined based on the theory proposed by Hoffman and Lauritzen (1976), in which they treat the growth rates of spherulites the same way as their constituent lamellae. This is given by

$$G = G_o(\Delta T) \exp [-U^*/R (T_c - T_\infty)] \exp [-K_g/T(\Delta T) f] \tag{2.2}$$

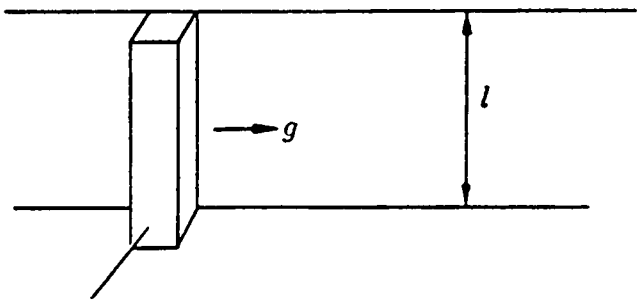


Fig. 2.5 A simple nucleation model for long chains. The first stem is of length l and attaches to the surface. Subsequent stems are deposited adjacent to attached stems, so that the patch spreads in either direction with velocity g.

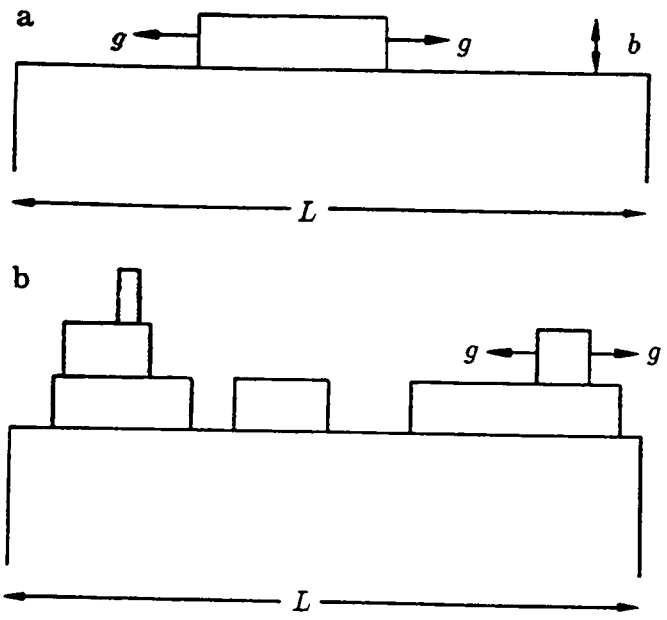


Fig 2.6 Growth on the surface of lamellae, viewed looking onto the fold plane, showing two different types of growth. In *a* a single strip spreads across the surface before another patch can nucleate. *b* shows several patches in the same layer, which may in turn support further nucleation events.

where G_o is the growth rate constant, U* represents the activation energy that governs the short distance diffusion of the crystalline element across the phase boundary. T_∞ is the temperature below which such motion ceases, ($T_\infty = T_g - 30K$) and is related to the glass transition temperature of the material used. The exponents of the second term are the Gibbs free energy contribution for growth of critical size surface nucleus, which is dependent on the degree of supercooling. The factor $f = 2T_c / (T_c + T_m^o)$, which is the correction factor for the variation with temperature of the heat of fusion ΔH_f.The term K_g (nucleation rate constant) can be expressed as;

$$K_g(I) = 4b_o \sigma\sigma_e T_m^o / K(\Delta H_f) \qquad (2.2a)$$

for regime I type of crystallization. σ and σ_e are the lateral and fold surface free energies, K is the Boltzman constant and b_o is the layer thickness. On similar lines, K_g for the regime II and regime III can be expressed as;

$$K_g(II) = 2b_o \sigma\sigma_e T_m^o / K(\Delta H_f) \qquad (2.2b)$$

$$K_g(III) = 4b_o \sigma\sigma_e T_m^o / K(\Delta H_f) \qquad (2.2c)$$

The plot of G versus the crystallization temperature (T_c) gives the growth rate variation with variation in T_c. The regime transitions can be illustrated by taking log of the equation (2.2) and taking a plot of $\log G + U^*/[2.303 R(T_c - T_\infty)]$ *versus* $1/[T(\Delta T)f]$. as illustrated in Fig. (2.7). The plots exhibit two intersecting straight lines of a slope difference of two as predicted by the

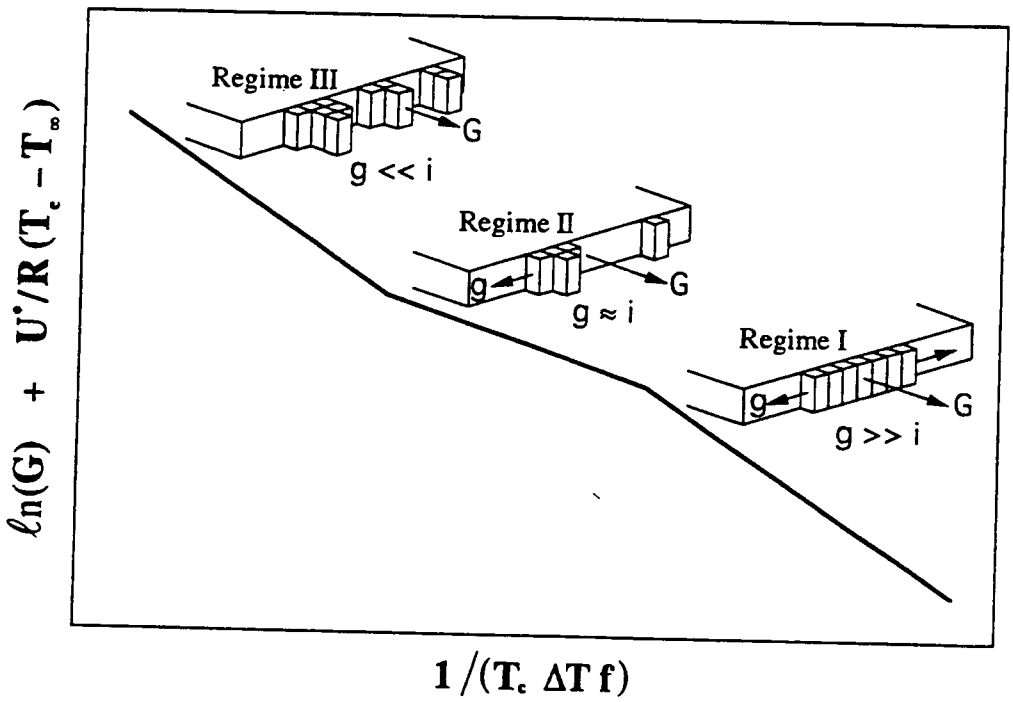


Fig 2.7 Regime I, II and III

equations (2.2 a, b and c). The major contribution to the fold surface free energy arises from the ability for a polymer chain to fold. The chain folding q,can be expressed based on σ_e and the cross sectional area of the polymer chain;

$$q = 2\sigma_e a_o b_o \qquad (2.3)$$

where, a_0b_0 represents the cross sectional area of the polymer chain.

Lauritzen - Hoffman theory for the study of growth data of polymers is based on the competition between the rate of deposition of the secondary nuclei (I) and the rate of lateral spreading (g). This leads to the three regimes; in regime I ($i << g$) which is evident at very low supercoolings close to the melting of the crystals. Regime II occurs when i and g are similar, and finally the third regime occurs when $i > g$ and is seen at very high supercoolings, which is common in all the processing techniques used for the fabrication of many polymers.

Regime analysis has been performed for various polymers, of which some are, PE, cis-PI, PEO, PDMT, Polylacticacid, (Vasanthakumari. and Pennings, 1983), POM (Galeski 1972), poly (3-hydroxybutyrate) (Barham. *et al.* 1984) and PPS (Lovinger 1985). Regime analysis on iPP has been envisaged by many researchers, Allen and Mandelkern reported a regime I/II transition at 56K (1987). Clark and Hoffman reported a II/III transition at ΔT - 48K, and also observed a downward change of slope with decreasing supercooling at the regime II/III occurrence (Clark and Hoffman 1984). Janimak (1991) has reported the presence of all the three regimes in fractions

of iPP (Ph.D. Dissertation, Univ. of Akron, 1991). Campbell and Phillips (1993) and recently Mezghani and Phillips (1994) have done extensive studies on the crystallization regimes of iPP at elevated pressures.

Modifications of the LH theory

In order to make the existing model more realistic in its predictions, modifications have been suggested. The major assumptions are still assumed to be good, where the growth rate is given by nucleation and spreading. The deposition of complete stems depend on the rate constants obeying

$$A_i/B_i = exp\ (\Delta F_T/KT) \qquad (2.4)$$

based on the Frank (1961) assumption where ΔF_T is the total change in free energy upon adding a new stem.

The earliest work with respect to modifications of the LH theory was its extension to multicomponent chains, so that the rate constants for adding stems to a nucleating strip depend not only on the number of stems already deposited, but also on the species of the final stem in the strip and the attaching stem (Lauritzen., Di Marzio and Passaglia, 1966).

The muticomponent theory has been used for cilia (Di Marzio 1967 and Sanchez and Di Marzio 1971), and crystallization of random copolymers where the main conclusion was that the compositions of the components in the crystal are determined by kinetic rather than equilibrium considerations.

Fractionation effects (Sanchez 1972) and the amount of adjacent reentry (Di Marzio and Passaglia 1987) have also been studied. Hoffman and Miller (Hoffman and Miller 1988) have modified the nucleation model by incorporating reptational motion at the crystal melt interface.

This reptation-like molecular weight dependence has been criticized by Point and Dosiere (1989) who question the application of Frank's model for the crystallization of polyethylene melt.

In order to account for the curved edges of polymer crystals, Mansfield (1988) introduced the moving boundary approach supported by computer simulations, this has been questioned by Point et al (1991) for its correctness. An alternate model developed by the late Sadler in the early 1980's, was based on continuous growth on a rough surface (Lauritzen 1973 and Kossel 1927). Here he assumes that the growth is controlled by the entropy barrier rather than the nucleation barrier. On this basis he also attempted to explain the regime transitions in polymers (Bennett *et al.* 1981). Apart from this multi path model suggested by Point, there are molecular nucleation theory by Wunderlich and Mehta (1974) and sliding diffusion model by (Hikosaka 1987).

2.3 Thermal Behavior of Polypropylenes

Copolymerization in polypropylene lowers the chain regularity, reducing the melting point and the sequence length of the crystallizing component. It also depresses the crystallinity, and broadens the melting and crystallization peaks, as formation of crystals of varying perfections is

allowed. Flory's theory of polymer melting does not assume defect incorporation into the crystal, but still predicts a depression in melting with an increase in comonomer content (Flory 1955). This prediction has been applied to propylene copolymers by Ke (1960) where he predicts a decrease in melting of 1.5 degree/mole% ethylene incorporation. Based on the work of Martuscelli (1986), and Greco *et al.* (1987) it can be concluded that the reduction in melting point with an increase in ethylene content is correct but that it is more significant in lower comonomer contents.

The equilibrium thermodynamic properties, especially the equilibrium melting point data has been very inconsistent in the literature. There have been two different values reported, one closer to 185°C and the other in the range of 210°C (Fatou 1971; Hoffman and Weeks 1962; Miller and Seeley 1982; Wuderlich 1988; Martuscelli 1984). Lately Phillips *et al.* (1994) have evaluated this problem with the help of SAXS to conclude that the value close to 185°C is more pertinent.

Theories of random copolymer crystallization have been developed based on interdependence of melting of crystals, the amount of non-crystallizable component that is incorporated in the crystal lattice and its kinetics (Flory 1955, Sanchez and Eby 1973; Helfand and Lauritzen 1973; Sanchez and Eby 1975). Depending on the type of comonomer incorporation in the crystal, copolymer crystallization can be classified as uniform inclusion of comonomer or total exclusion of comonomer Fig. 2.8. The former one suggested by Flory considers the polymer crystal to consist of only the rich

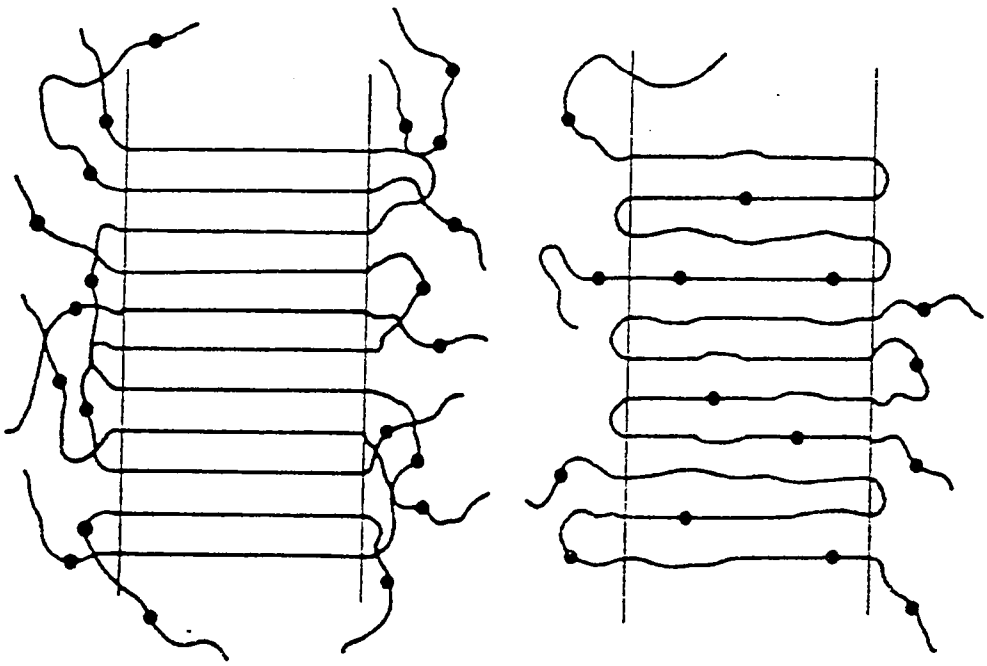


Fig 2.8 Inclusion and Exclusion models; two extreme representations of lamellar random copolymer crystals, the exclusion model (left) and inclusion model (right).

component A, while the dilute component is excluded from the crystal. The latter proposed by Sanchez and Eby, argues that the other extreme might be possible thermodynamically where the dilute component exists as included in the rich component. Both these models suggest the lowering of the equilibrium melting point with increase in comonomer content. Applying thermodynamics, x (mole fraction) is the overall fraction of the dilute component B in the copolymer AB. The probability that m units in a stem of n units will be B comonomers is given by the binomial distribution

$$\mu(m) = [n!/m!(n-m)!]x^m (1-x)^{n-m} \tag{2.5}$$

Helfand and Lauritzen gave the partition function Z as

$$Z = \sum_{m=0}^{n} \mu(m) \exp^{-\beta m\varepsilon} \sum_{m=0}^{n} z(m) = (1-x+xe^{-\beta\varepsilon})^n \tag{2.6}$$

where $\beta = 1/kT$, z is the partition function of a metastable state and the maximum is at the equilibrium. Sanchez and Eby give the difference in Gibbs free energy between a metastable crystal of concentration $x_c = m_c/n$ and the melt is given as;

$$\Delta G = \Delta G^o = RT \ln z(m_c) \tag{2.7}$$

$$and\ \Delta G = \Delta G^o - RT[\frac{x_{c\varepsilon}}{RT} + (1-X_c) \ln \frac{1-x_c}{1-x} + X_c \ln (\frac{x_c}{x})] \tag{2.8}$$

where $\Delta G^o = \Delta H^o_f (1-T/T_m^o)$ is the difference in the Gibbs free energy near the equilibrium melting temperature T_m^o, and ΔH^o_f is the equilibrium heat of

fusion of the homopolymer with A comonomers, and the excess free energy caused by the incorporation of the dilute component is *e*. If the free energy is equated to zero, then

$$\frac{1}{T_m} - \frac{1}{T_m} = \frac{R}{\Delta H_f}\left[\frac{x_c \varepsilon}{RT_m} + (1-X_c)\, ln\, \frac{1-x_c}{1-x} + X_c\, ln\left(\frac{x_c}{x}\right)\right] \qquad (2.9)$$

when $x_c = 0$ the equation reduces to Flory's exclusion equation

$$\frac{1}{T_m} - \frac{1}{T_m} = \frac{R}{\Delta H_f}\, ln(1-x) \qquad (2.10)$$

when $x_c = x$ the equation reduces to uniform inclusion model

$$T_m = T^{o}_{m}\,(1 - x\varepsilon / \Delta h^{o}_{f}) \qquad (2.10a)$$

when $x_c = x$ equilibrium, the equation becomes

$$\frac{1}{T_m} - \frac{1}{T_m} = \frac{R}{\Delta H_f}\, ln(1 - x + x\, exp^{-\beta\varepsilon}) \qquad (2.10b)$$

Thus the $\beta\varepsilon$ term seems to be the deciding factor if there is going to be inclusion or exclusion. If $\beta\varepsilon$ is large, it tends to satisfy the exclusion model since $x\, exp^{-\beta\varepsilon}$ tends to zero, while if $\beta\varepsilon$ is small i.e. ($<\leq 1$), the total inclusion model is satisfied.

Theoretically assuming the enthalpies to be additive, the difference in enthalpies of the two models can be obtained. Sanchez and Eby give the enthalpies of both the models (1973)

Inclusion model

$$\Delta H / X = \Delta H - X_b \Delta H_d - 2\Delta H_e / l \qquad (2.11)$$

Exclusion Model

$$\Delta H / X = \Delta H - 2\Delta H_e / l \qquad (2.12)$$

where ΔH_e is the excess enthalpy required in forming the basal surface of the copolymer crystal. X is the crystallinity and ΔH is the heat of fusion. In the inclusion model the dilute component affects the enthalpy whereas in the exclusion model it is unaffected. Thus a plot of heat of fusion/crystallinity vs. the comonomer content would give a simple way to quantify inclusion or exclusion.

2.4 Structure and Properties of Polypropylenes

The word "Polypropelen" was first used by Buterlov (1873), who produced oligomers by adding sulphuric acid to propylene. Amorphous polypropylene was first obtained by Fontana (Seymour *et al.* 1988) of Mobil Oil Co., by cationic process during the post World War II period. In 1954 Natta and Corradini (Natta 1960) announced the structural characteristics of isotactic crystalline polymers from α-olefins synthesized in their laboratory in Milan Polytechnic. These highly crystalline polypropylenes have gained prominence as raw materials for the production of plastics and textiles due to

their excellent thermal and mechanical properties, in comparison to their low costs.

If polypropylene was synthesized by head to tail polymerization, and not stereospecifically, the monomer assumes two equivalent specular conformations (Fig 2.9) that cannot in any way be superposed. This results in a random steric structure (Fig 2.10). The advent of the heterogeneous stereospecific catalysts reduced the possibility to only one of the two configurations. This is because the co-ordination of the π-bond with the transition element of the catalytic complex leads to the addition of the polarized olefin molecule to the growing chain in a specific fashion. Fig. (2.10). The sterically regular conformation that the chains assume is called isotactic (derived from the Greek word 'ίσος', similar and 'τάττω', to settle, Natta 1955). Natta and co-workers concluded that vinyl polymers whose monomeric units can follow a head to tail polymerization along the chain, are able to assume by rotation around single carbon-carbon bonds, sterically equal configurations, that is of repeating themselves by simple operations of transitions and rotation along an axis. (Natta and Corradini 1960).

Polypropylene can be obtained in the isotactic, syndiotactic and atactic forms, but particularly the isotactic form has stimulated growth mainly because of its commercial importance other than fundamental research interests. Syndiotactic polypropylene is also winning importance due to the launch of the metallocene catalyst systems.

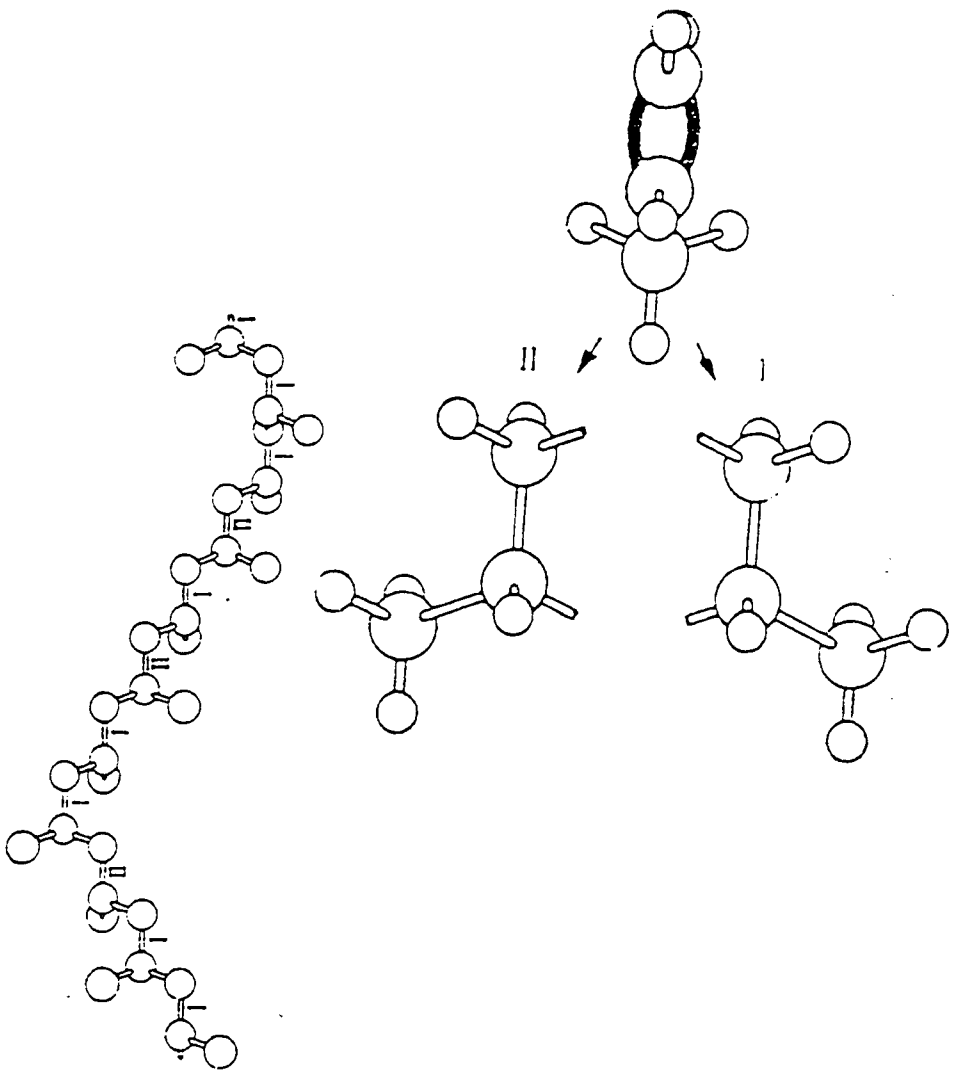


Fig 2.9 Conformation and configuration of Polypropylene.

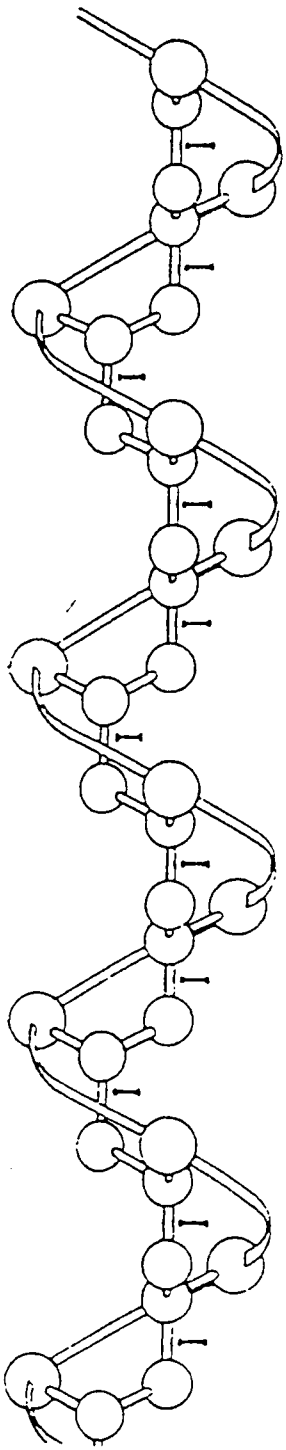


Fig. 2.10 Conformation of an isotactic chain of polypropylene in the crystal state

Chain Conformation of Isotactic Polypropylene.

In the polymorphs of polypropylene (α, β and γ), the chains are always in the conformation of a three fold helix (s (3/1)1 symmetry) with a 6.5Å repeat distance, but are packed in different ways, either in the monoclinic (Gruerra, Petraccone *et al.* 1984), hexagonal (De Rosa, G. Gruerra, Petraccone *et al.* 1984) or orthorhombic forms (Meille and Bruckner 1989).

A unique property in iPP is its ability to epitaxially crystallize with a number of polymers with their chain axis tilted at large angles (40-80°) relative to the helical axis direction present in the iPP substrate. This ability has lead to the understanding of the γ phase, where it permits a homoepitaxy with a tilt angle of 80°. γ iPP was first cited by Addink and Beinten (1961), who found diffraction lines which were not characteristic of the α & β form. Though the conditions for the formation of the gamma form have been many, the exact mechanism has been an enigma. Heterogeneity in the chain was regarded as the main reason for this type of formation and it was earlier observed in atactic PP and propylene copolymers.

Conditions for obtaining gamma form;

Phillips and Campbell (1991,1993) have observed the coexistence of gamma phase with the alpha for high molecular weight homopolymers crystallized at elevated pressures. Recently Mezghani and Phillips have shown the existence of 100 % γ phase in homopolymers at elevated pressures, and at very low supercoolings. (unpublished). Lotz and Kojima *et al.* have been successful in obtaining gamma phase from pyrolysis and special

synthesis (Kojima 1968). Morrow (1968) were also able to achieve a considerable amount of gamma phase from fractions of iPP with a molecular weight range of 1000-2000. Turner-Jones reported that by extracting stereoblock copolymers using xylene extraction (35-70° C) and recrystallizing these fractions at the very slow rate of 6°/hour, they developed the γ form. The most surprising route to develop the γ-form is by copolymerization of propylene with ethylene or but-1-ene, first reported by Turner-Jones (1971). The % ethylene they used was 4-10% and they concluded that a maximum amount is developed in the case of iPP with 6.5% ethylene. The molecular weights they studied were of the range of 300,000.

Recent studies by Meille and Bruckner (1989) have indicated that a new homogeneous catalyst system can help in achieving pure gamma phase. There have been many attempts to develop gamma form in fibers which were futile due to the formation of α-form owing to stress induced crystallization. Awaya (1966) was successful in obtaining some γ phase in biaxially oriented films. Bevis *et al.* (1994) were successful in obtaining gamma phase in injection molded iPP samples. They used shear controlled orientation injection molding and obtained gamma phase in highly oriented samples, together with a marked intensification of preferred orientation of the α-phase.

Crystal Structure of Polypropylene

- The α- phase monoclinic unit has dimensions ; a=6.66, b=20.78, c=6.495 and β = 99.6, reported by Turner- 1964), representing a small correction to the

original reports of Natta and Corradini (1960). This is found to be the most stable and prevalent form in normal polymer processing conditions.

- The paracrystalline form which is generally achieved at fast cooling rates, got its name as mesomorphic since it was the second modification of the α-form (Natta and coworkers 1959). This was earlier misunderstood to be amorphous polypropylene by Slichter and Mandell (1958) in their studies on rapidly quenched polypropylene. This phase is also called smectic phase or condis crystal (conformationally disordered) as termed by Wunderlich .

- Morrow and Newman (1968) proposed a triclinic structure for γ- phase iPP; a=6.54, b=21.40, c=6.5, β = 99.6 and γ = 99 after the initial work of Turner-Jones, who proposed a bidimensional cell (Meille and Bruckner 1991). Most recently Meille and Bruckner undertook extensive studies on x-ray diffraction coupled with electron diffraction studies and proposed a pseudo triclinic cell. This differs from the previous reports mainly in the value of α*, (for which Morrow and Newman acknowledged some ambiguity due to the thin crystals studied). This pseudo-triclinic cell can be transformed into a face centered orthorhombic cell a=8.54, b=9.93, c=42.41. This was suggested by them after trying different packing mechanisms to maintain parallelism in the triclinic cell. Thus they came up with a model which comprised chains parallel to both of the diagonals of the a-b plane (13.08, twice the helical period of 6.5Å and forming an angle of ≈80°, similar to chain axes of branched iPP crystals. This packing is given in (Fig 2.11)

• The structure of β-iPP also has been a longstanding structural puzzle, being identified first by Keith, Padden, Kissel and Wyckoff, (1959), but due to its mechanical and thermodynamic instability it was not fully characterized. The dimensions of possible lattices of β-iPP have been listed by Turner-Jones(1964). Recently Lovinger *et al.* (1994) have investigated the structure of β-iPP based on X-ray, electron diffraction and packing energy calculations. Since the structure was extensively disordered they concluded that two models could be envisaged, and they both satisfied a pseudo-hexagonal lattice. They can be simple trigonal; a = b = 11.03 and c = 6.49Å, if the coupling of the chiral domains are across the glide planes or if the domains are coherent, in a new achiral orthorhombic lattice; a=11.03, b=19.10 and c = 6.49Å.

2.5 Theories of Fractionation

Fractionation of polymers is the separation of heterogeneous macromolecules into fractions which are more homogeneous in nature. These fractions which are close to monodisperse are always sought as standard materials. The experimental method used for fractionation plays a key role in determining the type of fractions obtained, i.e., if it is by molecular weight, structural or chemical configuration.

Major advances in experimental techniques have taken place in the fractionation of polymers by molecular weight, since molecular weight distributions is the most common feature in all polymers. Experiments for fractionation by chemical and structural heterogeneities have been successful

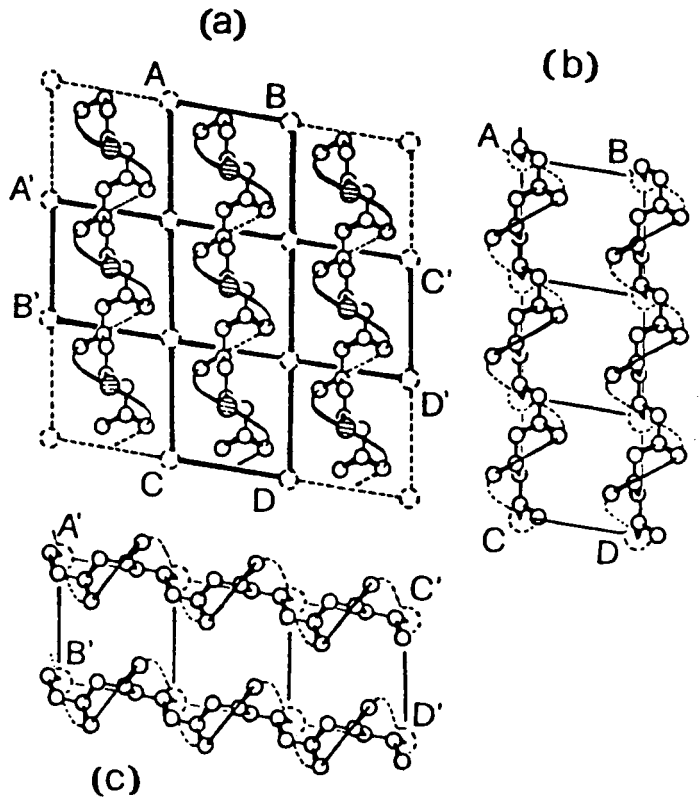


Fig 2.11 Possible orientations of chain axes in the crystal packing of iPP (a) A layer of left handed helices are shown, reproducing the lateral (010) face B of a-iPP. The methyl groups which protect out of the mean plane toward the reader are shaded, while broken line circles indicate the available sites of the methyl groups of the next layer. If the next layer is built up with helices of possible chirality (right-handed), as shown on the right side (b), a parallel arrangement of the chain axes allows for a favorable packing. If the helices of the same chirality are present in the next layer, as shown in (c), a tilting of the chain axes of the 81o is required for a favorable interdigitation of methyl groups to occur. (Bruckner 1991)

with specific modifications of the techniques used for molecular weight based fractionation. Numerous reviews have been published on fractionation based on molecular weight separations (Cantow 1967 and Tung 1977, Encyclopedia of Polymer Science and Technology 1988, Paukkeri and Lihtinen 1994) Fractionation methods can be classified as shown in Fig. 2.12

Fractionation of Copolymers

Solubility of a chemically homogeneous material depends on the molecular weight of the sample. In the case of copolymers, inhomogeneous materials, the solubility depends on both the chemical structure and the molecular weight. During the fractionation of copolymers by solubility behavior of individual molecules, a superposition of the contribution of molecular weight and structure occurs. In cases where there is a pronounced heterogeneity, the fractionation by molecular weight does not take place as it is over run by the variation in chemical composition. Solubility also depends on the solvent-nonsolvent system used for fractionation, and the temperature.

Fractionation by Solubility

Fractionation by solubility, using the Flory-Huggin's statistical thermodynamic treatment has been reviewed by many authors (Huggins *et al.* 1967, Higgins 1963 and Koningsveld 1970). The equations were restated for copolymers by Topchiev (1962).Accordingly the distribution of a copolymer between two phases in equilibria is given by:

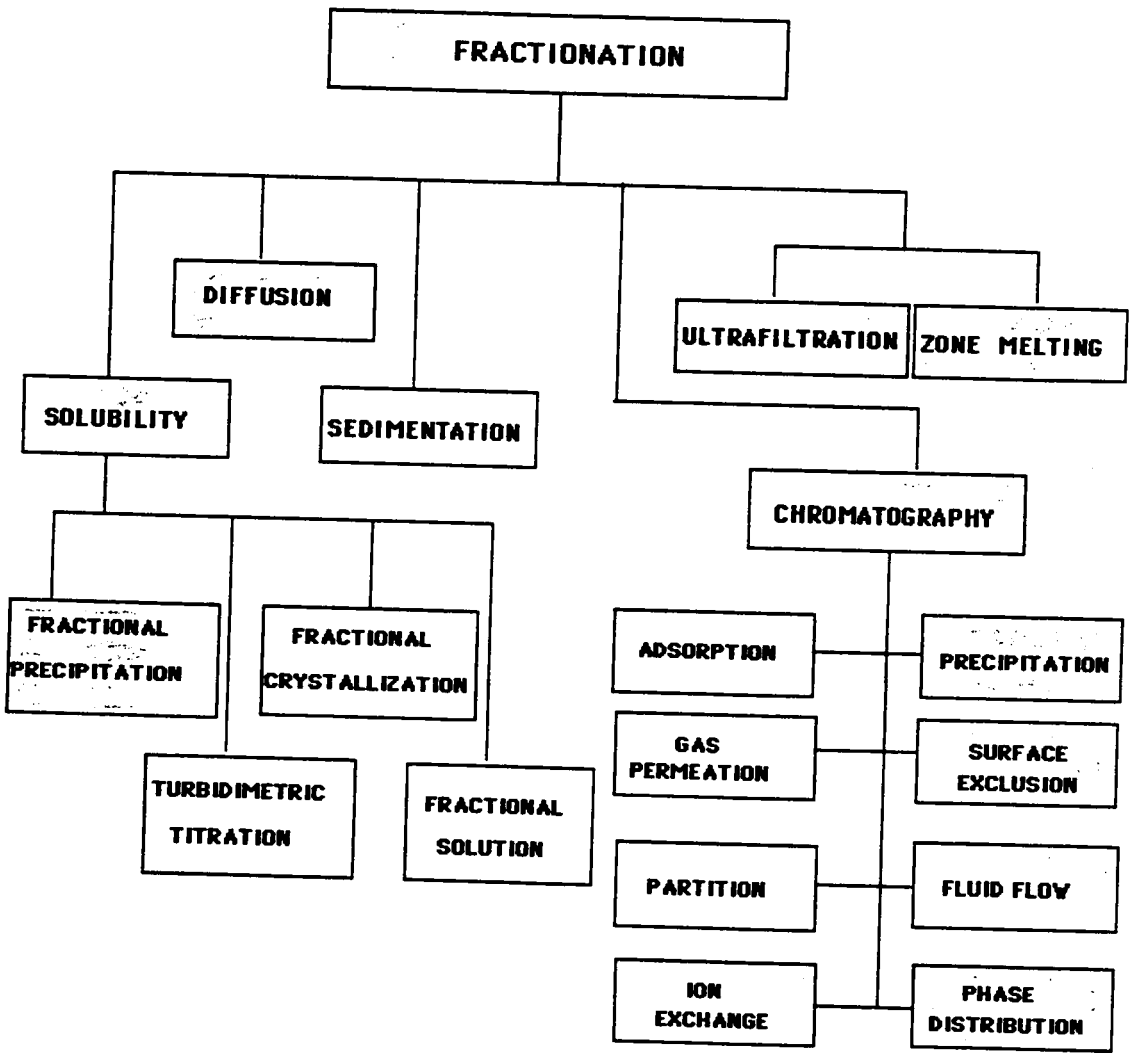


Fig. 2.12 Classification of Fractionation (Polymer handbook)

$$v'_{p\alpha} / v_{p\alpha} = exp\,[p(\sigma + K\alpha)] \qquad (2.13)$$

where p is the degree of polymerization, α the chemical composition (volume fraction of A monomer in copolymer A-B, $v'_{p\alpha}$ and $v_{p\alpha}$ are the volume fractions of a component (p,α) in precipitated and supernatent phases, σ is the fractionation parameter and K is given by

$$K = (v_1 - v'_1)(X_{1A} - X_{1B}) + (v_2 - v'_2)(X_{2A} - X_{2B}) \qquad (2.14)$$

for a two solvent system and

$$K = (v_3 - v'_3)(X_A - X_B) \qquad (2.15)$$

for a one solvent system. In these equations above v_1, v'_1 and v_3 are the volume fractions of the solvent 1, solvent 2, and the copolymer, the prime corresponds to the precipitated phase and X_{1A}, X_{1B} are the interaction parameters of solvent 1 or 2 with the monomer A or B. The equivalent of equation 2.13 for homopolymers is

$$v'_p / v_{p\alpha} = exp\,[p\sigma] \qquad (2.16)$$

where σ is a function of the volume fraction in each phase, of molecular weight and of the interaction parameter. If in a copolymer system $K=0$ then true molecular weight fractionation is expected, without being affected by the chemical composition. Thus it is always the case that the fractionation in

copolymers is not one directional but is dependent on chemical structure and molecular weight. Though there have been many advances in predicting the thermodynamics of the copolymer-solvent-nonsolvent system, only a good qualitative understanding can be achieved using experimentation. For efficient fractionation, it must be conducted using very dilute solutions

Fractionation of copolymers based on solubility is affected by the chemical nature of the polymers, if they are of different polarities it is comparatively easier to fractionate them. In the case of propylene copolymers with ethylene, fractionation is more difficult due to the similar chemical nature of the monomers. Recently there has been repeated interest in the fractionation of isotactic PP, based on tacticity and molecular weight. Kawamura *et al.* (1989), based on the understanding that iPP is a mixture of isotactic and atactic polymers produced at different sites, have successively extracted iPP with boiling n-alkane solvents. They conclude that tacticity and molecular weight fractionation occurs for the isotactic portion of iPP while only molecular weight fractionation occurs in the atactic rich portion of iPP. Paukkeri and Lehtinen (1994) have fractionated iPP synthesized from different heterogeneous Zeigler-Natta catalysts by using soxhlet extraction. They first extracted the polymer in n-pentane, and later the unfractionated polymers and their heptane soluble/insoluble fractions were analyzed using size exclusion chromatography. From their studies they concluded that estimation of isotacticity based on heptane insoluble fraction gives only a rough estimate of the stereoregularity of the polymer, since there are some syndiotactic and heterotactic PP also present in them.

Fractionation of copolymers is a powerful tool to determine the monomer sequencing and the heterogeneity of the copolymer. In the fractionation performed on copolymers the approximation that the solution behavior of the copolymer is close to that of the homopolymer has helped in better understanding. Detailed fractionation of propylene-ethylene copolymers has shown broad comonomer and molecular weight distributions both with vanadium and titanium based catalysts, except in the early studies done by Cozewith on vanadium catalyst, where he achieved very narrow distribution in fractions of the copolymers (Cozewith *et al.* 1971). Kakugo and coworkers (Kakugo *et al.* 1988*)* have studied propylene copolymers using TREF and deduced the presence of differing ethylene contents in the fractions. Galli *et al.* (1985.) have come to a similar interpretation based on their work on new titanium based supported copolymers. Random copolymers made from $MgCl_2$ based supported catalysts are also heterogeneous in their composition as a simple fractionation with ether and hexane gave a range of ethylene contents (Milani *et al.* 1986*).* There has been extensive work conducted in the understanding of the monomer sequencing in propylene copolymers. (van Schooten *et al.* 1961; van Schooten *et al.* 1963; Cozewith *et al.* 1971; Wilkes, 1973; Ray 1977; Randall 1978; Smith 1980; Galli, Milani and Simonazzi 1985; Martuscelli 1986; Milani *et al.* 1986; Cheng *et al.* 1987; Kakugo *et al.* 1988; Hayashi *et al.* 1988). Finally from all these extensive works it can be discerned that copolymers are typified by broad compositional distribution due to the presence of multiple catalyst species.

3 EXPERIMENTAL

3.1 Materials

The propylene copolymers for this work were provided by Exxon Chemical Company; iPP3 (3% weight ethylene copolymer, M_w = 300K) and iPP5 (5% weight ethylene copolymer, M_w = 300K) with similar molecular weights. In order for better understanding of these copolymers based on molecular characteristics, comonomer content and tacticity, they were solution fractionated using a soxhlet extractor.

3.2 Fractionation

The copolymers iPP3 (3% ethylene) and iPP5 (5% ethylene) were fractionated successively using solvents of increasing boiling point. These fractions were further analyzed for comonomer content, tacticity (FTIR), melting behavior (DSC) and molecular characteristics by GPC (awaiting results from Exxon)

Apparatus/ Materials

The apparatus used for this work were; two necked flask, soxhlet extractor (insulated), water cooled condenser, cellulose thimble, glass wool, hot plate with stirrer and heating mantle.

Materials

In order to obtain better surface interaction between the polymer and the solvent, fractionations are generally carried out in the powder form. For this purpose the polymer pellets were dissolved at 140°C in xylene containing an antioxidant, butyrated hydroxy toluene (1.5-2 g/L), using a heating mantle with a magnetic stirrer. The solution obtained was allowed to cool to room temperature and the polymer was precipitated by pouring the solution in cold methanol. The recovered polymer was filtered using a cellulose filter and dried under vacuum at room temperature.

The solvents used for fractionation were hexanes (69 °C), cyclohexane (80 °C), heptane (98 °C), toluene (111 °C), octane (125 °C) and xylene (144 °C). Butyrated hydroxy toluene (2, 6, di- tetr-butyl-4-methyl phenol) was used as an antioxidant and methanol as non solvent.

Experimental Setup

A typical experimental setup used is given in Fig 3.1. The powdered sample (~5-6 gms) along with glass wool is placed in a cellulose extraction thimble. The glass wool helps to increase the surface area of the polymer powder and also serves to keep the polymer from clumping together to form a large mass, when the solvent causes it to swell. The glass wool is also placed on top of the extraction thimble to stop the condensate from dripping directly onto the polymer. The thimble is placed in an insulated soxhlet, which helps in keeping the extraction temperature within 2 °C of the boiling point of the solvent.

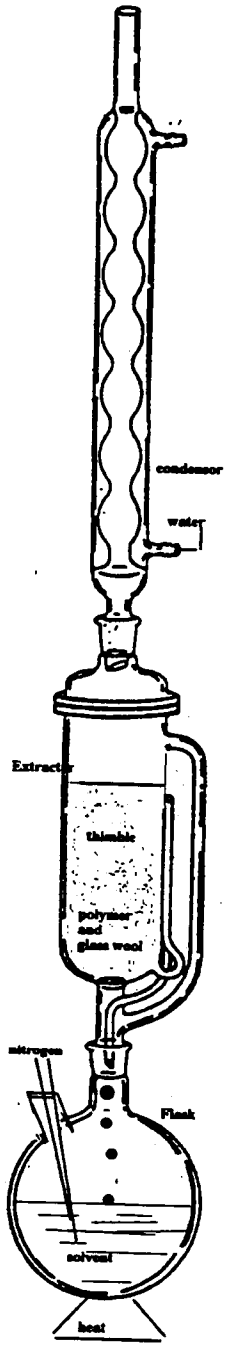


Fig. 3.1 Soxhlet Extraction setup for solution fractionation

It is very important to note that the top of the thimble should be above the level of the syphon tube, and the top of the polymer should be below the level of the syphon top.

The extraction solvent and the antioxidant are placed in the flask, the extractor on top of the flask and the water cooled condenser on top of the extractor. Nitrogen gas is dried through anhydrous calcium sulphate ("drierite") and bubbled into the solvent to eliminate oxygen. Then the solvent is brought to boil sufficiently to allow the extraction cup to fill and dump every 10 minutes; this can be adjusted by controlling the regulator. In order to achieve steady state the extraction was continued for 24-30 hours. After cooling, the polymer is recovered by precipitating in cold methanol. The polymer is further dried at room temperature under vacuum. This procedure is continued for all the solvents successively. To obtain accurate extraction yields, after each solvent extraction, the thimble is removed, dried and weighed.

3.3 Sample Preparation

The polymer samples in powder form are expected to have good homogeneity, so these were used to make films by pressing into films between cover slips in a Mettler FP52 hotstage at 180 °C for 3-5 minutes followed by quenching in water. Care was taken not to pressurize the sample at low temperatures to avoid orientation of the polymer chains. These films were used for DSC, FTIR and PLM studies. A hole of 5mm diameter was drilled in 1.2 mm thick microslides, and these were used as moulds for preparing samples for WAXD studies in the hot stage.

3.4 Differential Scanning Calorimetry

Thermal studies for all the polymer fractions were carried out using the Perkin Elmer DSC Series 7 equipped with an updated computer interface. The DSC was calibrated using pure lead for correcting both the heat flow and the temperature. The melting/crystallization behaviour of all the fractions were found after holding them at 180°C for 5 minutes. All experiments were conducted under dry nitrogen gas purge at 20 ml/min.

Isothermal experiments were conducted at various crystallization temperature to obtain the equilibrium melting point using the Hoffman and Weeks method. The samples were first heated to 180°C and held for 5 minutes, for erasing their thermal history. Then the melt was quenched at 80 °C/min. to the pre-selected crystallization temperature and held for predetermined times. A short time was used only to develop small crystals, which were melted at a rate of 10 °C/min. Besides the peak temperature, the melting temperature by modified-return to baseline method was also determined. A small portion of the samples prepared for WAXD were also dynamically melted at 10 °/min to obtain their latent heat of fusion.

3.5 Polarized Light Microscopy

Polarized light microscopy studies were carried out to determine the linear growth rates and morphology of the copolymers. A Nikon polarized microscope hooked with attached TV, video camera and a VCR were used for

this investigation. All the experiments were conducted using two Mettler hot stages under an atmosphere of dry nitrogen at atmospheric pressure. The hot stage was calibrated using a type J calibrated thermocouple. The sample films were pressed under cover slips (about 10 mm thickness) in hot stage I at 180°C for 8 minutes. They were then transferred suddenly to hot stage II at a pre-selected isothermal crystallization temperature. The measurement commenced only after 5-10 seconds time lag, which is normally taken into consideration for thermal equilibration. Growth rate measurements for axialites / spherulites were recorded using the video camera, and successive measurements were done prior to impingement at regular time intervals. In order to obtain accurate results at least ten measurements were carried out at each temperature (T_C) and the measurements had a standard deviation of $\pm$ 5%. Linear growth rates were obtained from the slope of sperulitic radius versus time.

3.6 Wide Angle X-ray Diffraction

WAXD studies were used to determine the effect of comonomer content (at different crystallization temperatures) on the crystal lattice. CuKα radiation was used for WAXD studies in a Rigaku-Denki diffractometer. The reflection mode was used to determine the diffraction pattern of the copolymer fractions. The 1.2 mm thick samples were completely crystallized on a Mettler hot stage and quenched in ice water before analyzing. The diffractometer was calibrated for alignment using a standard silicon specimen (peak at 28.47 °.). A chart recorder was used to measure the relative

intensity versus 2θ for an anglular range of 30° to 10°. The % gamma content, and the crystallinity were measured.

3.7 Fourier Transform Infrared Analysis

Infrared analysis was obtained using a BioRad spectrometer, all the spectra being obtained for the mid-infrared region (4000 - 500 cm^{-1}). Inhomogenities in films were handled by making five recordings from different regions of each sample. The scans were then transferred to spectrum fit software (unscrambler) where the different areas were integrated. Calibrations for comonomer content and % isotacticity were based on C^{13} nmr experiments. The band areas were preferred to peak heights, as they were found to be independent of spectral resolution, band asymmetry and splitting (Skaare *et.al.*,1992). Thus the effect of crystallinity and band splitting becomes less critical when band areas are employed. All the spectroscopic analyses were conducted at ambient temperature.

3.8 Nuclear Magnetic Resonance

NMR measurements were recorded at 127°C in a Bruker AX-400 spectrometer operated at 100 MHz. The sample solutions for a 5-mm-o.d. glass tube were prepared in o-dichlorobenzene (90 vol %)/benzene-d_6 (10 vol%) with 10 w/w % of the polymer. Benzene-d_6 was used for the ^2H NMR internal lock. For all the measurements an aquisition time of 1.5s and a pulse interval of 8-20 s was used.

It has been earlier reported that 10s is sufficient to satisfy the spin-lattice relaxation time, T_1, of the methyl group which is the slowest relaxing nucleus with a T_1 of 2s at 125 °C. (Mandelkern 1977 and Randall 1976))

4 RESULTS

4.1 Fractionation

Successive fractions of copolymers iPP3 and iPP5 were recovered after solvent extraction using a soxhlet extractor. A good mass balance was achieved by weighing the dried thimble after each extraction. The weight fraction recovered from each successive solvent is illustrated in Fig. 4.1-4.2 and Table 4.1- 4.2. All the fractions of iPP5 and iPP3 were recovered in toluene, while those of iPP3 were also recovered using higher boiling octene and xylene. It can be observed based on the weight recovered from each successive extraction that majority of the fractions dissolved in the lower boiling solvents.

In order to understand the molecular, thermal and structural characteristics of the copolymer fractions, they were characterized using NMR, FTIR, DSC and X-ray diffraction. Information about tacticity, molecular weight, comonomer content, comonomer sequencing, melting, crystallization and presence of the gamma phase were obtained. Analysis of propylene copolymers using NMR and FTIR has been studied by a number of researchers to relate the effect of comonomer content, comonomer sequencing and tacticity to copolymerization (van Schooten *et al.* (1961), Wei (1961), Corish *et al.* (1964), Bly *et al.* (1966), Zambelli A *et al.* (1975), Randall (1982,

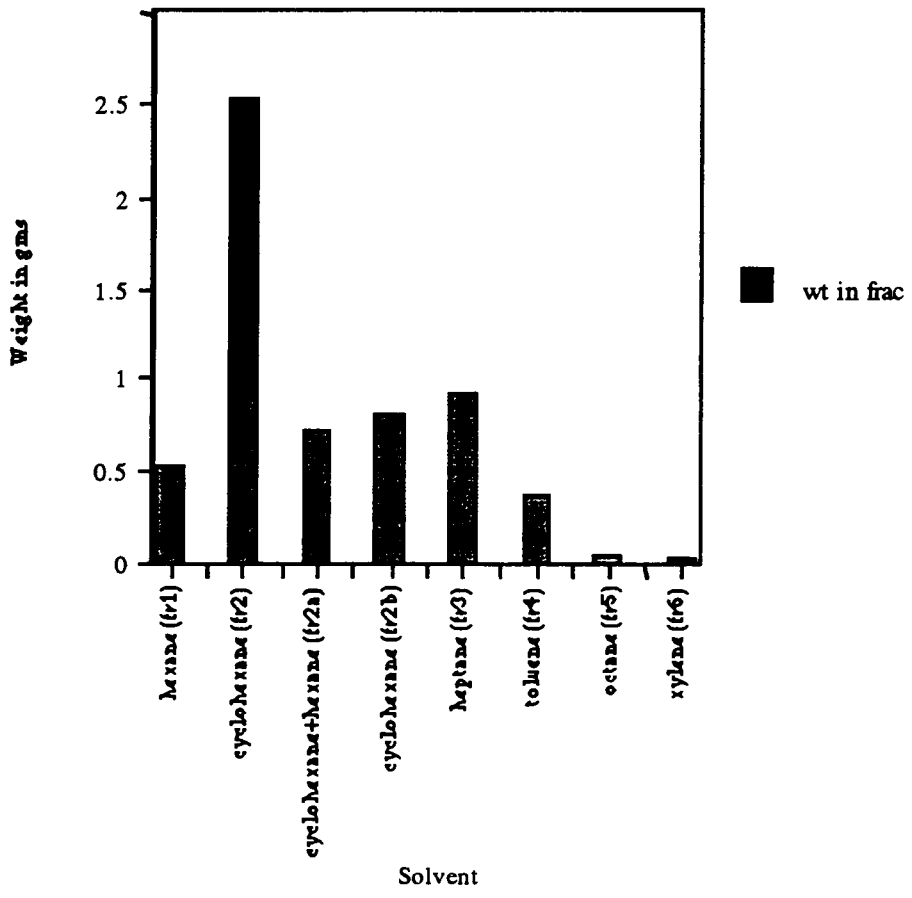


Fig. 4.1 Fractionation of 3% ethylene containing Propylene copolymer

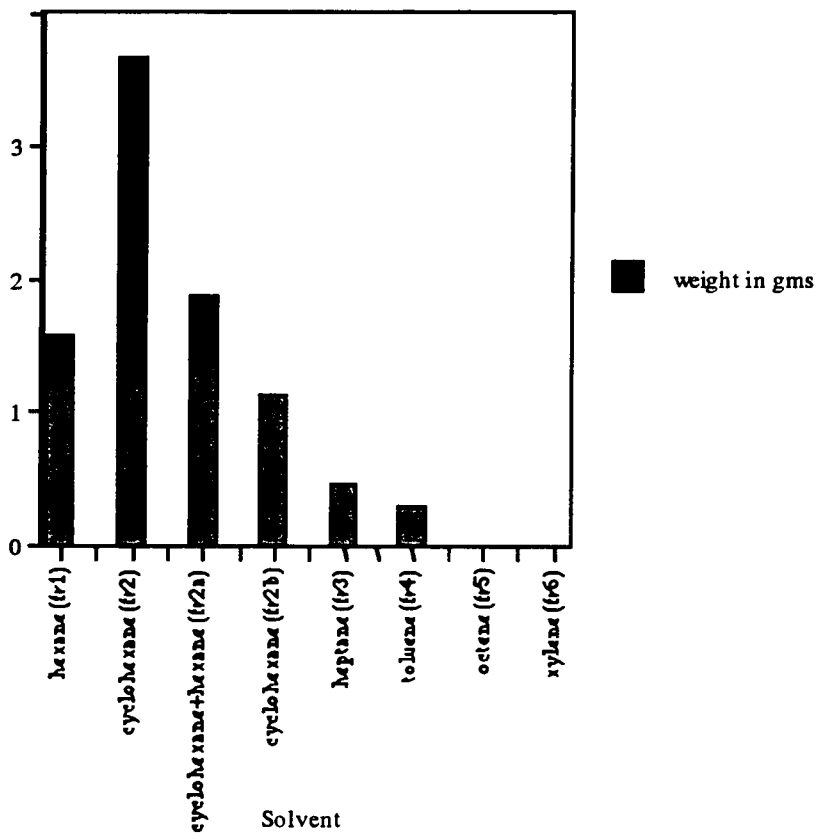


Fig. 4.2 Fractionation of 5% ethylene containing Propylene copolymer

Table 4.1 Fractionation of 3% Propylene copolymer

Fraction	Solvent	Wt of fraction in gms	wt % of ethylene	
1	hexane	0.505	10.6	15.10
2	cyclohexane	2.52	2.22	3.29
2a	cyclohexane+hexane	0.7	3.66	5.39
2b	cyclohexane	0.8	2.17	3.22
3	heptane	0.9	0.96	1.43
4	toluene	0.35	0.62	0.93
5	octane	0.025	0.55	0.82
6	Xylene	-	0.51	0.76

Total weight used in this fractionation was 4.8 gms.

Table 4.2 Fractionation of 5% Propylene copolymer

Fraction	Solvent	Wt of fraction in gms	% of ethylene	mole % of ethylene
1	hexane	1.56	10.050	14.35
2	cyclohexane	3.63	3.376	4.98
2a	cyclohexane+hexane	1.85	4.960	7.26
2b	cyclohexane	1.1	1.719	2.56
3	heptane	0.43	3.319	4.90
4	toluene	0.28	2.314	3.43
5	octane	_	_	
6	Xylene			
Fractionation of 5% Copolymer				

Total weight used in this fractionation 6.4 gms

1976), Pek Choo *et al.* (1984), Zhu *et al* (1984), Cheng (1984), Inoue *et al.* (1988), Doi(1984), Cozewith (1987), Doi *et al.* (1987) Ser van der Ven 1990, and recently by Skaare *et al.* (1992)). The use of NMR for these interpretations is undoubtedly the better, although FTIR is quicker and gives reasonable understanding when calibrated with the results obtained from NMR.

4.2 Calculation of % Ethylene content from IR

Detailed investigations on the determination of comonomer content in propylene ethylene copolymers have been performed in detail over the last three decades in the near and mid infrared regions using IR and FTIR by Corish *et al.* (1964) van Schooten *et al.* (1961), Wei (1961), Pek Choo *et al.* (1984), Bly *et al.* (1966) and recently by Skaare *et al.* (1992). For this analysis, samples of known comonomer content (determined from ^{13}C NMR) were used as standards for calibration to determine the comonomer content from FTIR.

Typical FTIR spectra for fractions obtained from the two copolymers are shown in Figs. 4.3 and 4.4. The recent work done by Skaare *et al.* on propylene ethylene copolymers in the 720-732 cm^{-1} (PE doublet) and the 900 cm^{-1} (PP) bands confirmed the reliability of using these peaks as a good reference for calibration. The same methodology is used in the present work to obtain the calibration curve. The 732-720 cm^{-1} doublet is caused by correlation splitting due to the in-phase and out-of-phase CH_2 rock in the crystalline sample. The IR scans of the fractions clearly show the steady increase in area

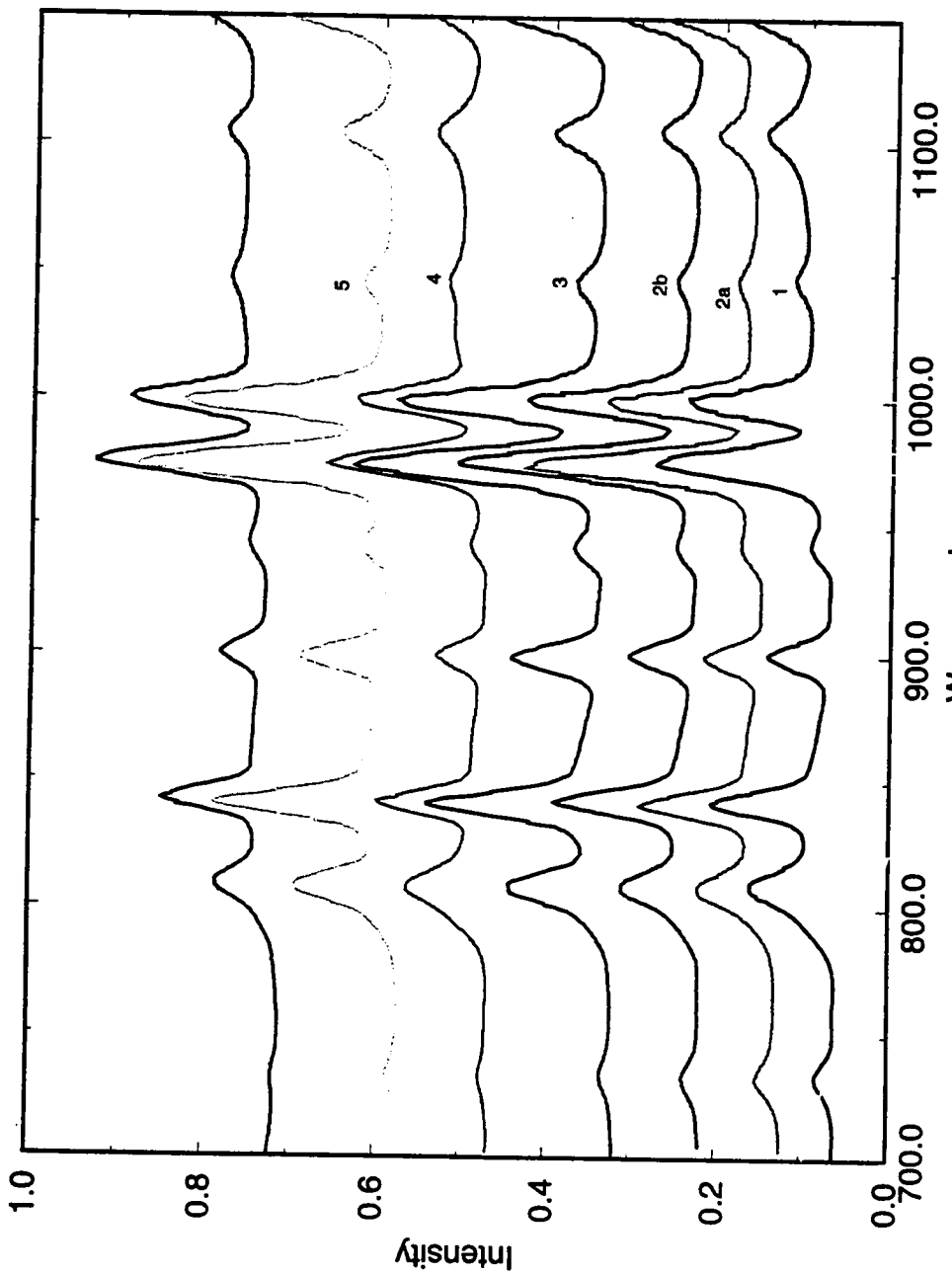


Fig. 4.3 FTIR analysis of 5% copolymer fraction.

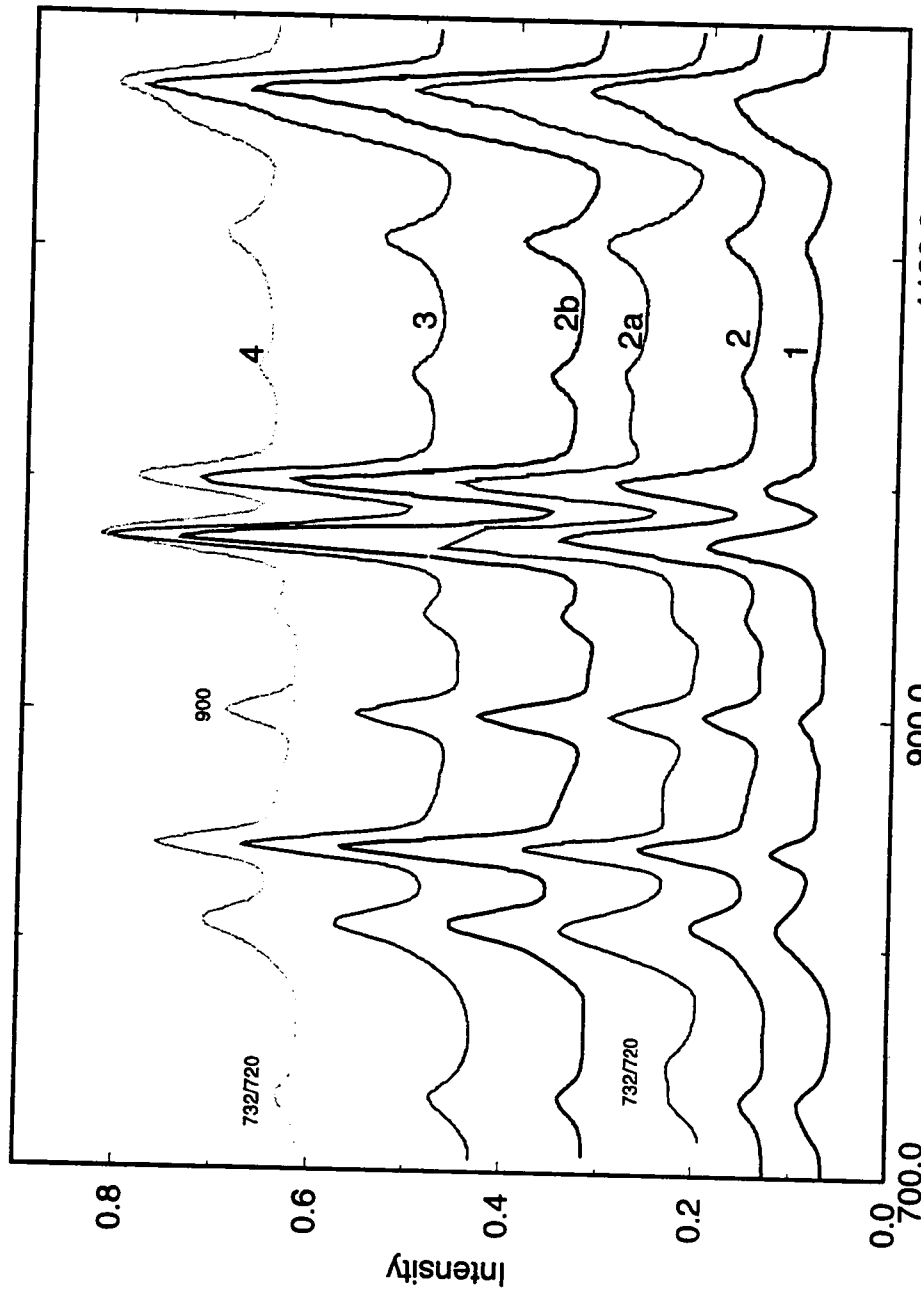
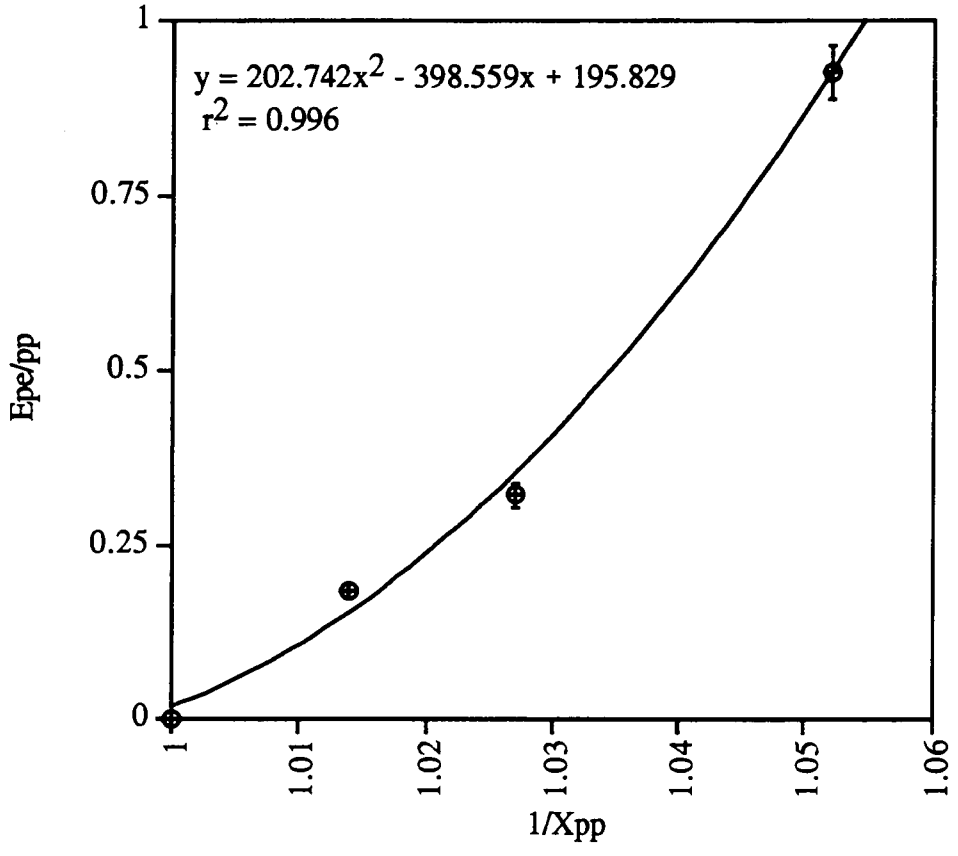


Fig. 4.4 FTIR analysis of 3% copolymer fraction.

/ intensity of the 720-732 cm^{-1} ethylene peak with respect to the 900 cm^{-1} propylene peak as the comonomer content is increased. The calibration graph (Fig. 4.5) was obtained by taking the ratio of molar absorptivities of the reference samples in (732-720 / 900 cm^{-1}) region and plotting them against the mole fraction of propylene. All the copolymer fractions were analyzed in this region to determine their comonomer content. Calibration was done by used the comonomer content data obtained from ^{13}C NMR as the reference. The distribution of comonomer content in each fraction is clearly illustrated in Fig. 4.6. The % error/deviation in determining these values are illustrated as error bars on the plots. From Fig. 4.6 it is also observed that all the fractions from both the copolymers had comonomer content ranging only from 0.5% - 10% of ethylene.

4.3 Determination of Isotacticity from NMR and FTIR

The NMR spectra of the two samples with known isotacticity index (heptane insoluble) are shown in Figs. 4.7 and 4.8. The methyl regions of the spectra are shown in Figs. 4.9 and 4.10. Chemical shift calculations were based on the internal standard of the solvent. The pentad assignments shown in Table. 4.3 (Randall 1971) are based on those proposed by Zambelli *et al.* (1975) and theoretically supported by Tonelli (1978). The pentad sequences are described in terms of combinations of m (meso [like configuration, isotactic]) and r (racemic [opposite configuration, syndiotactic]) diad. The pentad tacticity values were estimated based on the relative peak area calculations suggested by Randall, (1976). As observed from the low tacticity sample spectrum, some pentad resonances split further, this occurrence



⊕ Epe/pp= ratio of molar absorptivity

** Xpp is based on %wt fraction

Fig. 4.5 Calibration for the determination of comonomer content in propylene copolymers.

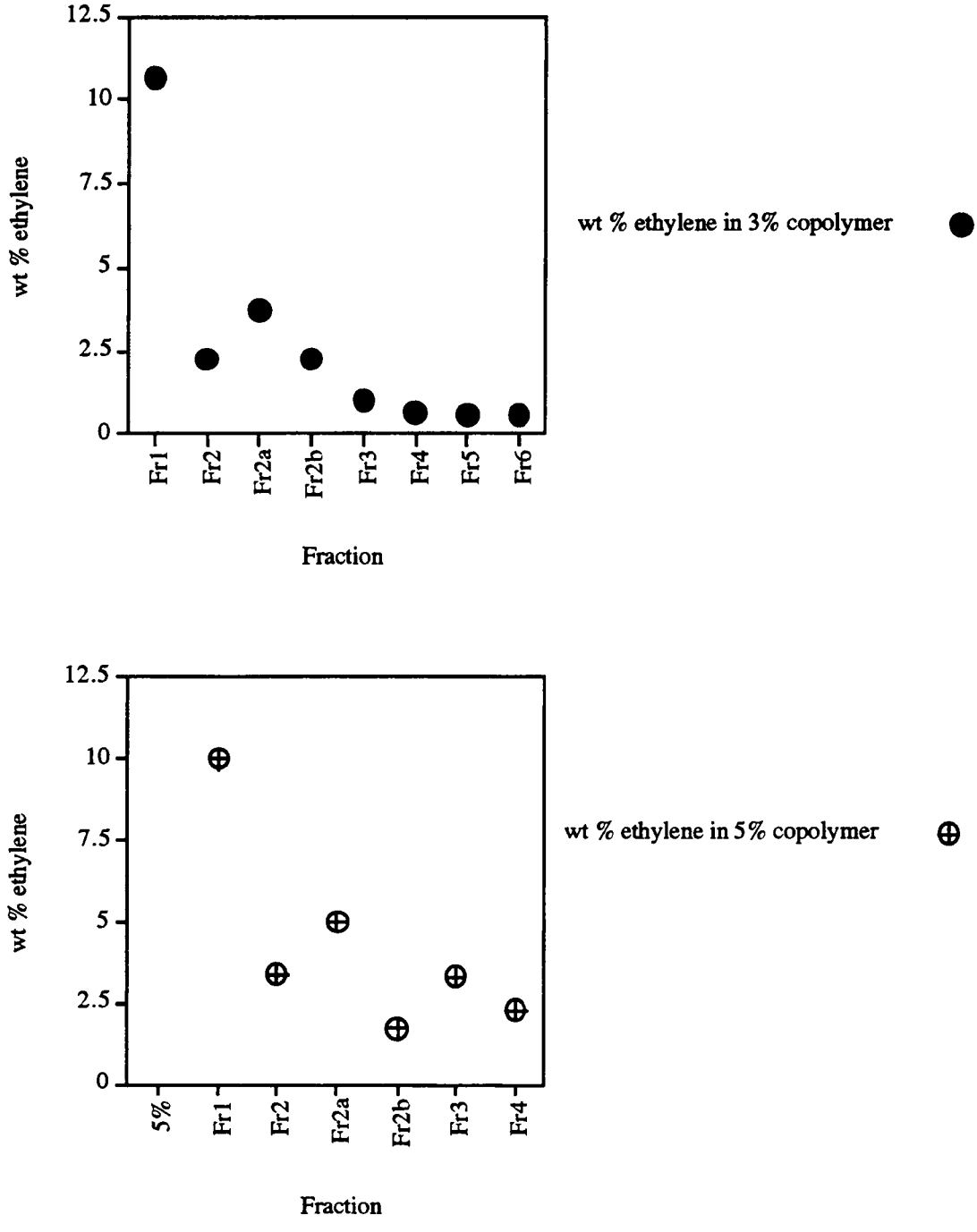


Fig.4.6 Weight % ethylene present in each fraction

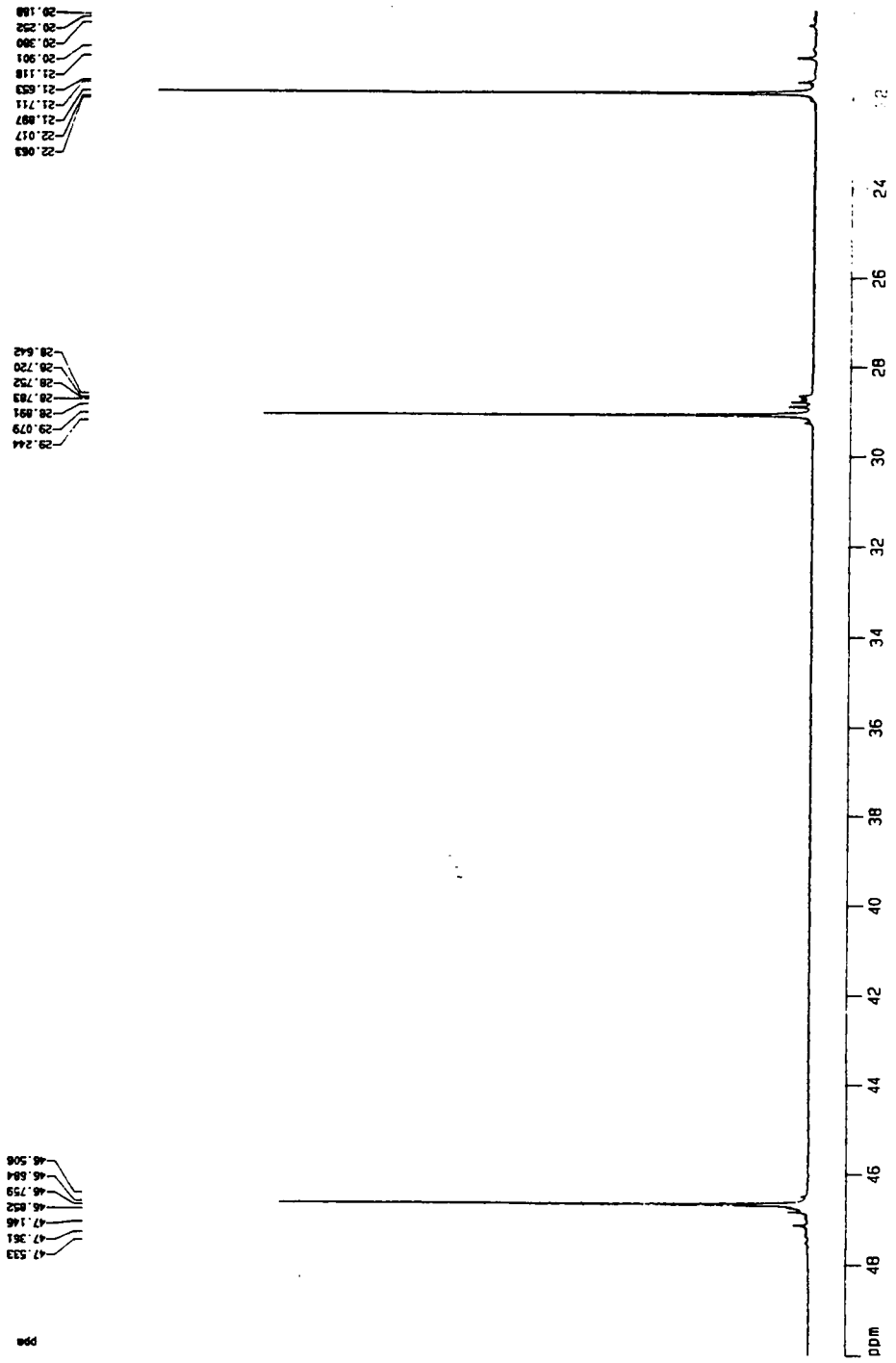


Fig. 4.7 NMR spectrum of low tacticity iPP sample with 91% heptane insoluble isotacticity.

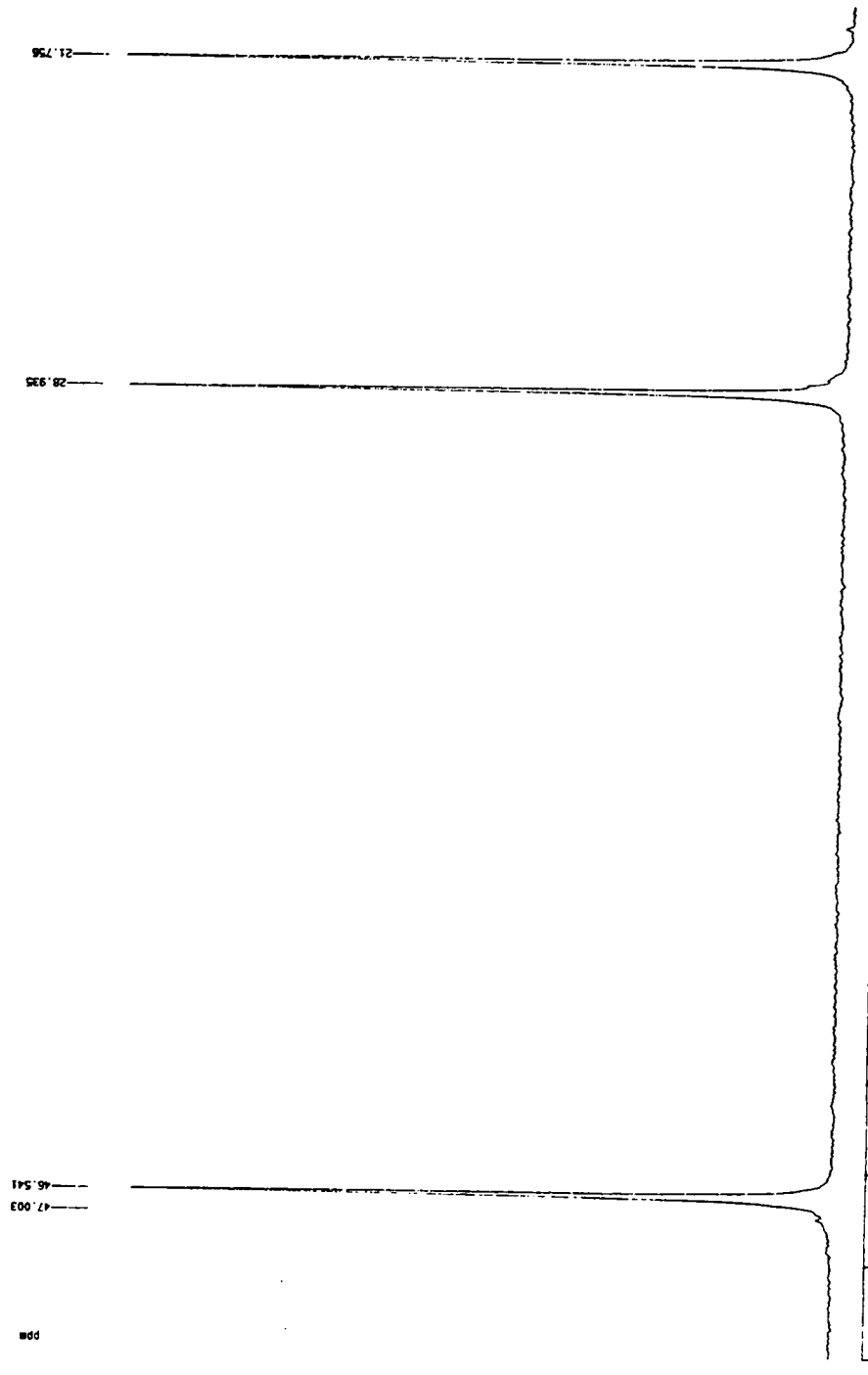


Fig. 4.8 NMR spectrum of high tacticity iPP sample with 99% heptane insoluble isotacticity

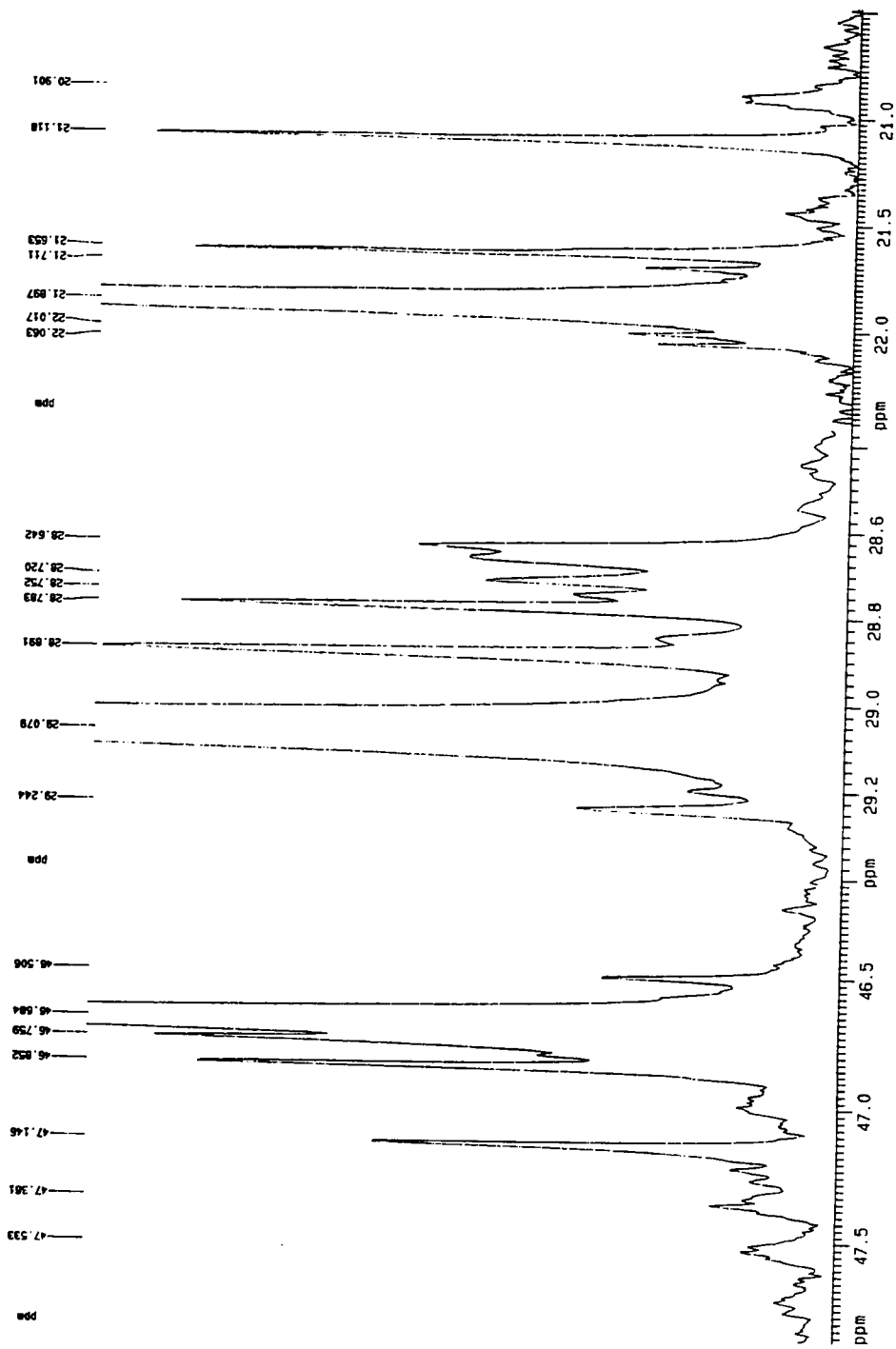


Fig. 4.9 NMR spectrum (methyl region) of low tacticity iPP sample with 91% heptane insoluble isotacticity

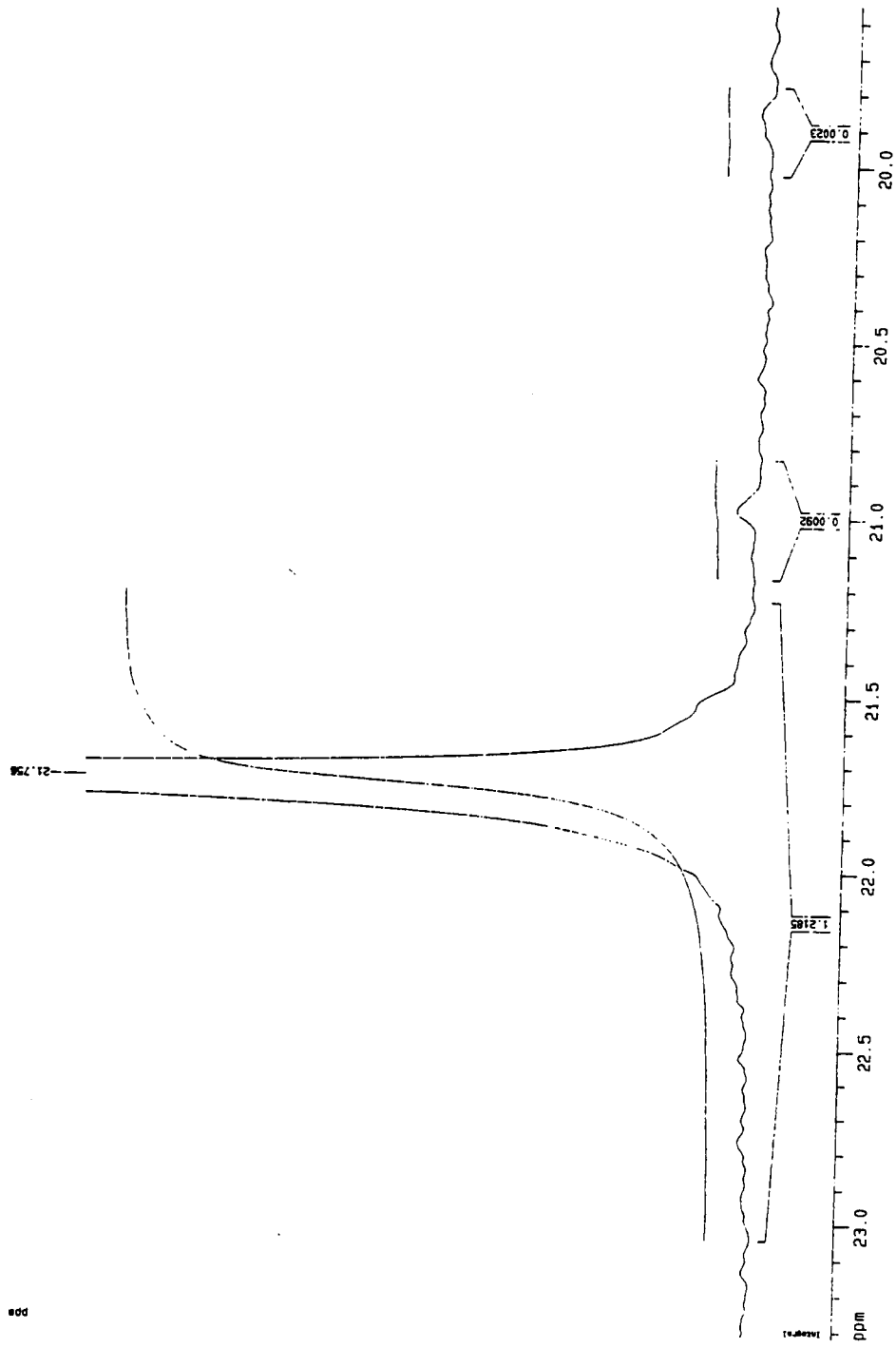
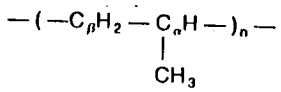


Fig. 4.10 NMR spectra (methyl region) of high tacticity iPP sample with 99% heptane insoluble isotacticity

Table 4.3 Spectral assignment for Polypropylene NMR spectrum.



δ (PPM)	Assignment	δ (PPM)	Assignment	δ (PPM)	Assignment
47.69	C_β (rmr+rrr)	28.78	C_α (rr)	20.12	CH_3 (mrrm)
47.53	C_β (rrr+rmm)	21.91	CH_3 (mmmm)		
47.39	C_β (rmm+rrr)	21.67	CH_3 (mmmr)		
47.26	C_β (rmm)	21.49	CH_3 (rmmr)		
47.03 (shoulder)	C_β (rrm+mmm)	21.14	CH_3 (mmrr+mmrm)		
46.89 (shoulder)		20.97	CH_3 (mrmm+rrmr)		
46.84		20.74	CH_3 (rmrm)		
29.23	C_α (mm)	20.44	CH_3 (rrrr)		
29.04	C_α (mr)	20.31	CH_3 (mrrr)		
28.91		20.27			

Analysis conditions

Nucleus : ^{13}C
Frequency : 88 MHz
Spectrometer : Caméca 350
Detection technique : FT – 550 pulses
Flip angle : 38° – Repetition time : 1 s
Solvent : 1,2,4-Trichlorobenzene
Temperature : 140° C
Reference : HMDS (δ = 0 PPM)
Lock : $NO_2C_6D_5$

probably being due to the presence of heptad configurations (Tonnelli *et al.* 1981). In order to account for this splitting they were estimated as the sum of pentad intensities. The presence of heterotactic material in the form of syndiotactic and other lower order conformations can be seen clearly in the low tacticity sample.

The ratio of A(998) / A(974) peak areas for the high tacticity polypropylene and low tacticity polypropylene were plotted against their known tacticities. This resulted as the calibration plot. Similar IR analysis was done for the fractions, and their tacticities were determined by fitting their absorbance ratio (A(998) / A(974)) on the calibration plot. This method has been followed, based on the extensive analysis on polypropylene fractions in the literature (Paukkeri *et al.* 1993,1994 and Burdfield and Loi 1988). The calibration of these samples based on the isotacticity values obtained from ^{13}C NMR and known heptane insoluble isotacticity index (in order to determine the tacticity of iPP quickly, the industry defines the heptane insoluble / xylene insoluble portions to be its isotactic content) are plotted to their observed absorbance ratios. This is illustrated in Fig. 4.11. The isotacticities of the fractions are given in Table 4.4, and compared with the mole and weight % ethylene in Figs. 4.12-4.13. The isotacticity showed a steady increase from the lower boiling fractions to the higher boiling fractions for the successive fractionations performed.

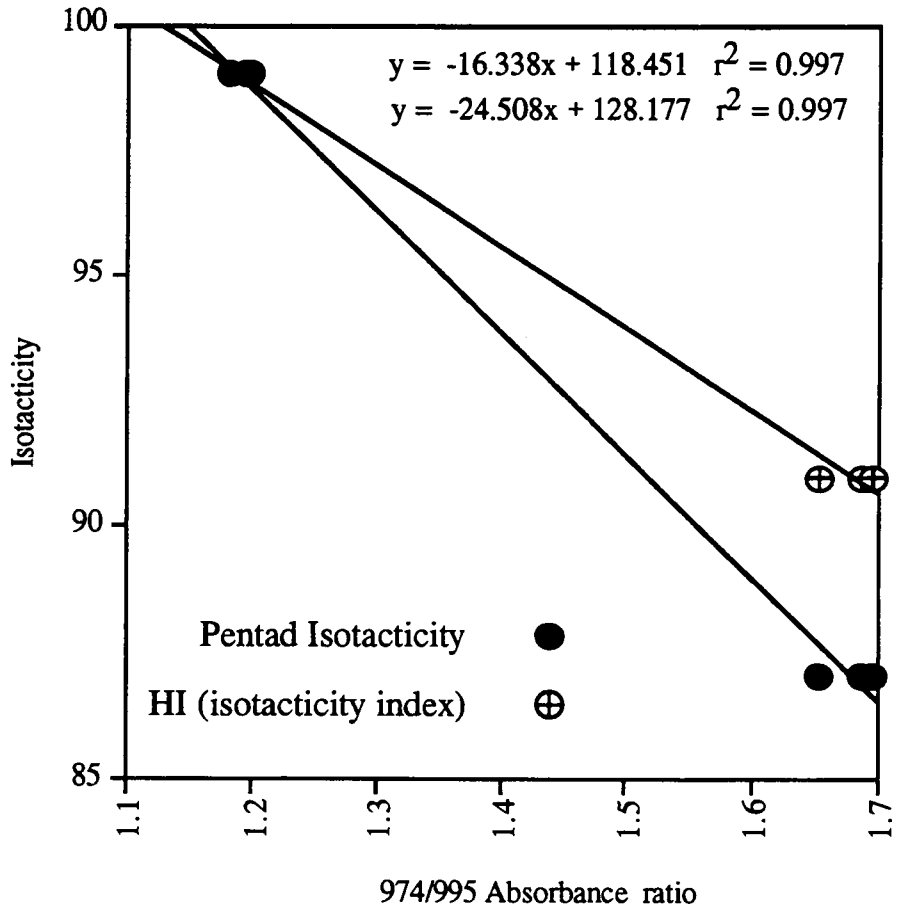


Fig. 4.11 Calibration for determining the % Isotacticity

Table4.4:- Tacticity and % Ethylene content calculated from IR and NMR

Fraction	wt % ethylene	mole %ethylene	Pentad Isotacticity	mole % chain atacticity	HI Isotacticity	% atacticity (HI)
	10	14.35	84.49	15.51	89.33	10.67
Fr2	3.4	4.98	89.34	10.66	92.56	7.44
Fr2a	5	7.26	85.32	14.68	89.88	10.12
Fr2b	1.7	2.56	89.74	10.26	92.83	7.17
Fr3	3.3	4.9	90.37	9.63	93.25	6.75
Fr4	2.3	3.43	91.91	8.09	94.27	5.73
	10.59	15.1	84.68	15.32	89.45	10.55
Fr2	2.2	3.29	89.42	10.58	92.62	7.38
Fr2a	3.7	5.39	85.88	14.12	89.92	10.08
Fr2b	2.2	3.22	89.7	10.3	92.8	7.2
Fr3	1	1.43	92.14	7.86	94.43	5.57
Fr4	0.61	0.93	94.69	5.31	96.13	3.87
Fr5	0.55	0.82	95.01	4.99	96.17	3.83
Fr6	0.51	0.76	95.29	4.71	96.53	3.47

HI = Heptane insoluble fraction (this is a method for determining the % stereoregularity, though not accurate)

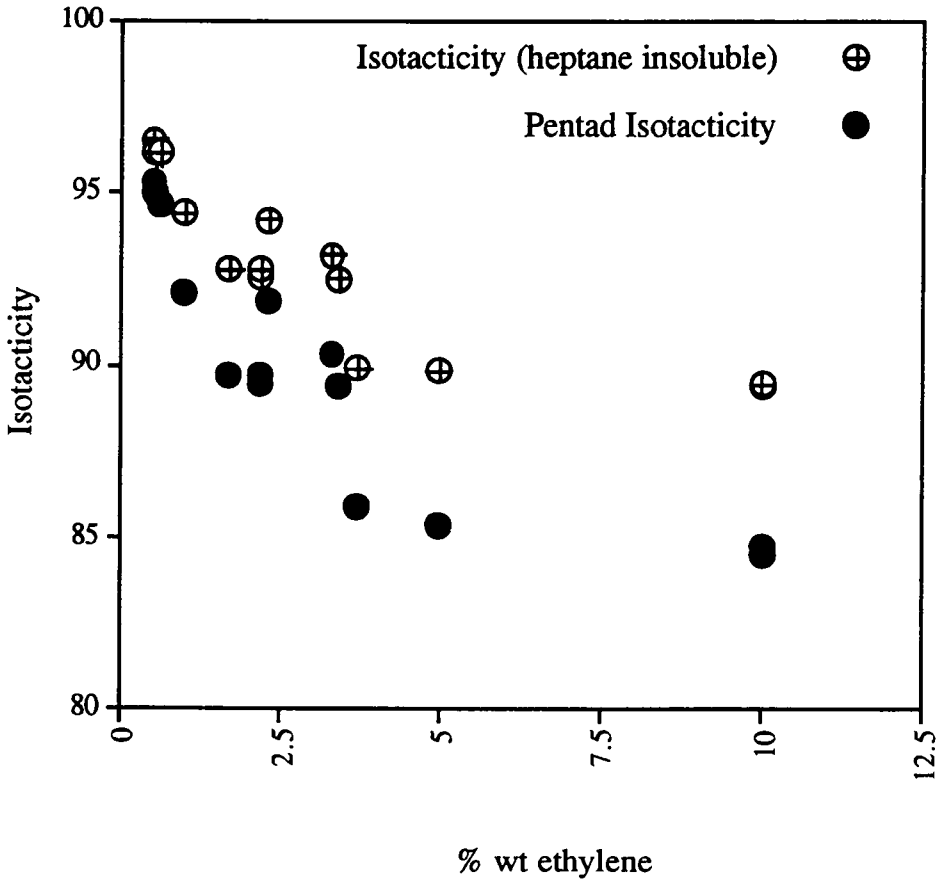


Fig 4.12 Isotacticities of fractions as a function of wt % ethylene content

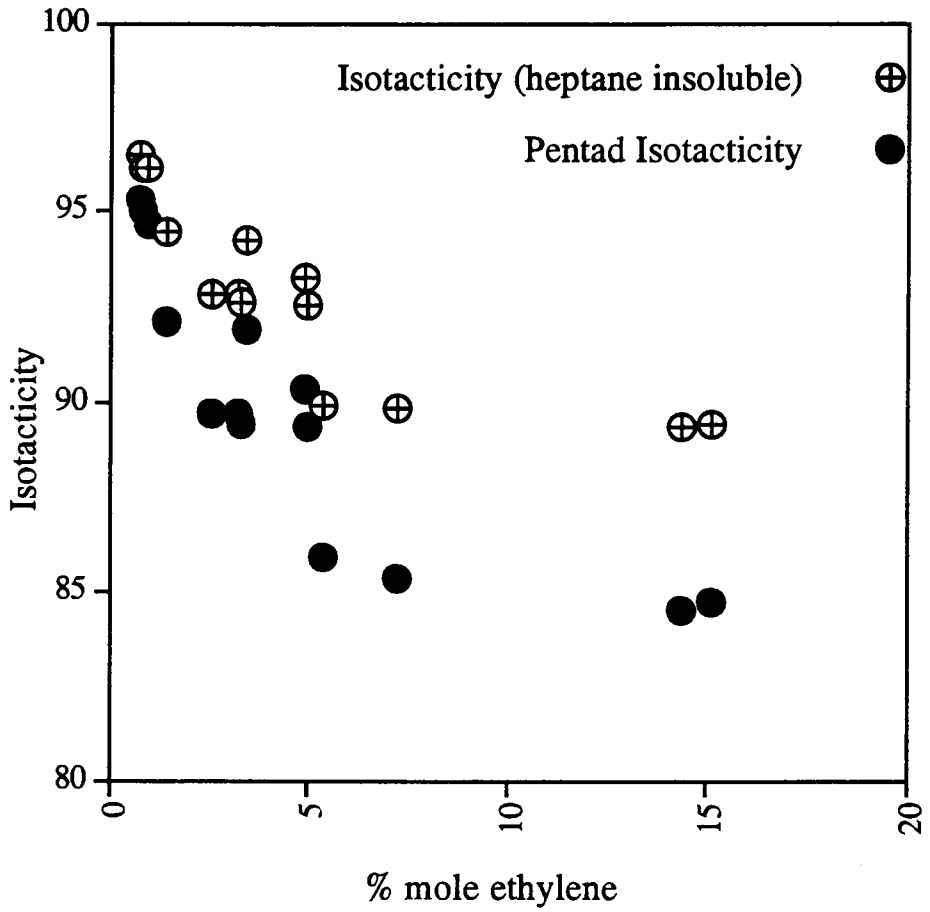


Fig. 4.13 Isotacticities of fractions as a function of mole % ethylene content.

4.4 Thermal Properties

Melting from DSC

Melting studies on the fractions were obtained from DSC. The melting of each sample was carried out at 10 °C/min. Details of the melting studies are given in Fig 4.14-4.15 and Table 4.5. The unfractionated copolymers iPP3, iPP5, xiPP3 and xiPP5 had a broad range of melting with the presence of double melting peaks. Fractionation reduced the presence of the double melting peaks, though they were still present in two of the higher melting fractions. The melting temperature of the fractions increased with the decrease of % ethylene and atacticity (Fig. 4.16) in each fraction. Extractions of the iPP3 and iPP5 in boiling xylene were done initially to remove impurities (additives). This resulted in a slight increase in the melting points for xiPP3 (extracted iPP3) and xiPP5 (extracted iPP5) by 1-2 °C which may be due to the removal of some atactic / low molecular weight material. The identification of the residues caused by xylene extraction has been briefly discussed by Williams (1995).

Crystallization from DSC

Crystallization of the fractions and unfractionated copolymers was performed by melting them completely and cooling them at a rate of 10°. C/min. The data on crystallization and their scans are shown in Figs. 4.17-4.19 and Tables 4.5. There was a steady increase in the crystallization temperature of the fractions with decrease in ethylene and atacticity content

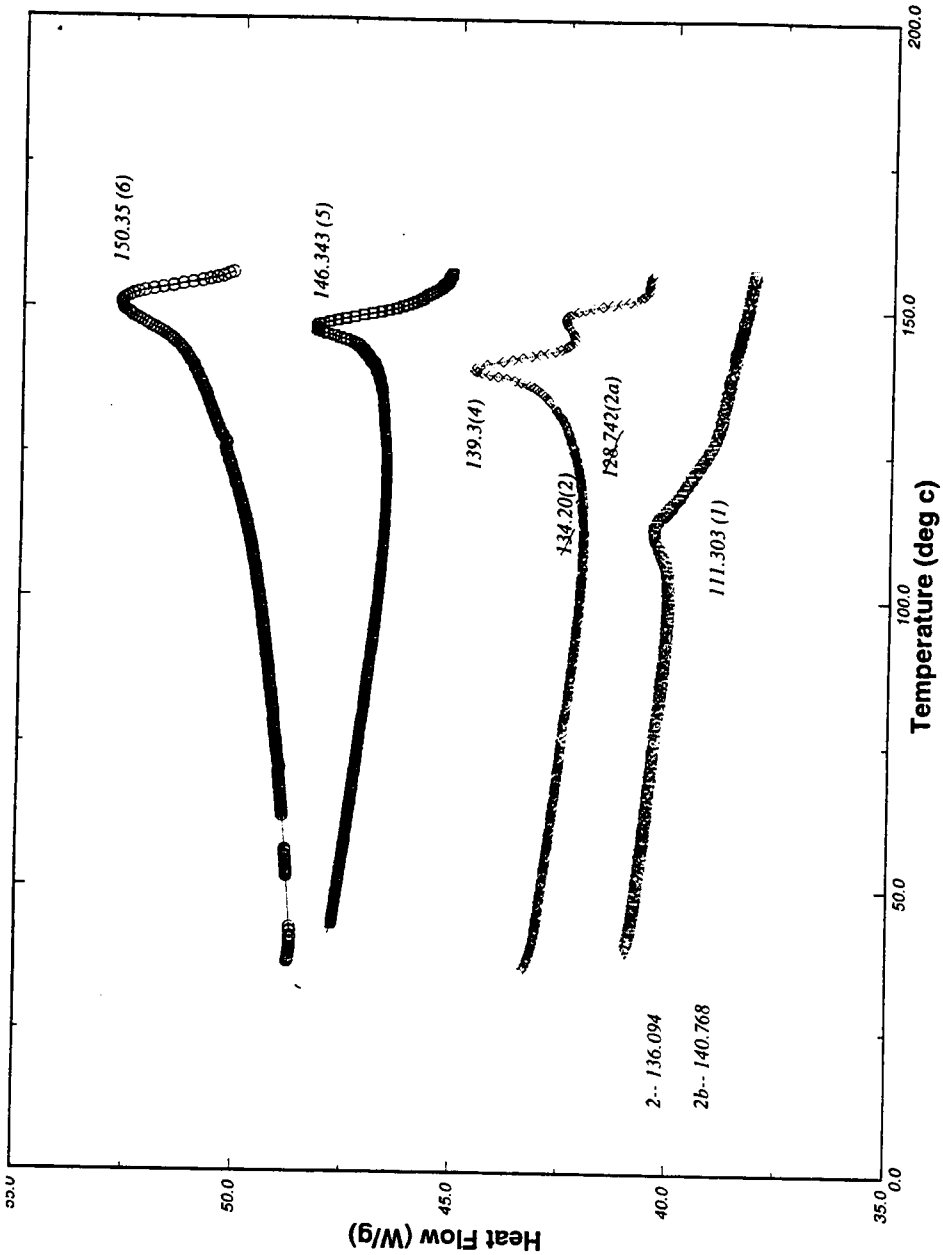


Fig. 4.14 DSC melting scans for the 3% copolymer fractions when melted dynamically at 10°/min

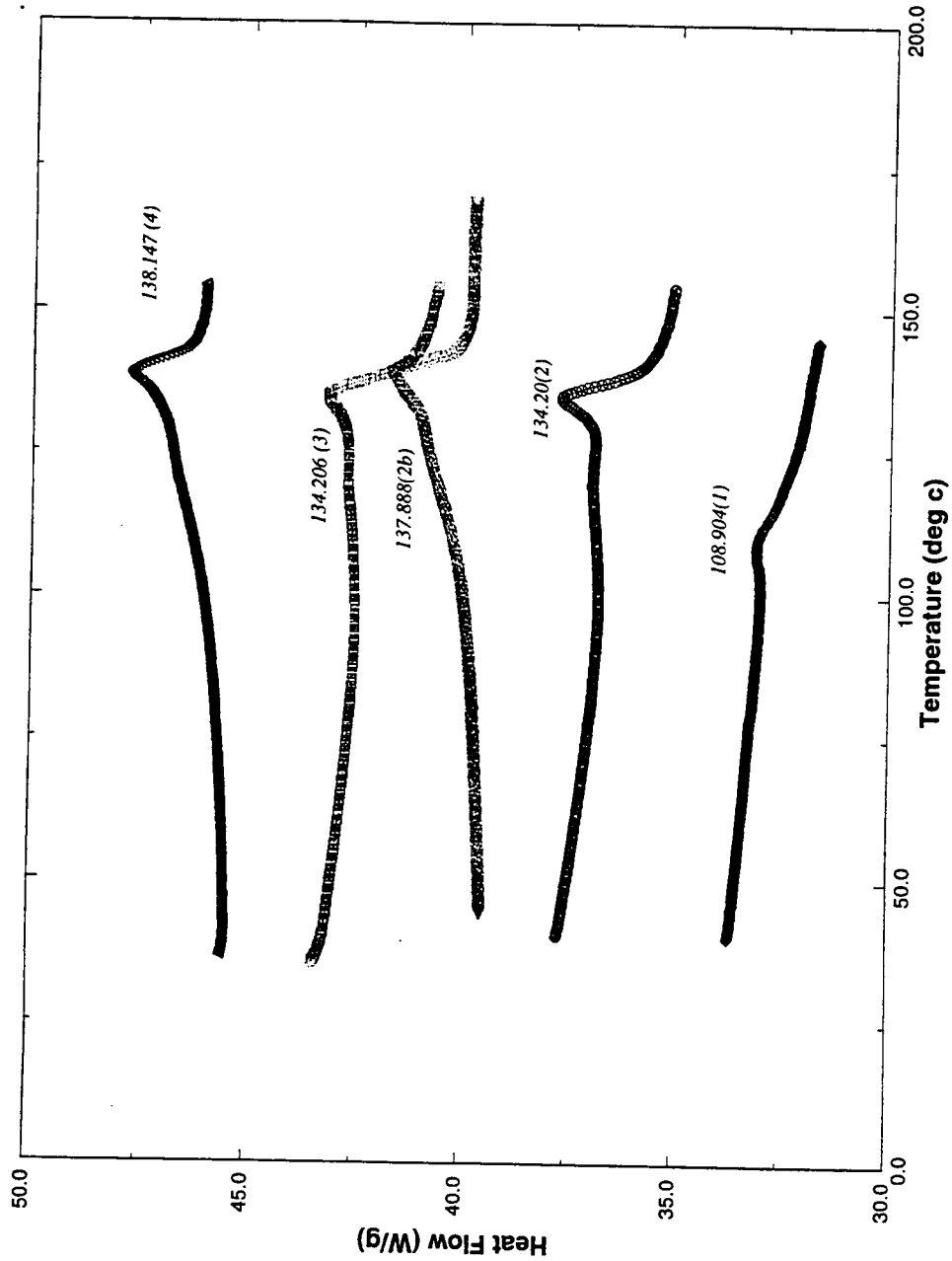


Fig. 4.15 DSC melting scans for the 5% copolymer fractions when melted dynamically at 10°/min

Table4.5 Melting and Crystallization data from DSC

Fraction	wt % ethylene	mole %ethylene	Pentad Isotacticity	mole % atacticity	Tm From DSC	Tc from DSC
					degC	degC
Fr1(5%)	10.00	14.35	84.49	15.51	108.90	70.72
Fr2	3.40	4.98	89.34	10.66	134.20	96.68
Fr2a	5.00	7.26	85.32	14.68	129.94	93.10
Fr2b	1.70	2.56	89.74	10.26	137.89	101.93
Fr3	3.30	4.90	90.37	9.63	134.21	97.93
Fr4	2.30	3.43	91.91	8.09	138.15	98.24
Fr1(3%)	10.59	15.10	84.68	15.32	111.30	72.84
Fr2	2.20	3.29	89.42	10.58	136.09	97.57
Fr2a	3.70	5.39	85.88	14.12	128.74	93.03
Fr2b	2.20	3.22	89.70	10.30	140.77	99.09
Fr3	1.00	1.43	92.14	7.86	139.8/144.8	103.65
Fr4	0.61	0.93	94.69	5.31	139.3/146.1	102.57
Fr5	0.55	0.82	95.01	4.99	146.34	107.13
Fr6	0.51	0.76	95.29	4.71	150.35	107.20

(Fig 4.17). The fractions from the lowest boiling solvent showed crystallization in the 70-72 °C range. All the other fractions showed a range of 90-105 °C. The crystallization peaks observed in these fractions were sharper compared to the melting peaks of the copolymer fractions.

Glass Transition

The DSC exotherms of the copolymers generated are illustrated in Figs. 4.20-4.23. The unfractionated copolymers iPP3 and iPP5 showed transitions at -6 °C and -9 °C while the fractions showed lower glass transitions. All the samples showed a broad transition between -25 °C and 25 °C. The glass transition temperature of the fractions in Table 4.6 are based on measuring the mid point of the transition range. When these transition temperature are plotted against % ethylene, (Fig. 4.24) the zero extrapolation gives a T_g of -11.8 for PP which is comparable to the values reported for polypropylene in literature (Campbell 1991). It is clearly seen that there is a presence of multiple transitions in the fractions compared to the unfractionated material. In the case of the fractionated material the appearance of multiple peaks may be evidence that there is segregation taking place between the phases.

4.5 X-ray Diffraction Studies

WAXD studies of the fractions and the unfractionated copolymers were used for detecting the α / γ ratio in these copolymers. Each of these fractions was crystallized at various isothermal temperatures, one set being

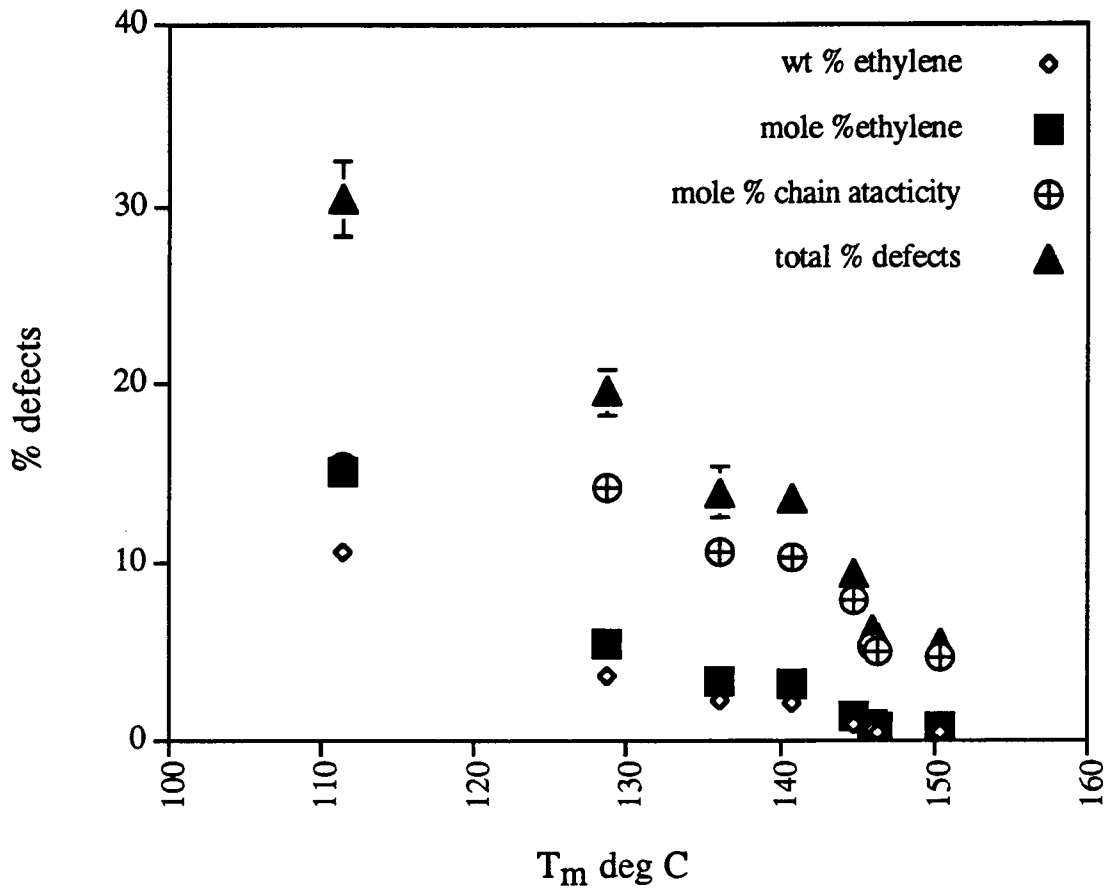


Fig. 4.16 Depression in melting of fractions with increase in defects.

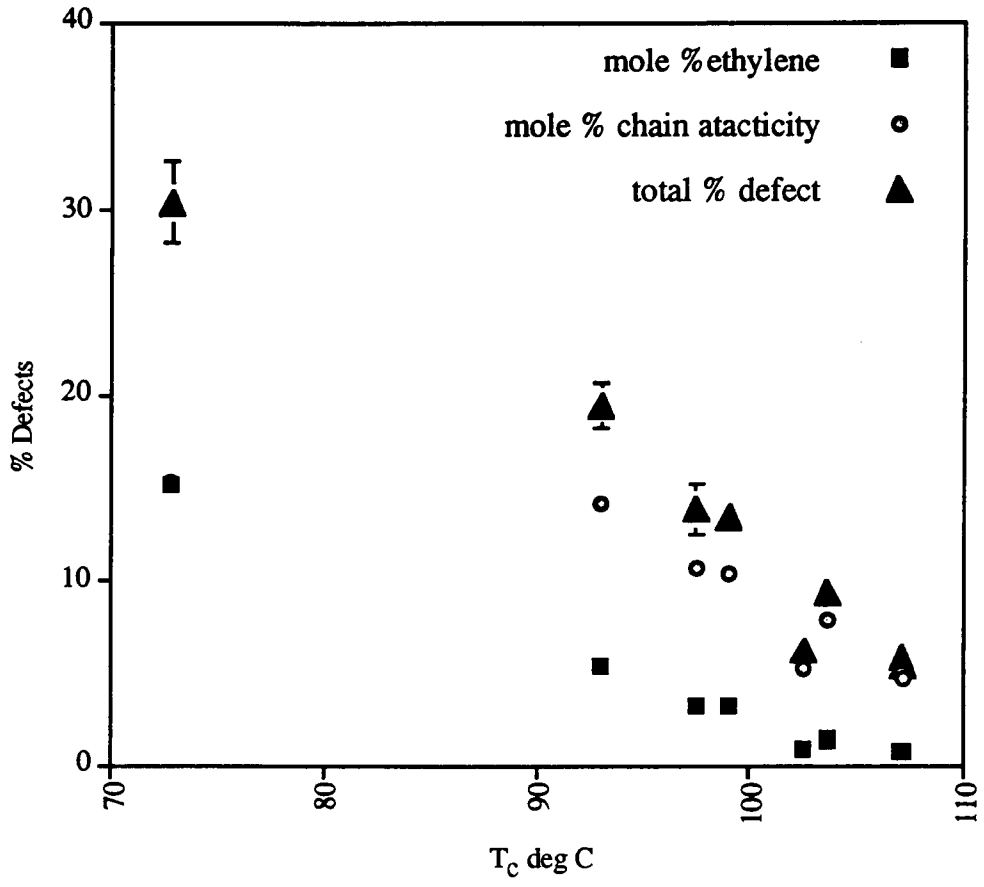


Fig. 4.17 The effect of defects on the crystallizability of the fractions.

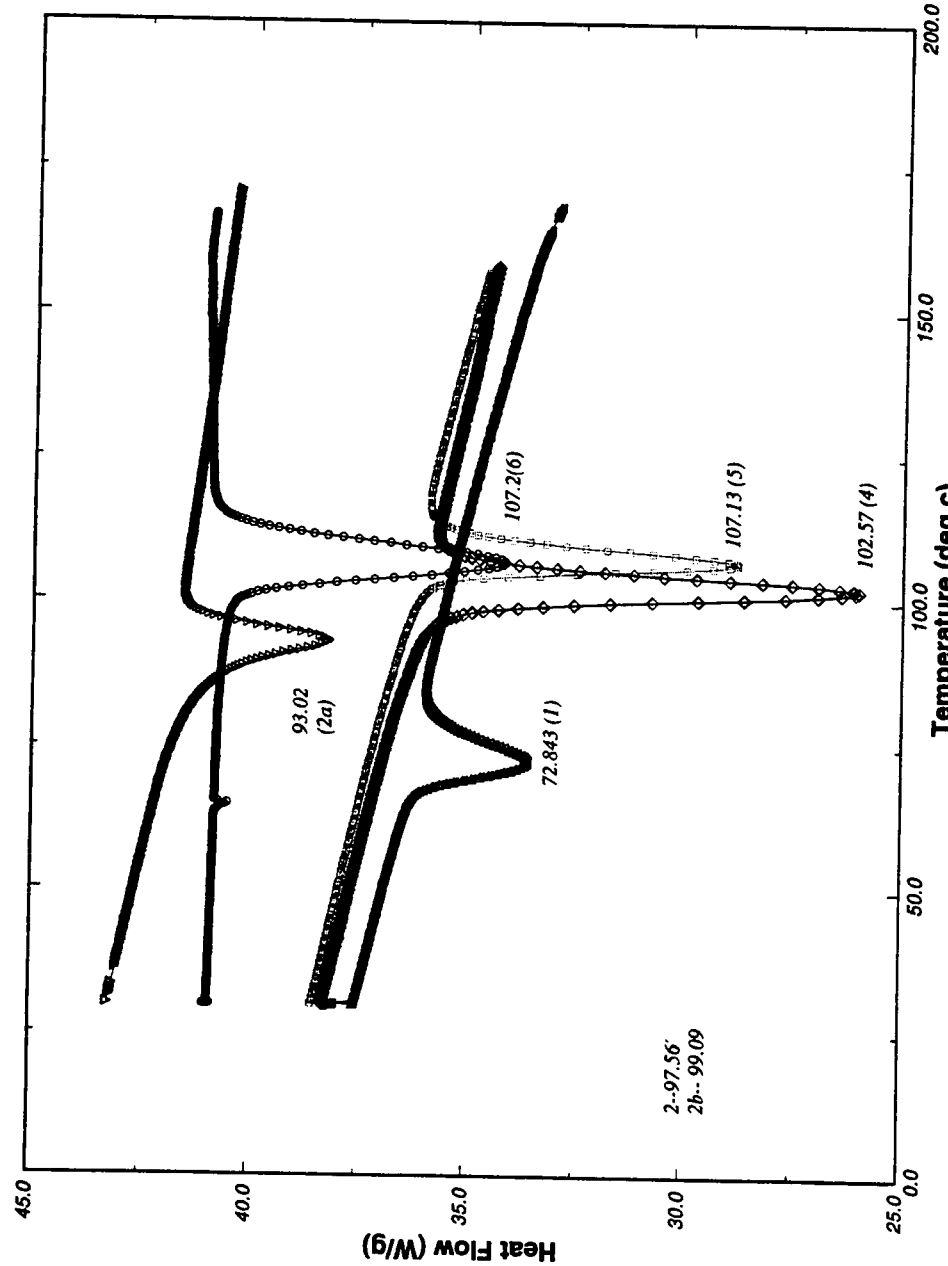


Fig. 4.18 DSC crystallization curves for the 3% copolymer fractions when cooled dynamically at 10°/min

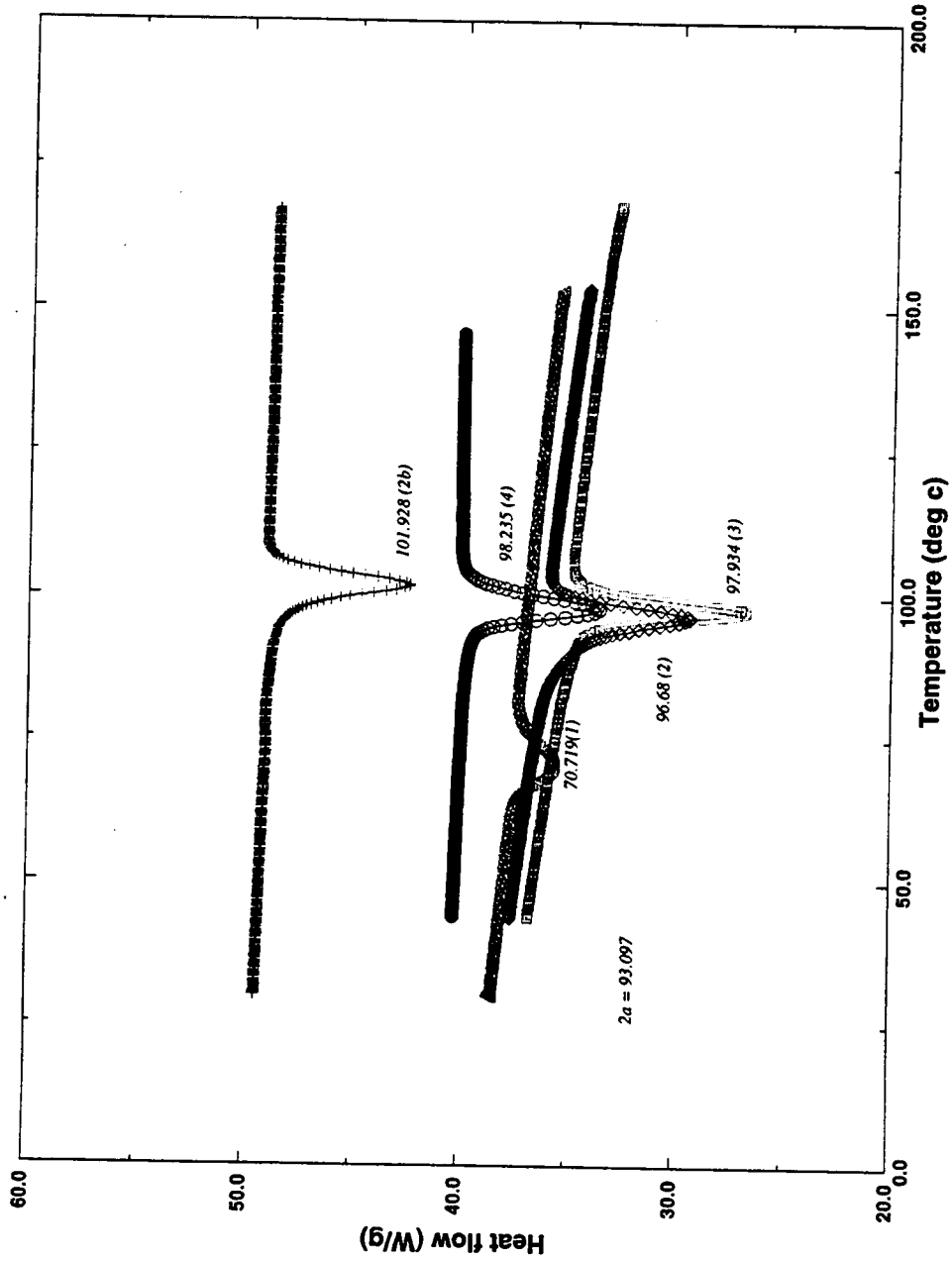


Fig. 4.19 DSC crystallization scans for the 5% copolymer fractions when cooled dynamically at 10°/min

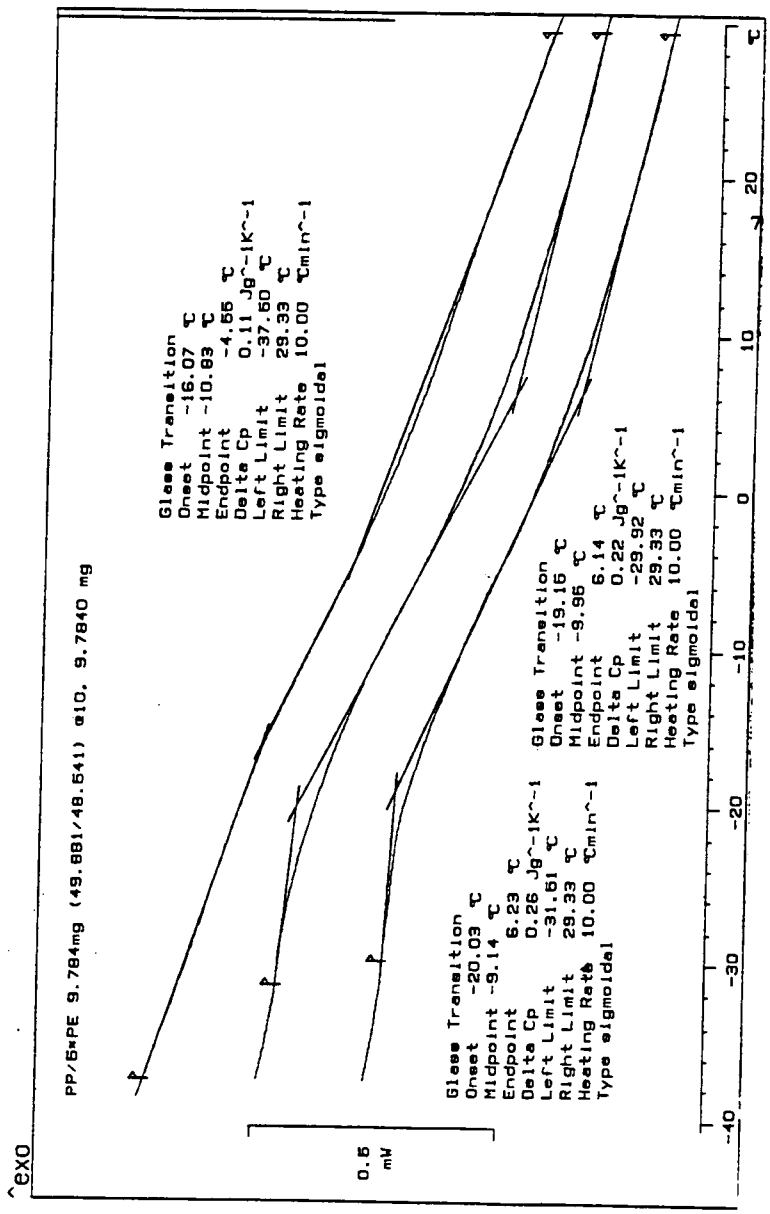


Fig 4.20 DSC exotherms for glass transition determination of the unfractionated 5% sample at a heating rate of 10°/min.

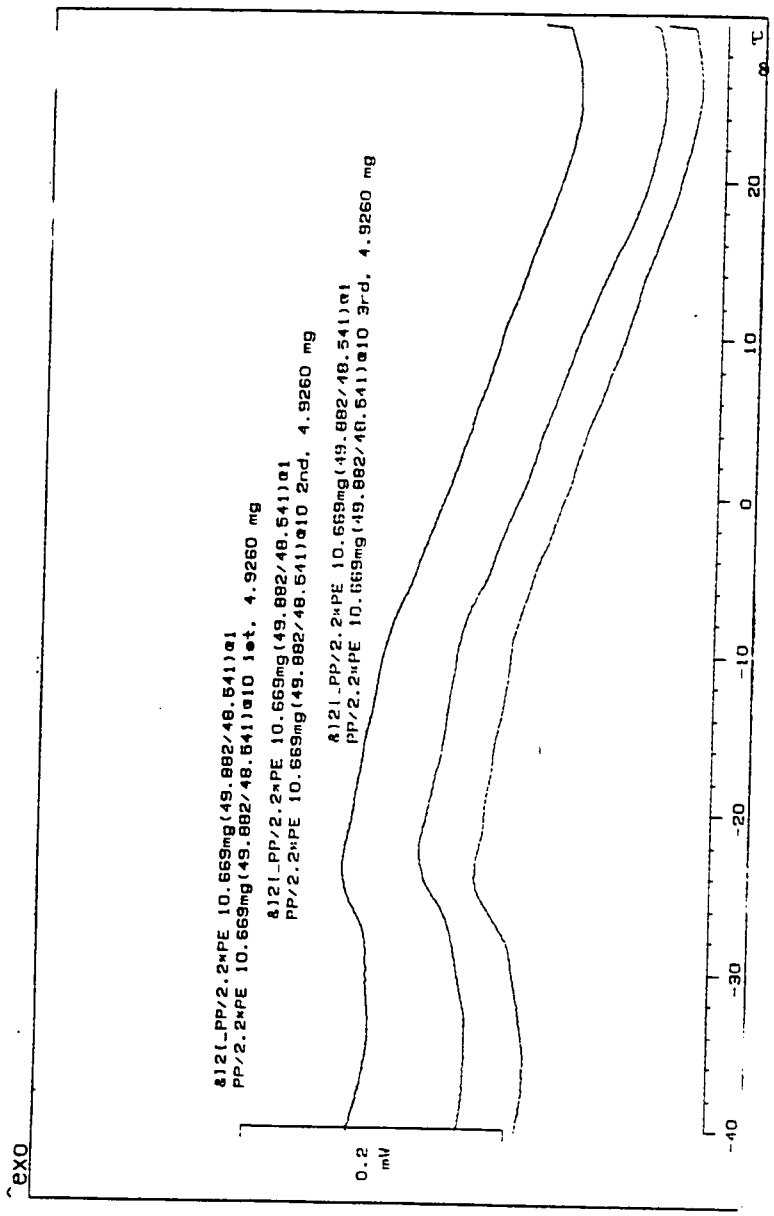


Fig 4.21 DSC exotherms for glass transition determination of the 2.2% fraction sample at a heating rate of 10°/min

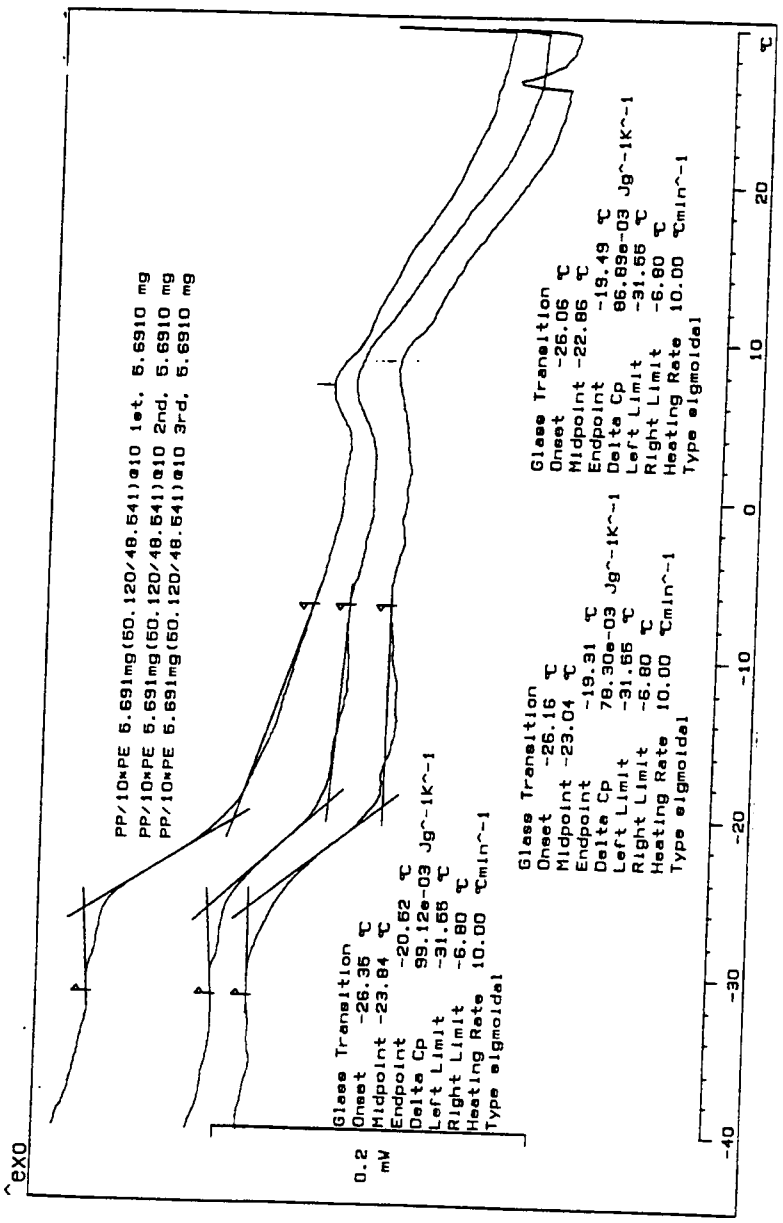


Fig 4.22 DSC exotherms for glass transition determination of the 3.7% fraction sample at a heating rate of 10°/min

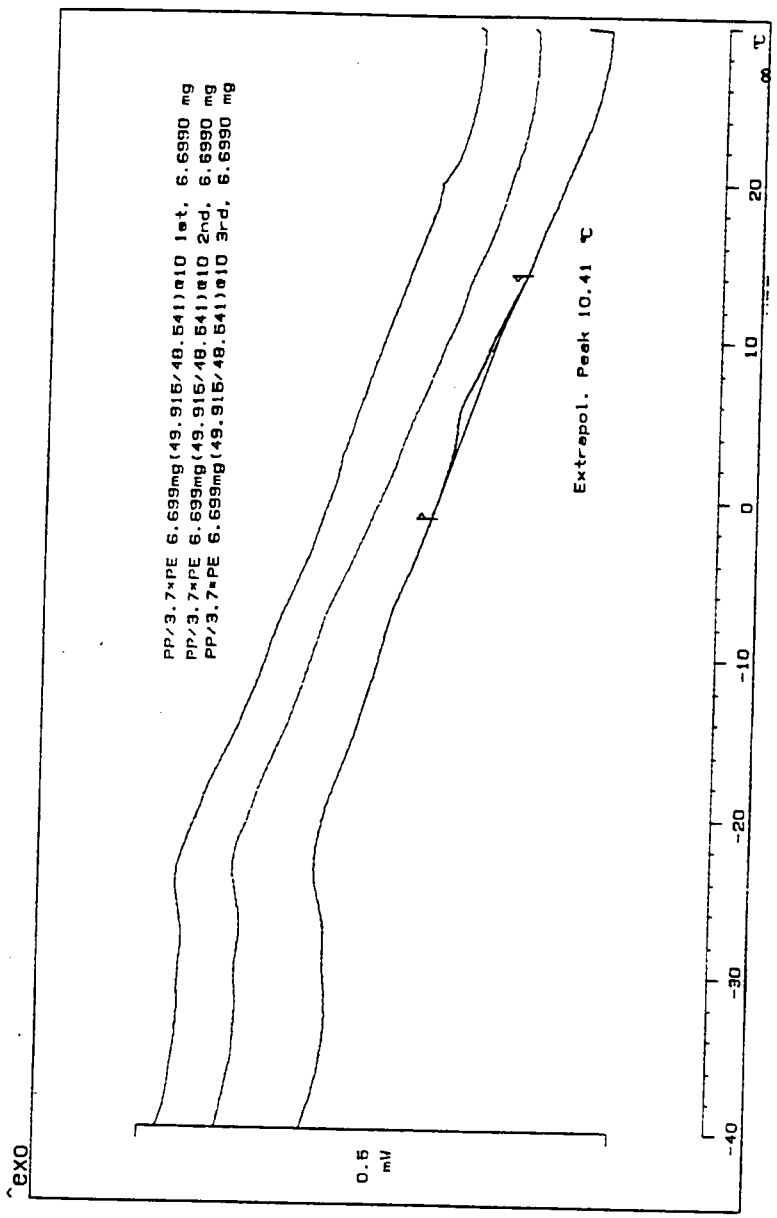


Fig 4.23 DSC exotherms for glass transition determination the 10% fraction sample at a heating rate of 10°/min

Table 4.6 Glass Tansition determined from DSC for the copolymer fractions

Glass transitions from DSC		
wt % ethylene	mole % ethylene	Tg
u3%	4.43	-6.00
u5%	7.32	-9.60
2.20	3.22	-14.00
3.70	5.39	-16.00
5.00	7.26	-17.30
10.00	14.35	-23.00

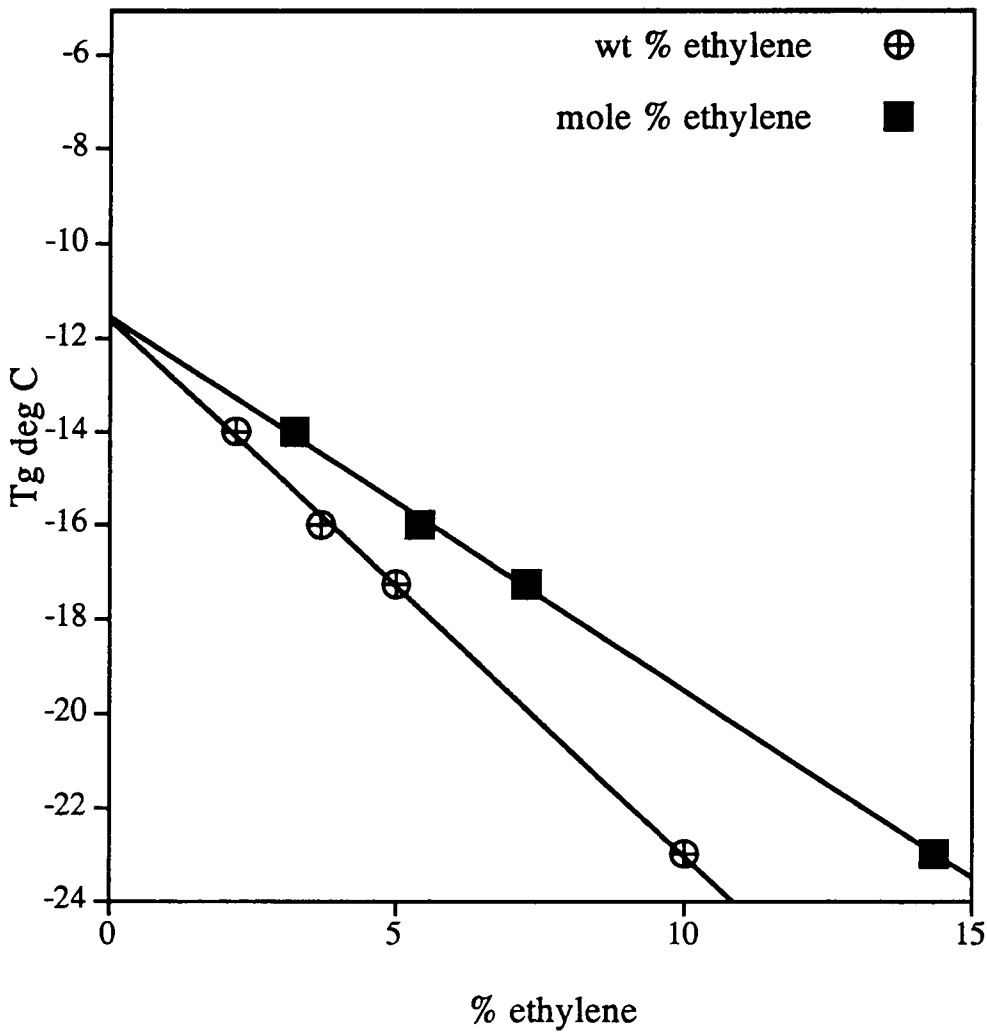


Fig. 4.24 Comonomer content Vs. T_g for various fractions

crystallized at 10 °./ min. The presence or the absence of distinctive α (18 - 19°) and γ (19.2-20.5°) peaks in these regions confirm the existence of these phases.The amount of γ phase present represented as an index for each fraction is illustrated in Table 4.7. Diffraction scans of these copolymers at the three different supercoolings studied are shown in Figs. 4.25 - 4.27. It can be observed that the γ content decreases with increasing boiling fraction at a particular supercooling, which implies that the presence of γ content in this copolymer is a function of the comonomer content as plotted in Fig 4.28. Apart from this each copolymer fraction was also studied as a function of supercooling. This is illustrated in Figs 4.29-4.34. From this analysis, it can be seen that the % gamma is not only a function of the comonomer and atacticity content but is also a function of supercooling. All the samples studied here were crystallized completely in the hot stage and left for enough time to equilibrate. This was possible for most of the samples except for the 5% and 10% copolymer fractions which did not crystallize completely at 100 and 110 °C. These samples were removed after 25-35 days since they started degrading in their thinner sections. There is a clear change in morphology from the 1% copolymer fraction to the 10% fraction.

4.6 Copolymer Morphology

The observed morphology of the copolymer fractions was strongly dependent on the comonomer content. Since the copolymers had a high nucleation density, they were not suitable for studies of the growth kinetics. Extraction of these propylene copolymers solved the problem by reducing the nucleation density. The morphology of various fractions and the two

Table 4.7 Gamma content represented as an index, at different supercoolings.for the fractions

% Gamma phase in the Fractions						
wt % ethylene	u5%	u3%	2.20	3.70	5.00	10.00
mole % ethylene			3.29	5.39	7.26	14.35
10 deg C	26.95	6.24	68.72	42.01	66.08	70.59
90 deg C	23.39	21.56	58.52	29.12	60.24	82.49
100 deg C	57.26	43.59	83.24	43.41	82.72	91.49
110 (stabilized) deg C	64.83	51.12	87.49	62.89	88.69	84.63
110 (quenched) deg C	46.62	39.48	77.35	58.11	76.68	80.52

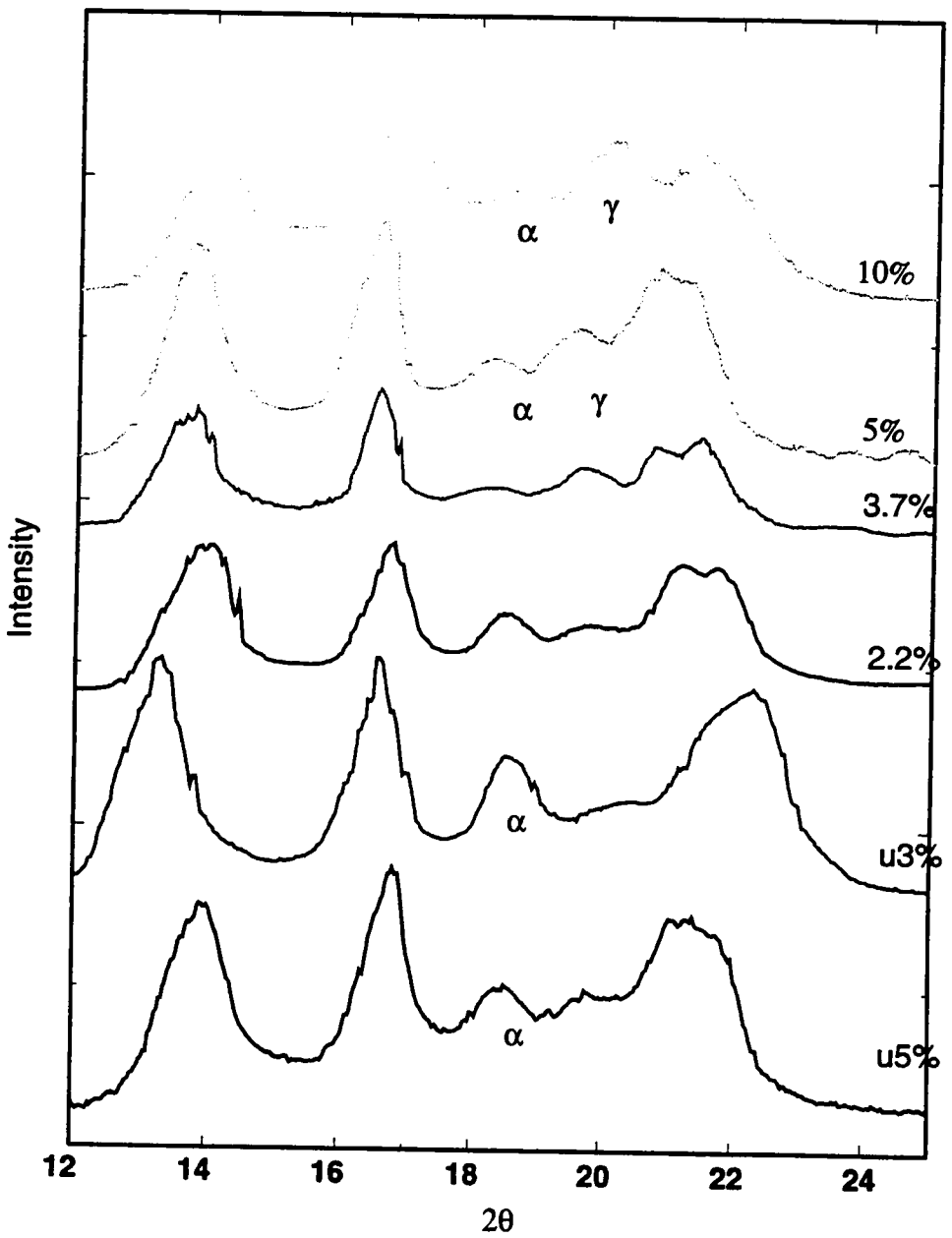


Fig.4.25 WAXD studies of Propylene copolymer fractions crystallized at 90°C isothermally in a hot stage.

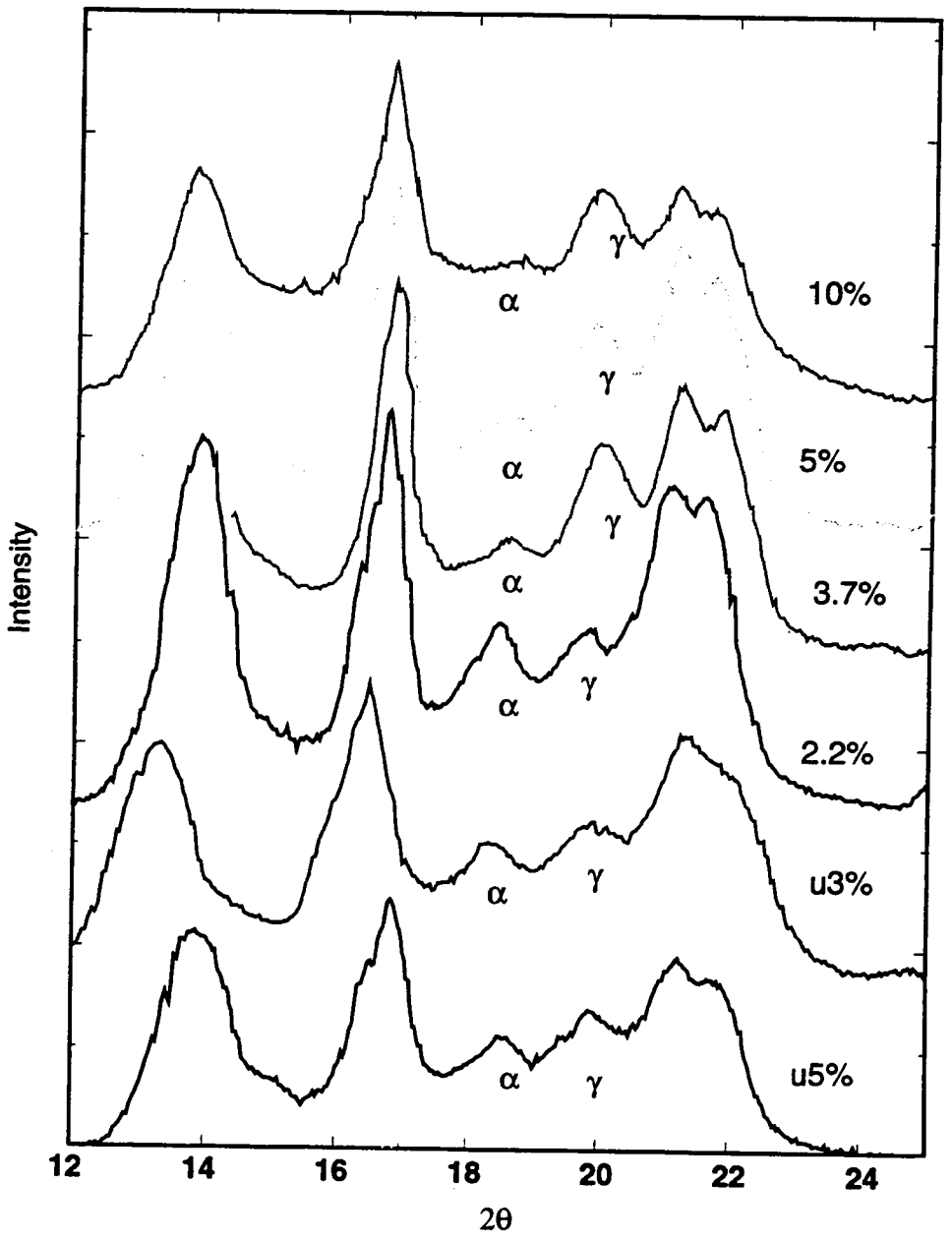


Fig. 4.26 WAXD studies of Propylene copolymer fractions crystallized at 100°C isothermally in a hot stage

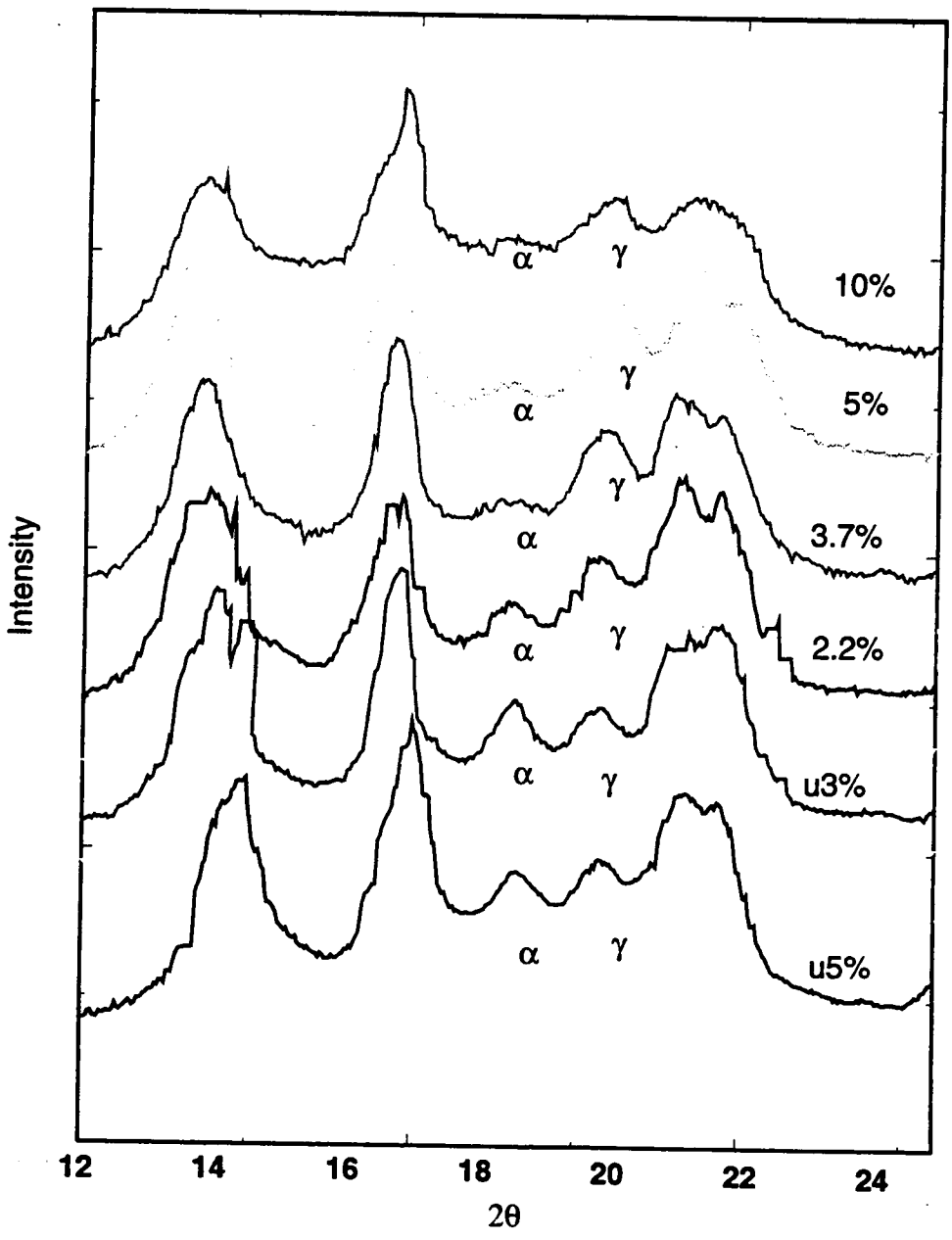


Fig. 4.27 WAXD studies of Propylene copolymer fractions crystallized at 110°C isothermally in a hot stage

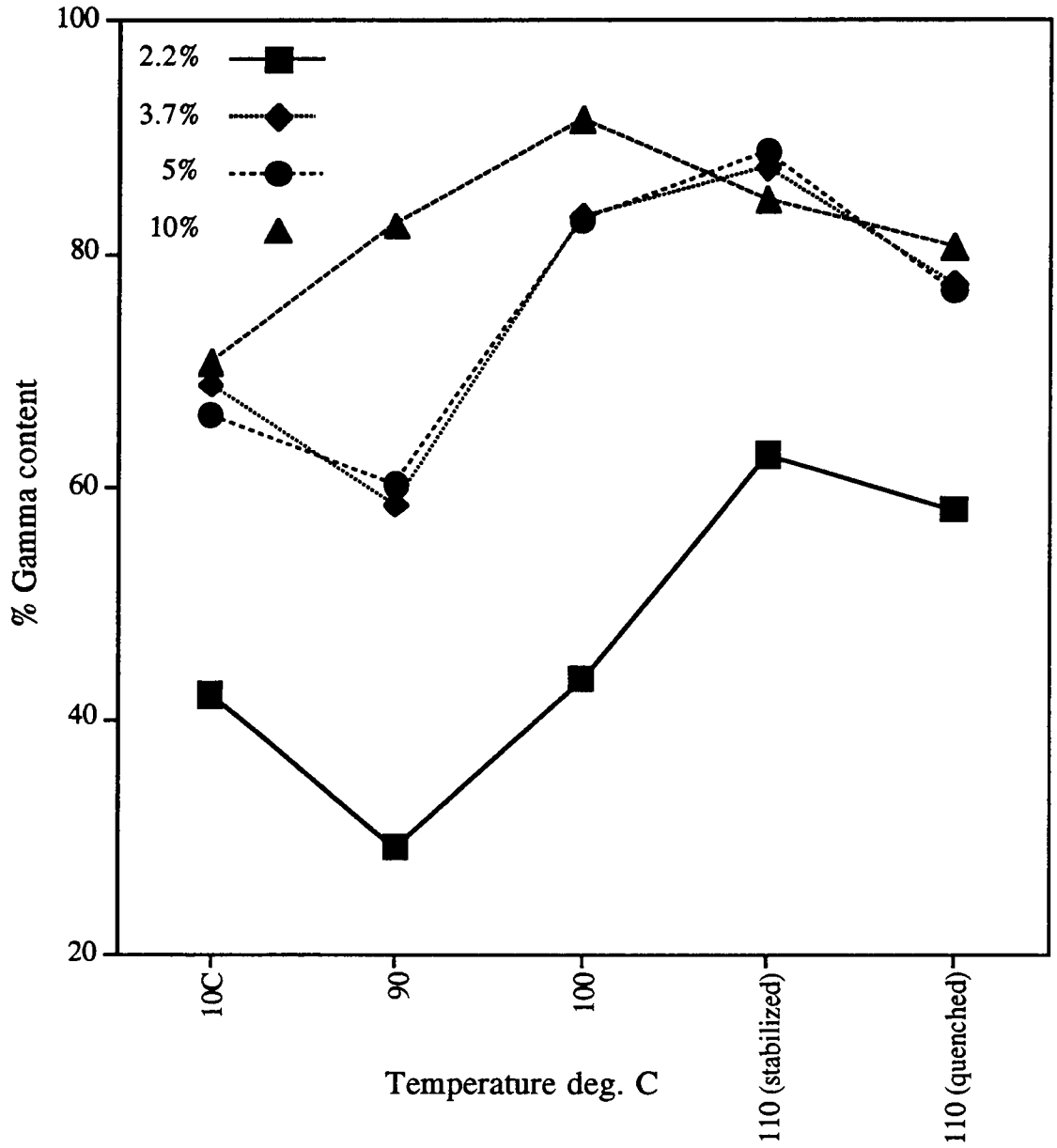


Fig. 4.28 Plots to show the increase in gamma content with change in supercooling and comonomer content. (note: the 10% comonomer containing fractions did not crystallize completely.)

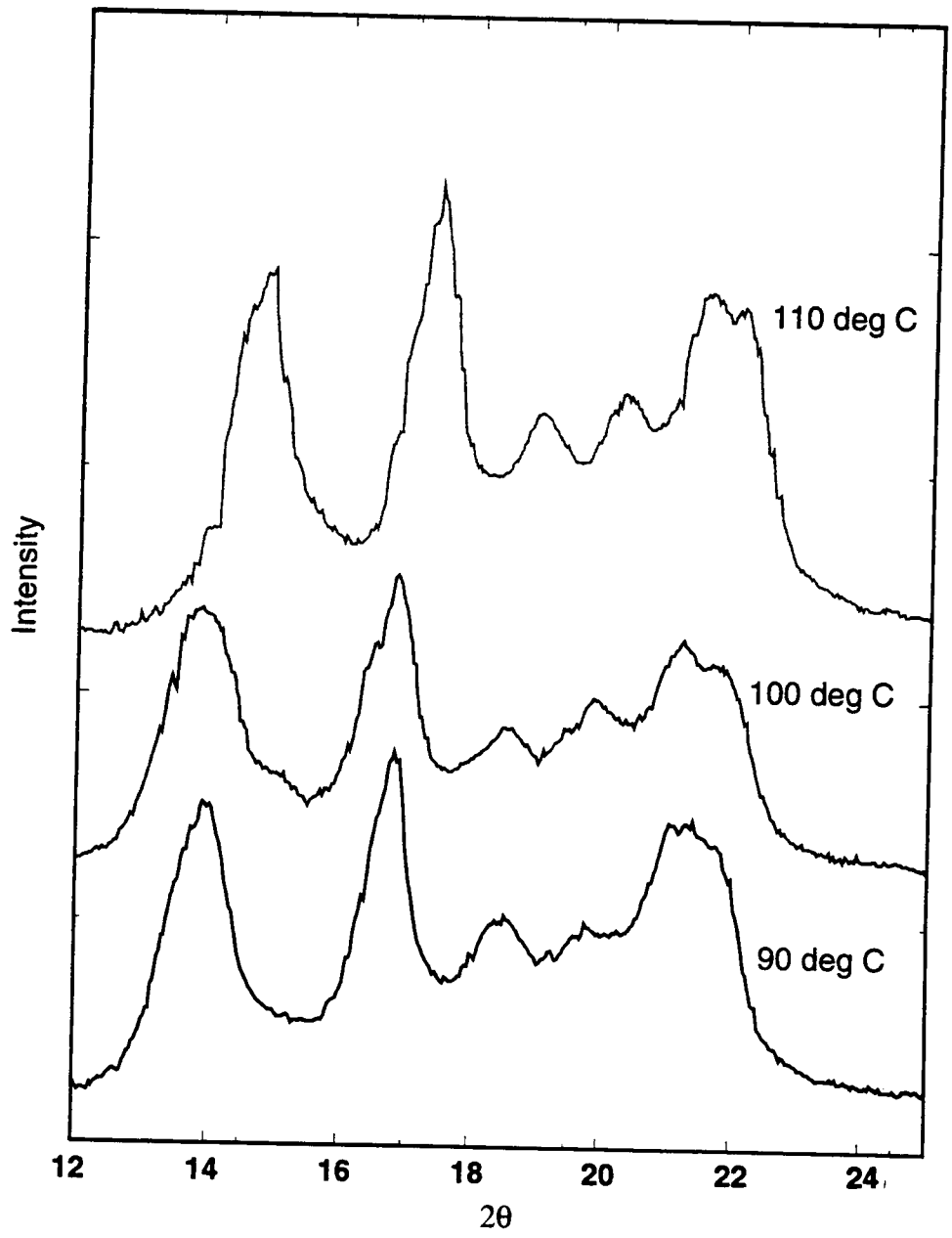


Fig. 4.29 WAXD studies of unfractionated 5% Propylene copolymer crystallized at various isothermal temperatures.

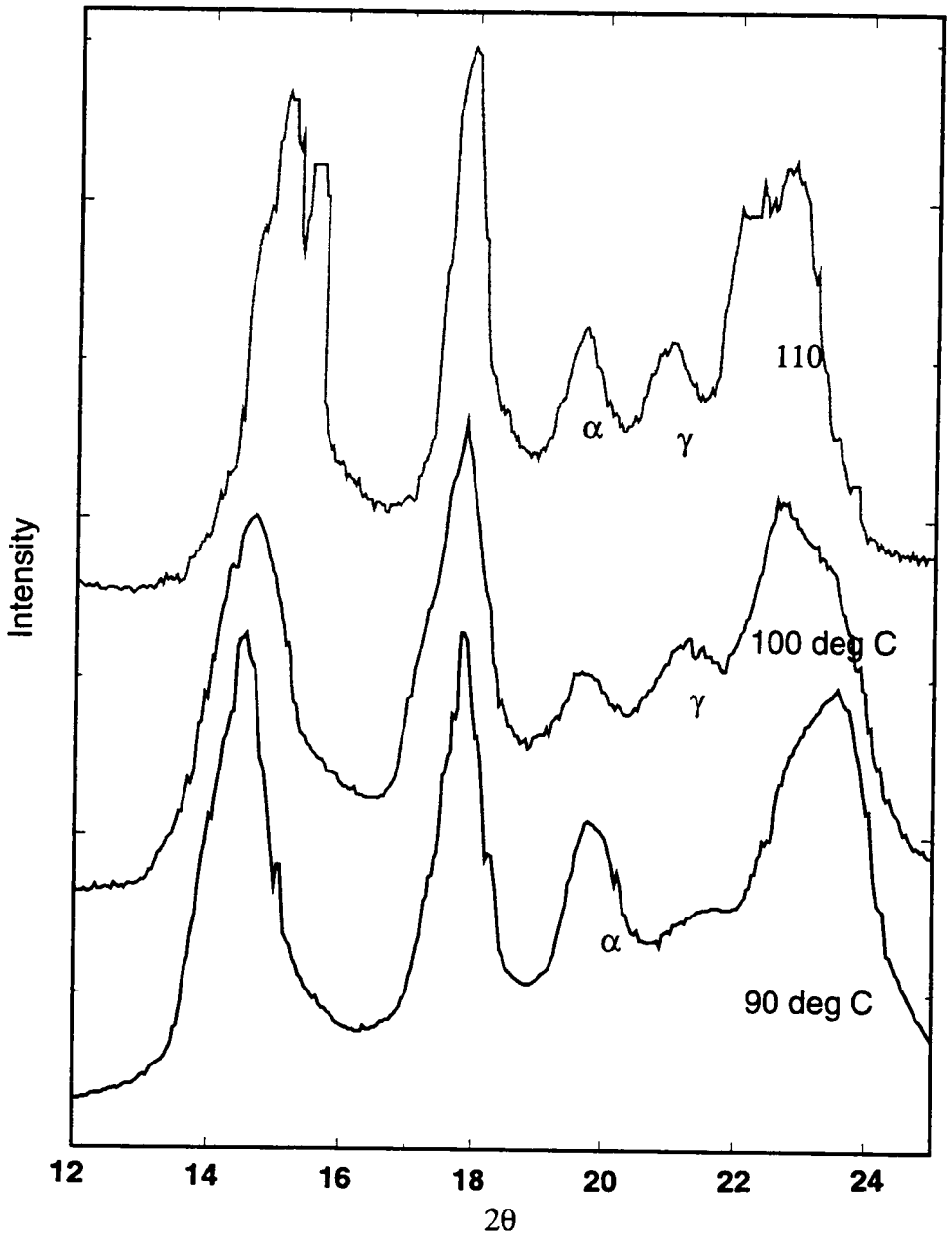


Fig. 4.30 WAXD studies of unfractionated 3% Propylene copolymer crystallized at various isothermal temperatures.

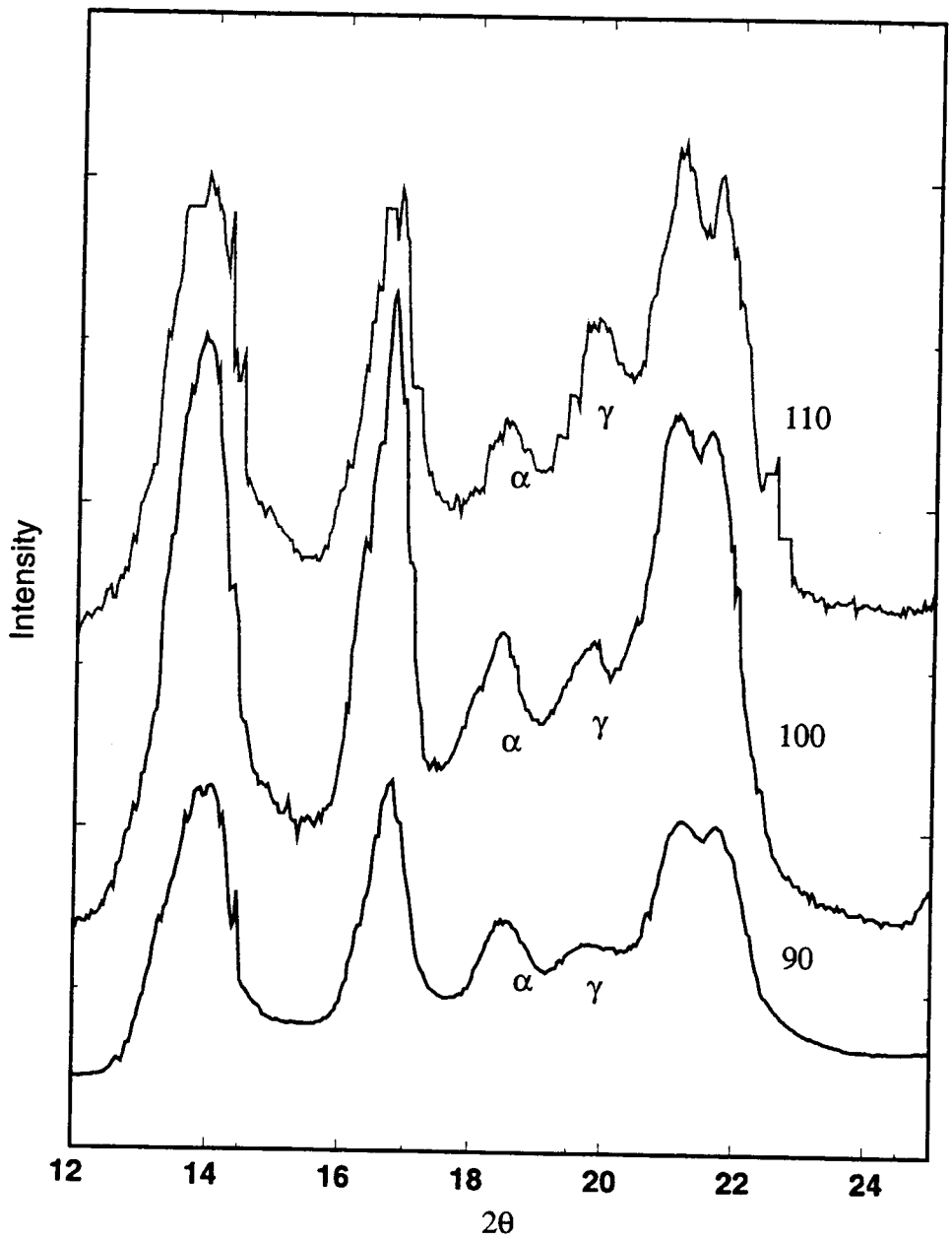


Fig. 4.31 WAXD studies of 2.2 wt % (ethylene) Propylene copolymer fraction crystallized at various isothermal temperatures.

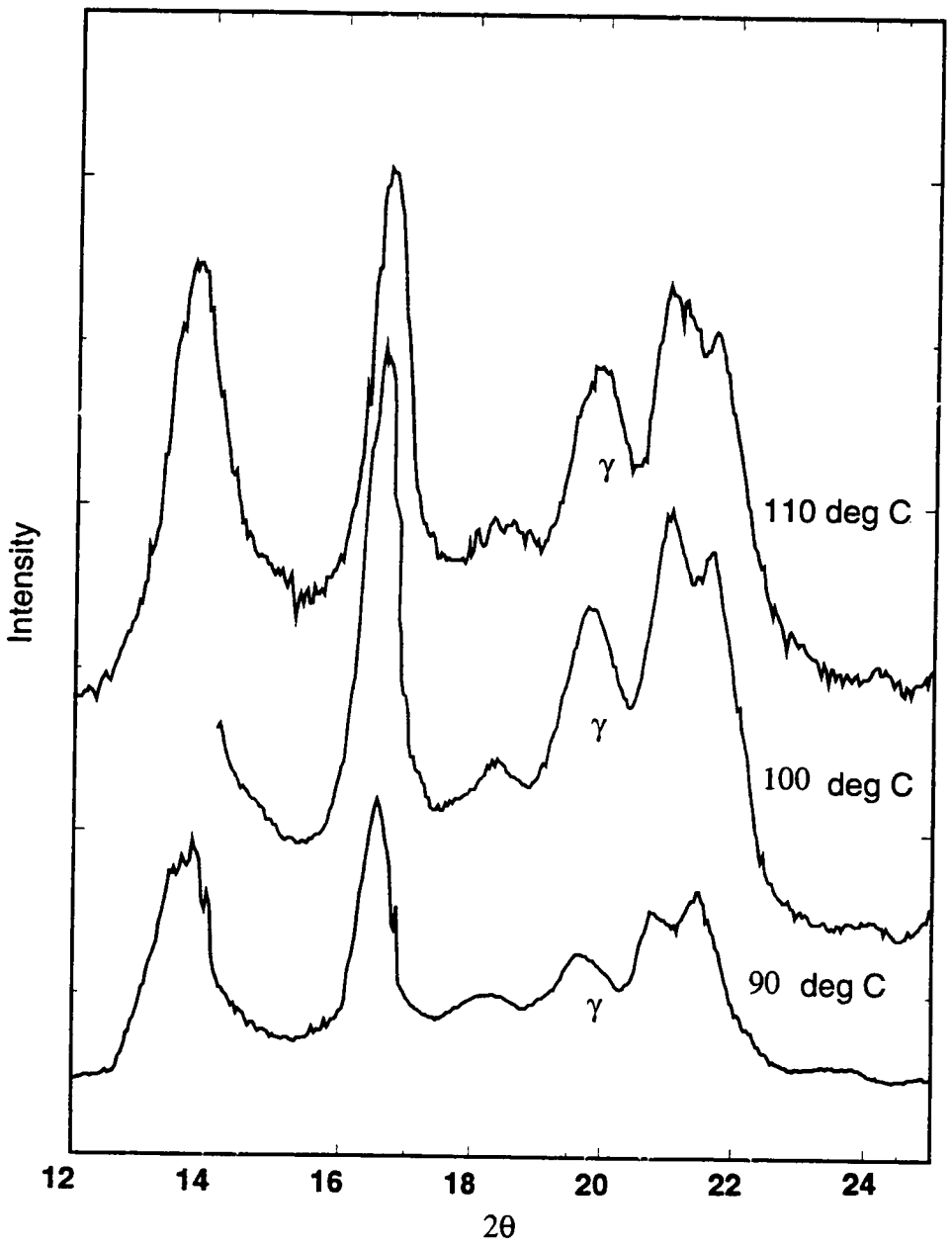


Fig. 4.32 WAXD studies of 3.7 wt % (ethylene) Propylene copolymer fraction crystallized at various isothermal temperatures.

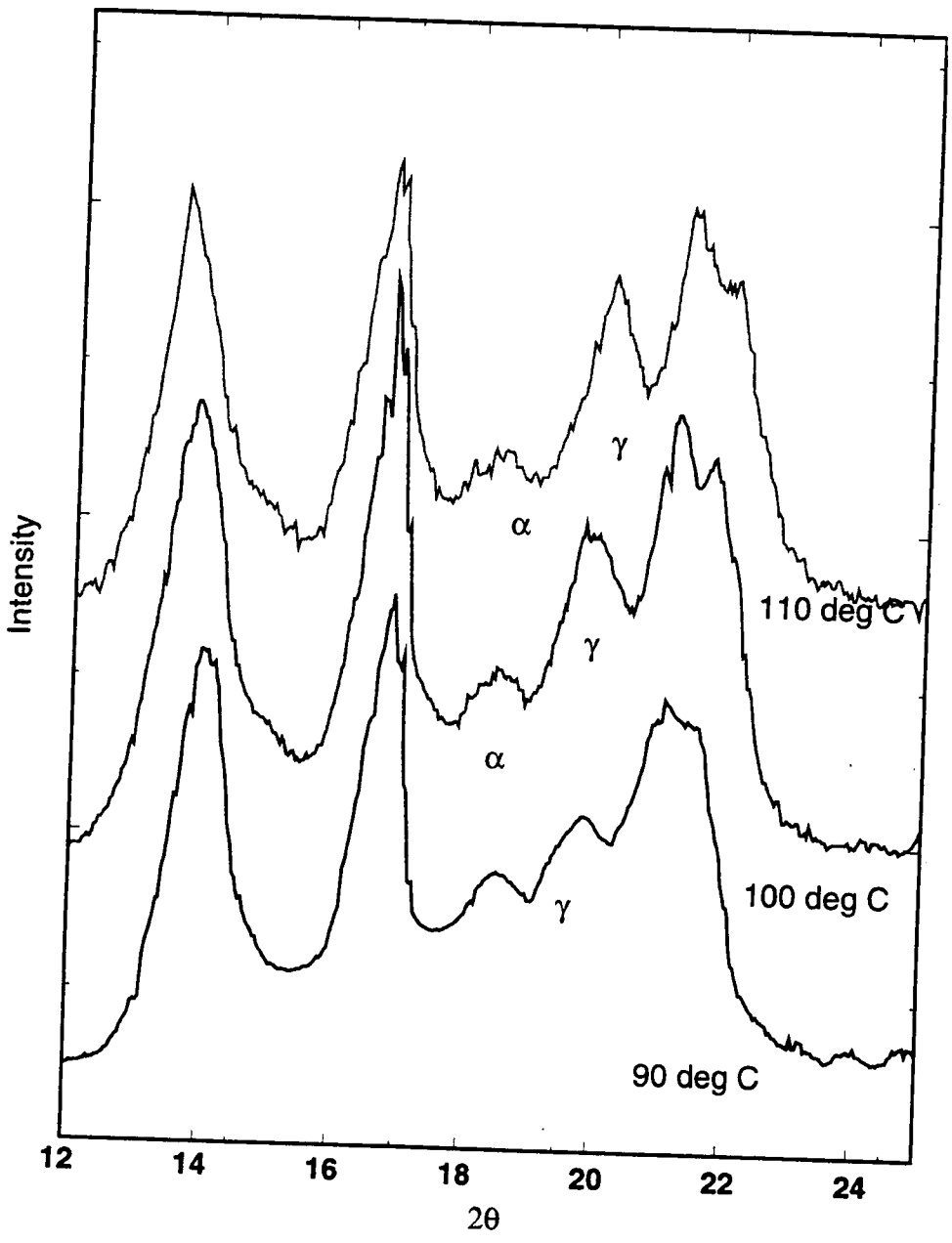


Fig. 4.33 WAXD studies of 5 wt % (ethylene) Propylene copolymer fraction crystallized at various isothermal temperatures.

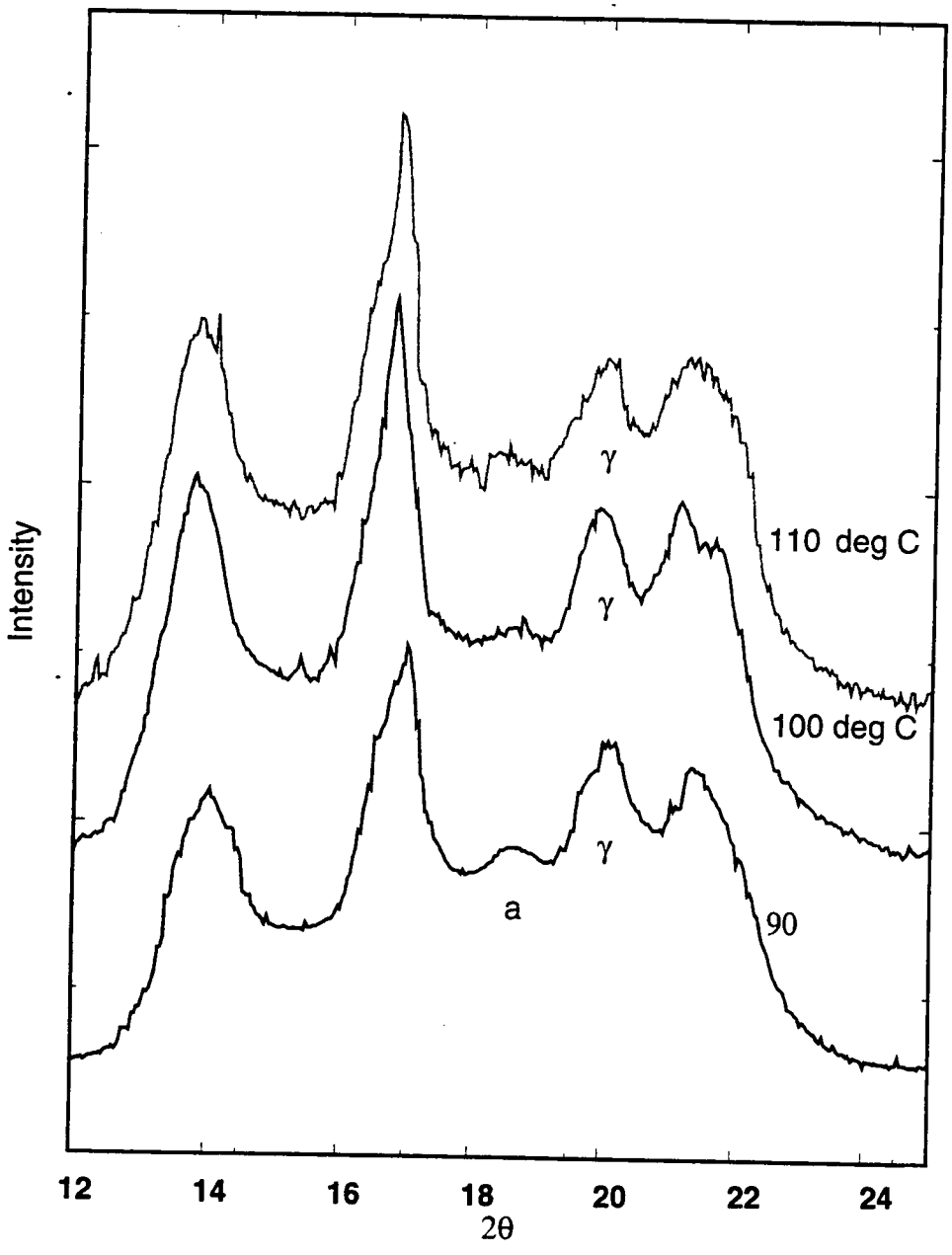


Fig. 4.34 WAXD studies of 10 wt % (ethylene) Propylene copolymer fraction crystallized at various isothermal temperatures.

copolymers xiPP3 and xiPP5 were studied in detail during the growth studies. There is a clear change in morphology from the 1% copolymer fraction to the 10% fraction. For all the fractions studied, the nucleation density at higher supercoolings was greater and this behavior increased with the comonomer content. This is illustrated in the Figs. 4.35-4.38. The 1% and the 2.2% fraction showed morphologies close to that of isotactic polypropylene, except that their spherulites were more distorted and consisted predominantly of positive spherulites. In addition the 2.2% also showed a few axialites. The 3.7% and 5% fractions changed drastically to a totally axialitic type of growth, the category 1 type of crystals proposed by Keller and Norton (1984). Here a single nucleating entity initiates crystal growth in all directions and thus crystal growth is uncorrelated. Although, if combined with some fanning and branching, it can lead to the formation of a spherulite. This growth observed in other polymers has been considered to be due to a coincidental consequence at high to medium supercooling. These are shown in Figs. 4.39-4.40. At low supercoolings, these crystals closely approach of the nucleating influence of heterogeneities Keller (1984). This might be a clear indication of the reduction in crystallinity in the higher ethylene content copolymers since there is a tendency to form open spherulites. It has been shown that lower molecular weight fractions in polyethylene have exhibit axialitic morphology (Hoffman *et al.* 1975). Thus lowering the molecular weight might reduce the tendency to form fully developed lamellae. The morphology of 10% fractions are typically open spherulites similar to that found in low crystallinity polymers, like *cis*-polyisoprene, where there are prolific branches seen at all supercoolings. Morphologies of this fraction is shown in Figs. 4.41-4.42.

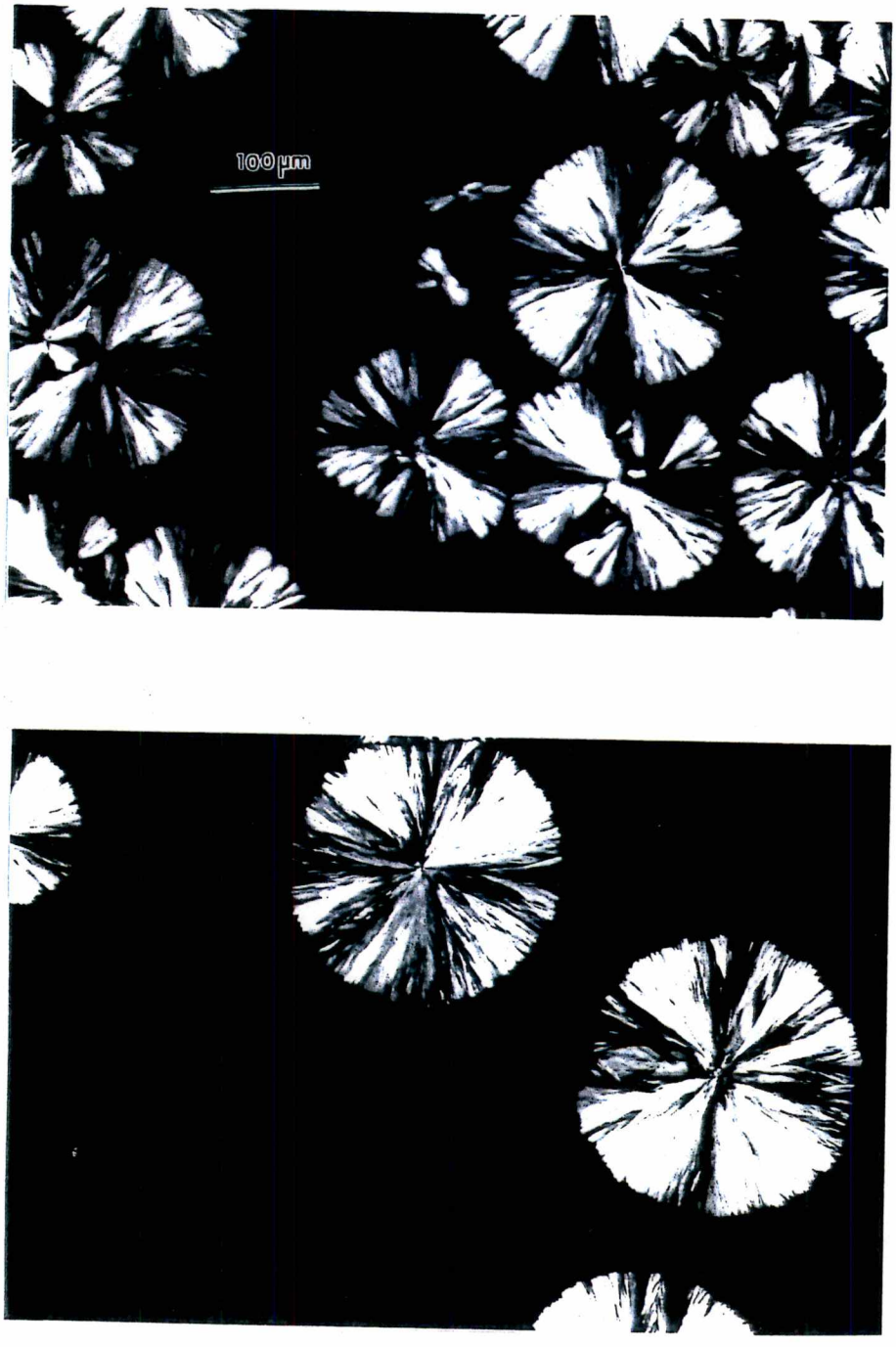


Fig. 4.35 Crystalline morphology of 1% fraction at, supercooling = 60 (top) and (bottom) supercooling = 52 (20 mag).

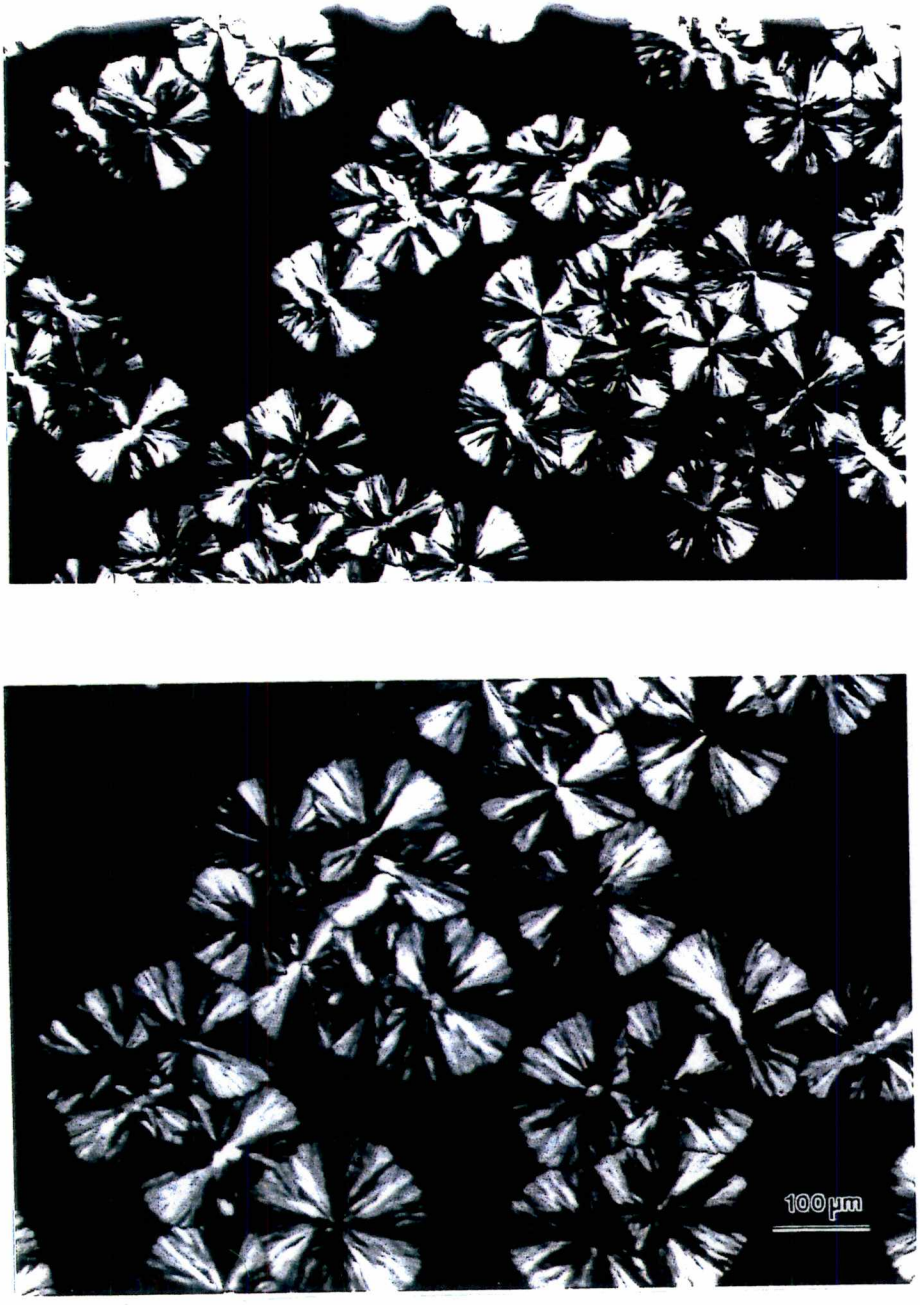


Fig. 4.36 Crystalline morphology of 1% fraction at, supercooling = 50 (20 mag).



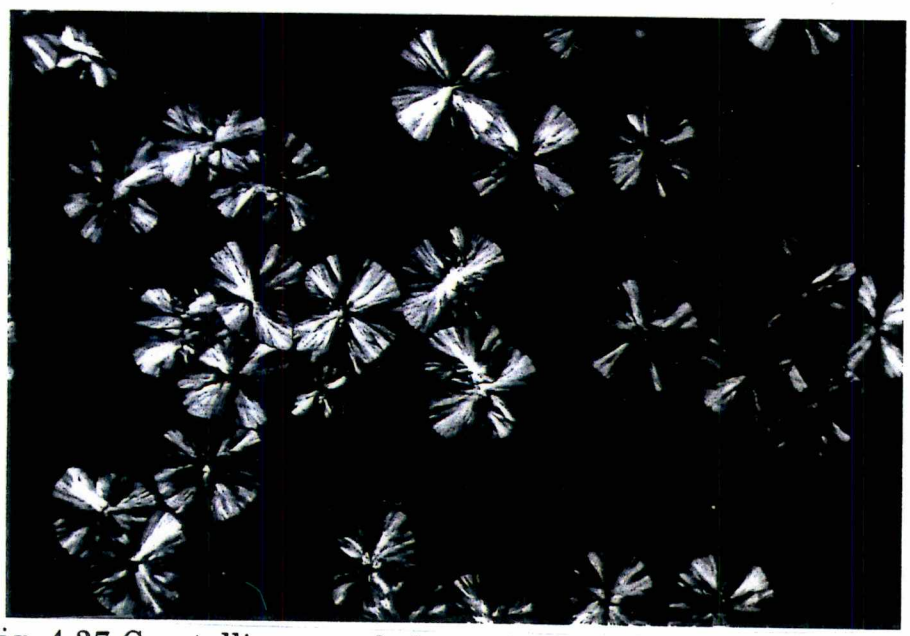


Fig. 4.37 Crystalline morphology of 2.2% fraction at, supercooling = 54 (top) and (bottom) supercooling = 50 (20 mag).

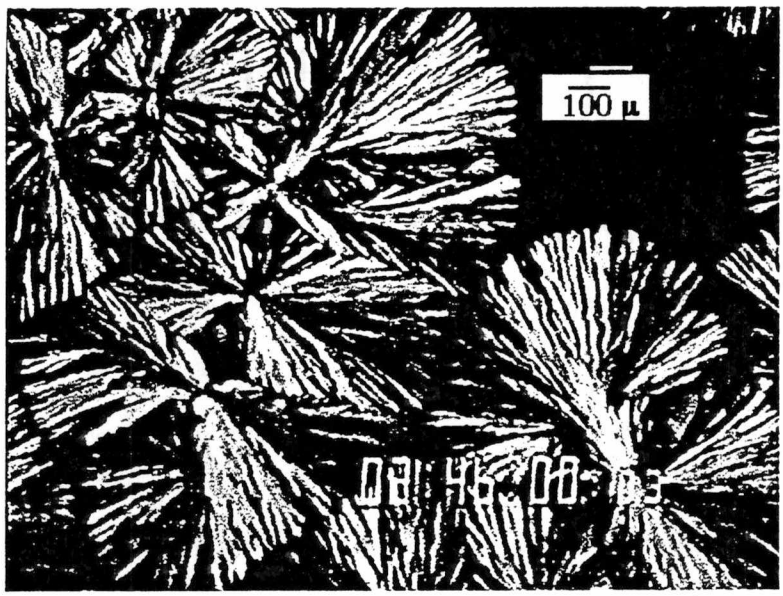


Fig. 4.38 Crystalline morphology of 2.2% fraction at a (supercooling =50) showing sheaf like morphology

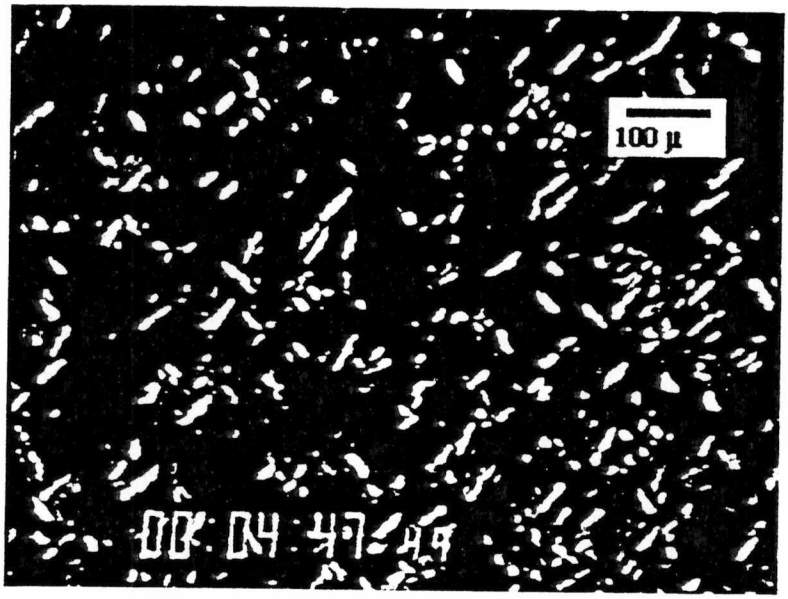


Fig. 4.39 Crystalline morphology of 3.7% fraction at high supercooling, axialitic morphology

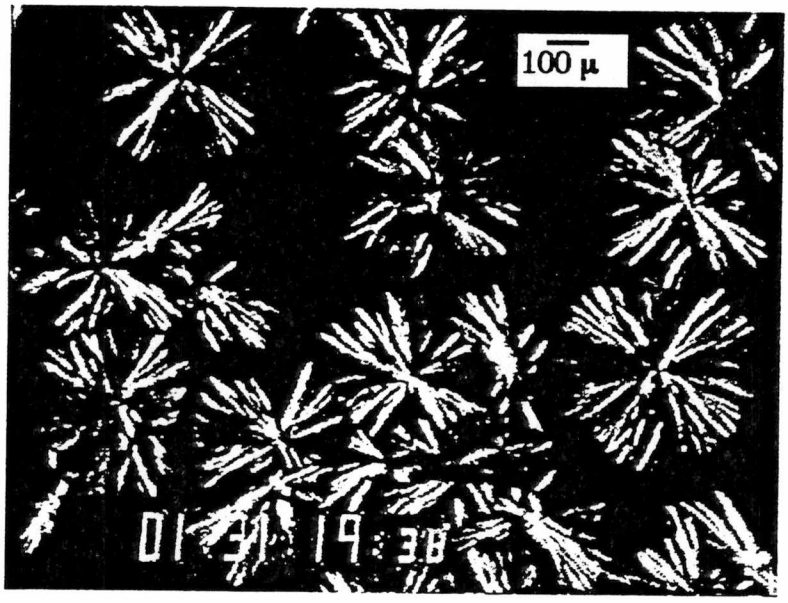


Fig. 4.40 Crystalline morphology of 2.2% fraction at low supercooling, axialitic morphology

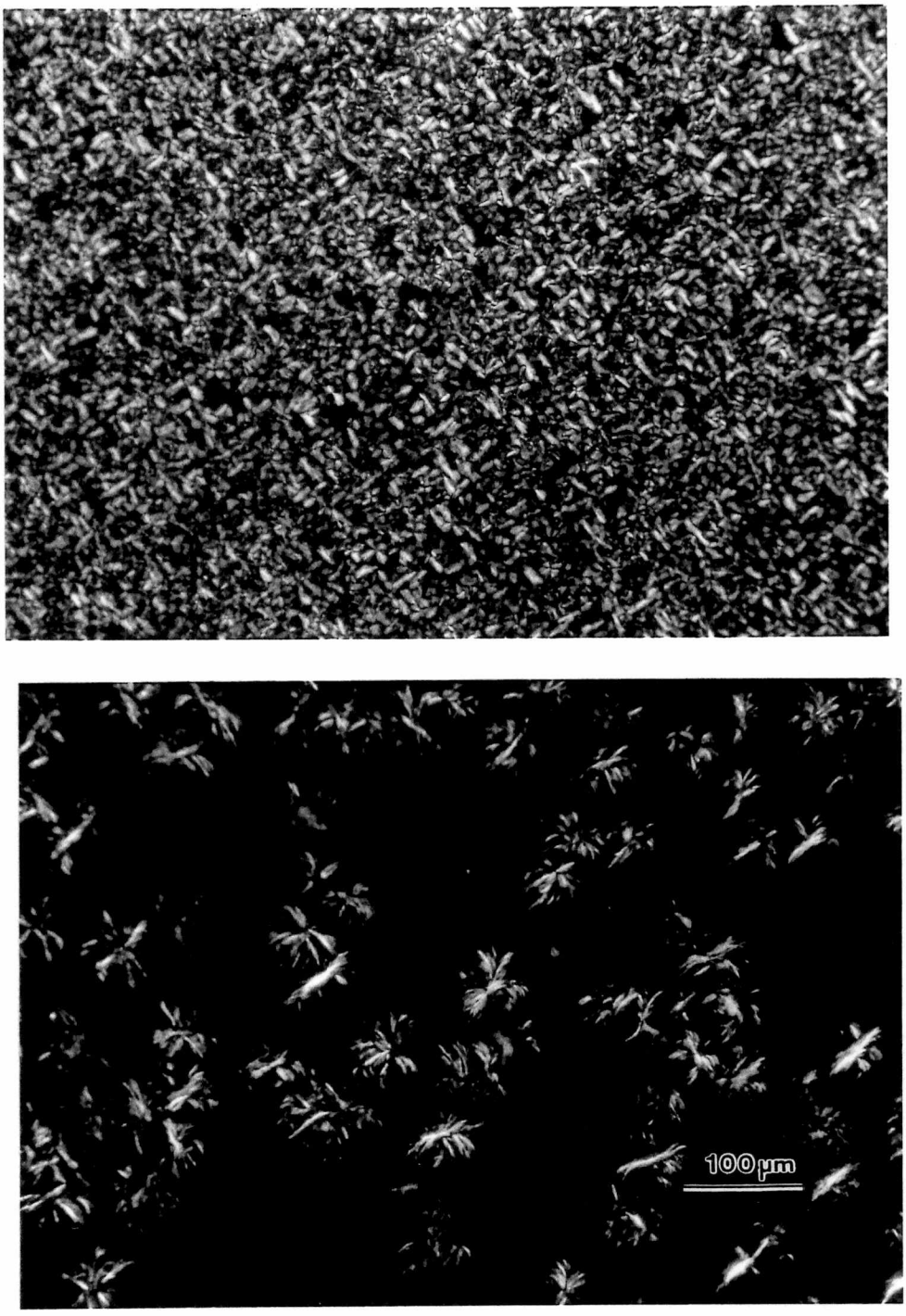


Fig. 4.41 Crystalline morphology of 10% fraction at, (top) supercooling = 60 and (bottom) showing prolific branching at supercooling = 50. (20 mag)

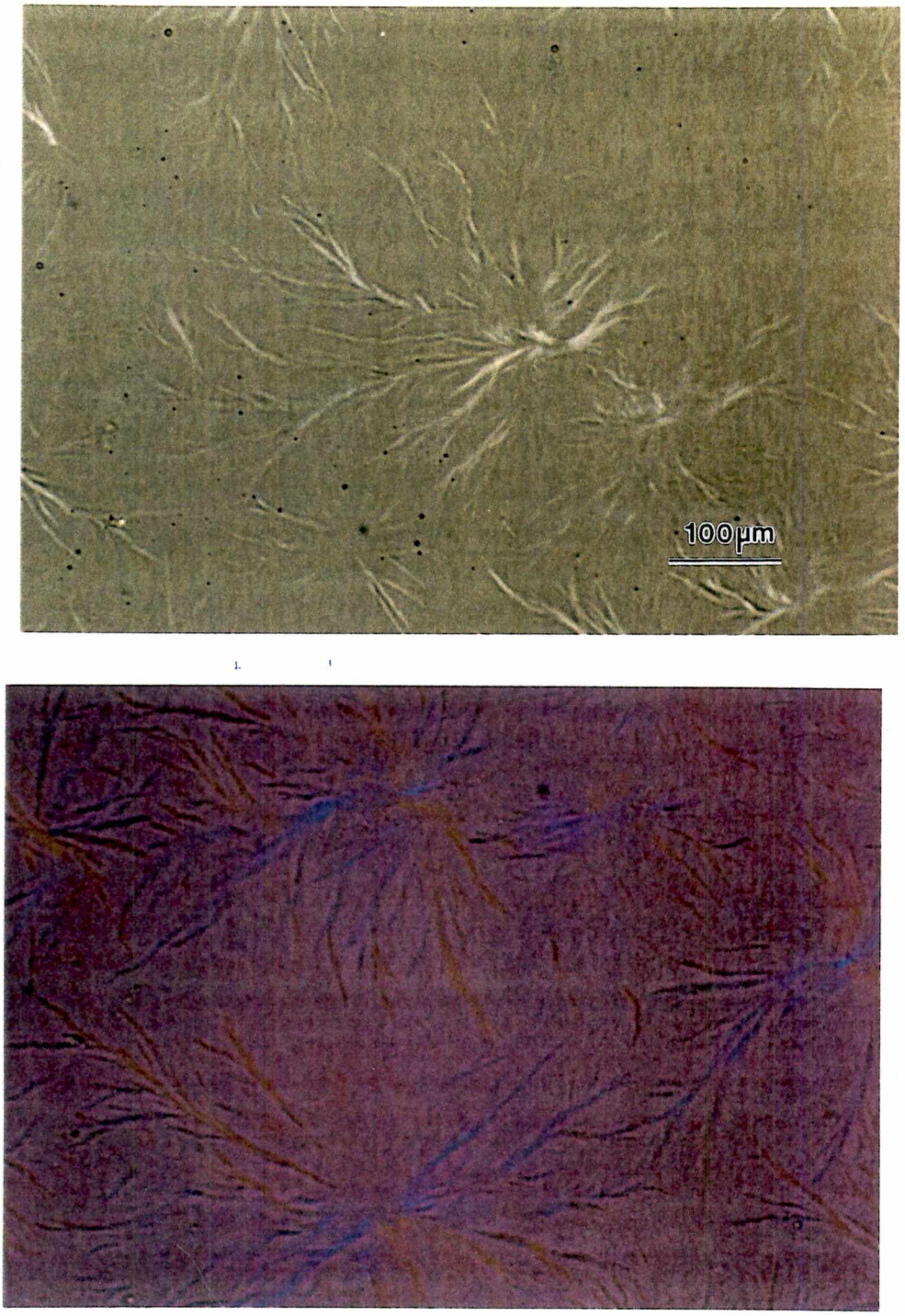


Fig. 4.42 Crystalline morphology of 10% fraction at supercooling = 37 (20 mag)

4.7 Crystallinity

Crystallinity of the fractions was calculated using WAXD. The advantage of using WAXD for determination of crystallinity is that it is the only method which examines the three dimensional order of the polymer directly. Calculation of the crystallinity was done by assigning the crystalline region as C and the amorphous region as A_m. The ratio of the areas in the crystalline region against the total area gives the crystallinity index

$$X_C = (C) / (A_m + C)$$

Error Limits

Selection of the baseline is the most probable case of error. In order to reduce the error in weight of each peak, they were weighed several times and their mean was taken for average crystallinity index.

4.8 Latent Heat of Fusion

The heat of fusion of a polymer depends on the crystallinity of the polymer and crystal perfection. The heats of fusion of the copolymer fractions were estimated from the total peak areas of the DSC endotherms. The latent heat of fusion was determined by

$$\Delta h_f^* = (\Delta h_f / \text{crytallinity}) \times 100.$$

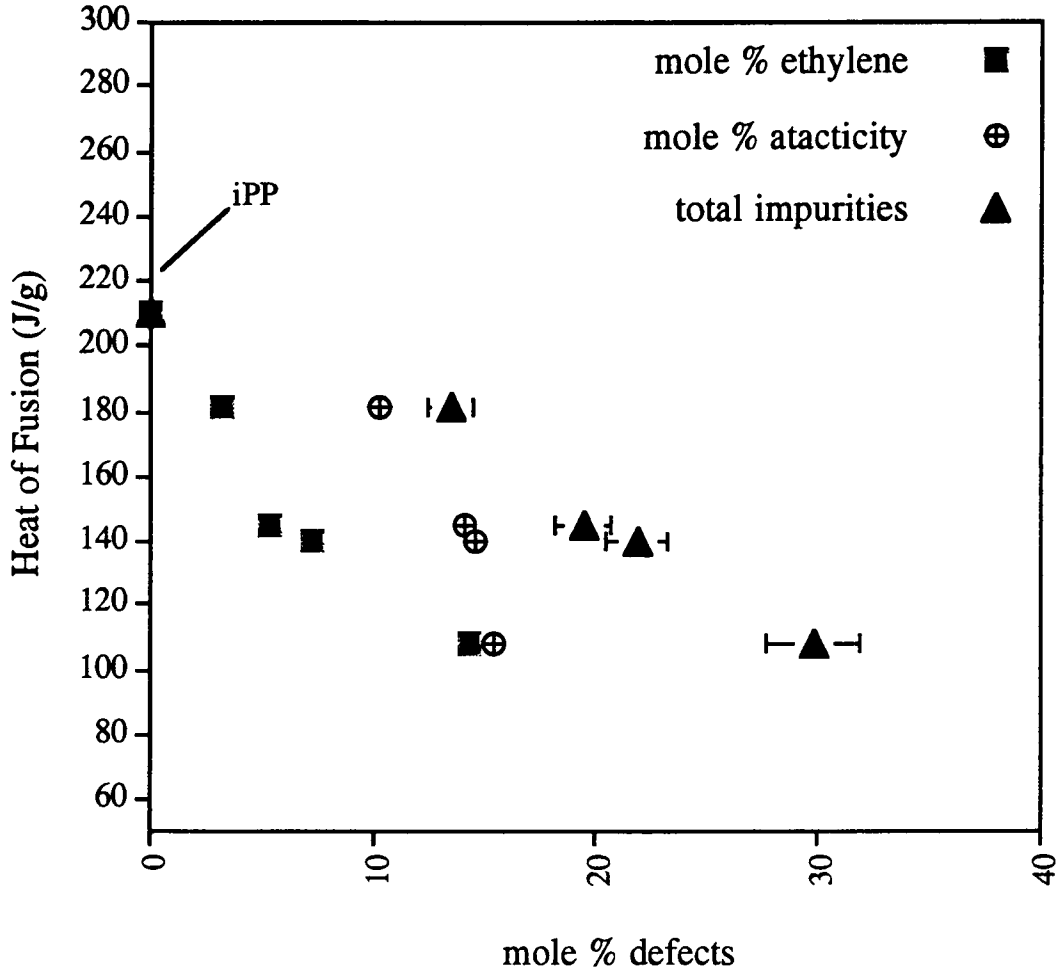


Fig. 4.43 Latent heat of fusion for the copolymer fractions calculated based on the crystallinity determinations from WAXD.

The latent heats of fusion for the copolymers are given in Fig. 4.43. It can be observed that the copolymers have a lower heat of fusion than the homopolymer. This reduction in heat of fusion is due to the incorporation of chain defects in the polymer. Therefore, as the comonomer content is increased, chain irregularity increases and the heat of fusion reduces. From the plot of latent heat of fusion vs. the comonomer content a simple methodology to quantify inclusion or exclusion can persued. From Fig. 4.43, and equations 2.11 and 2.22, there is a clear deviation from the exclusion model. The slope of this plot gives the heat of fusion of the defect which is attributed to the presence of the comonomer. A similar analysis is also completed by taking into account the chain defects caused by stereo-irregularities in the copolymer fractions. From this, it can be seen that the reduction in the heat of fusion caused by stereoirregularities is not only due to atacticity but also the presence of comonomer. It is seen here that the incorporation of the comonomer has a synergistic effect in increasing the stereoirregularity of the polymer. In order to understand this better, comparisons with the studies of Janimak (1991) who studied the effect of tacticity on crystallization of iPP, have been made. In the previous study a decrease of only 12 J/g was observed for an increase in stereoirregularity from 2.2 to 21 %. This restates that the effect of comonomer is substantially greater in decreasing the heat of fusion in these copolymers.

5 DISCUSSION

5.1 Fractionation

Fractionation is a powerful tool in reducing the heterogeneity in polymers. Homogeneity in copolymers can be mainly based on comonomer content, tacticity and molecular characteristics. The method of fractionation plays a key role in determining the type of homogeneity that can be in homopolymers or copolymers. This aspect has been well illustrated by Paukkeri *et al.* (1994) in their extensive studies on polypropylene homopolymer fractions.

The comonomer content of various fractions was determined based on FTIR experiments aided by NMR results. The lowest boiling solvent helped in recovering higher ethylene containing fractions, and the highest boiling solvent the least ethylene containing fraction. When the iPP3 and iPP5 fractions are compared based on weight recovered from each fraction and their comonomer content, it is obvious that the iPP5 fractions from lower boiling solvents have more % by weight of ethylene content in lower boiling solvents. In order to test for the authenticity of the fractionation and the corresponding % comonomer content, analysis was done to determine the weight % of ethylene recovered in each fraction. The summation of total weight % of ethylene recovered was divided by the total weight recovered, this resulted in values of 2.81 (for iPP3) and 5.09 (for iPP5).This methodology also confirms

that the % error involved in the FTIR analysis is reasonable. In both the sets of the fractions the majority of the ethylene content ranged between 2-10%.

The presence of crystalline ethylene can be identified if there is splitting of 732-720 cm^{-1} doublet peaks (van Scooten 1961) and this is more common in high ethylene containing samples. This can help in determining the comonomer sequencing in these copolymer fractions. In all the samples analyzed, the doublet 732-720 cm^{-1} overlapped to form a single peak. This is an indication that there are not more than three to a maximum of four methylene segments present on the chain consecutively and confirms the absence of long blocky segments in the copolymer. These fractions are relatively randomly distributed like the unfractionated samples.

Decrease in tacticity with increase in comonomer content has been reported by Zannneti *et al.*: similar observations have been noticed for both the sets of copolymers fractionated. The reduction of tacticity in the 10% copolymer was comparatively less compared to the rest of the samples. In spite of calibrating the FTIR using NMR results, it should be noted that the measurement of tacticity is related to the tacticity helix and not to the stereochemical order of the chain. From the FTIR analysis, it can be concluded that the fractionation of the two copolymers has been achieved both by tacticity and comonomer content. The incorporation of comonomer decreased the regularity of the chain for the obvious reason that it is an impurity. An interesting approach of the effect of ethylene incorporation has shown that ethylene might just act as a chain inverting site for the propylene chain (Ser Van der Ven 1990). It should be noted that the extent of decrease in mole % ethylene in each extraction is low compared to the increase in

stereoirregularities, except for the highest ethylene containing fraction. This effect can be observed in Fig. 5.1

In both sets of the copolymer fractions, the presence of comonomer and reduction in tacticity had distinct effects in depressing the melting temperature. As expected, fractionation narrowed the comonomer distribution and this had a great effect on the melting behavior of the crystals. The 10% fractions had the lowest melting range while the 0.5% copolymer fraction had the highest melting range. Most of the fractions observed did not show double melting behavior, as seen in the unfractionated samples. The presence of double melting peaks in a low ethylene fraction is probably due to distinct segregation of narrow comonomer contents. Though the effect of copolymer segregation might be more prominent, the effect of segregation due to molecular weight and recrystallization (Petraccone et al, 1988 and Kamide and Yamaghuchi 1972) should not be forgotten. Based on melting studies, it is seen that fractionation has been quite effective since separation based on closer comonomer distribution was achieved.

The effect of comonomer and atacticity content on melting is quite similar in the fractions. The extent of decrease with comonomer as defects was large compared to tacticity effects. Both showed a linear decrease in melting when the comonomer /atacticity contents are plotted against the T_m in Fig. 5.2. It should not be forgotten that the effects of these two types of defects are interdependent.

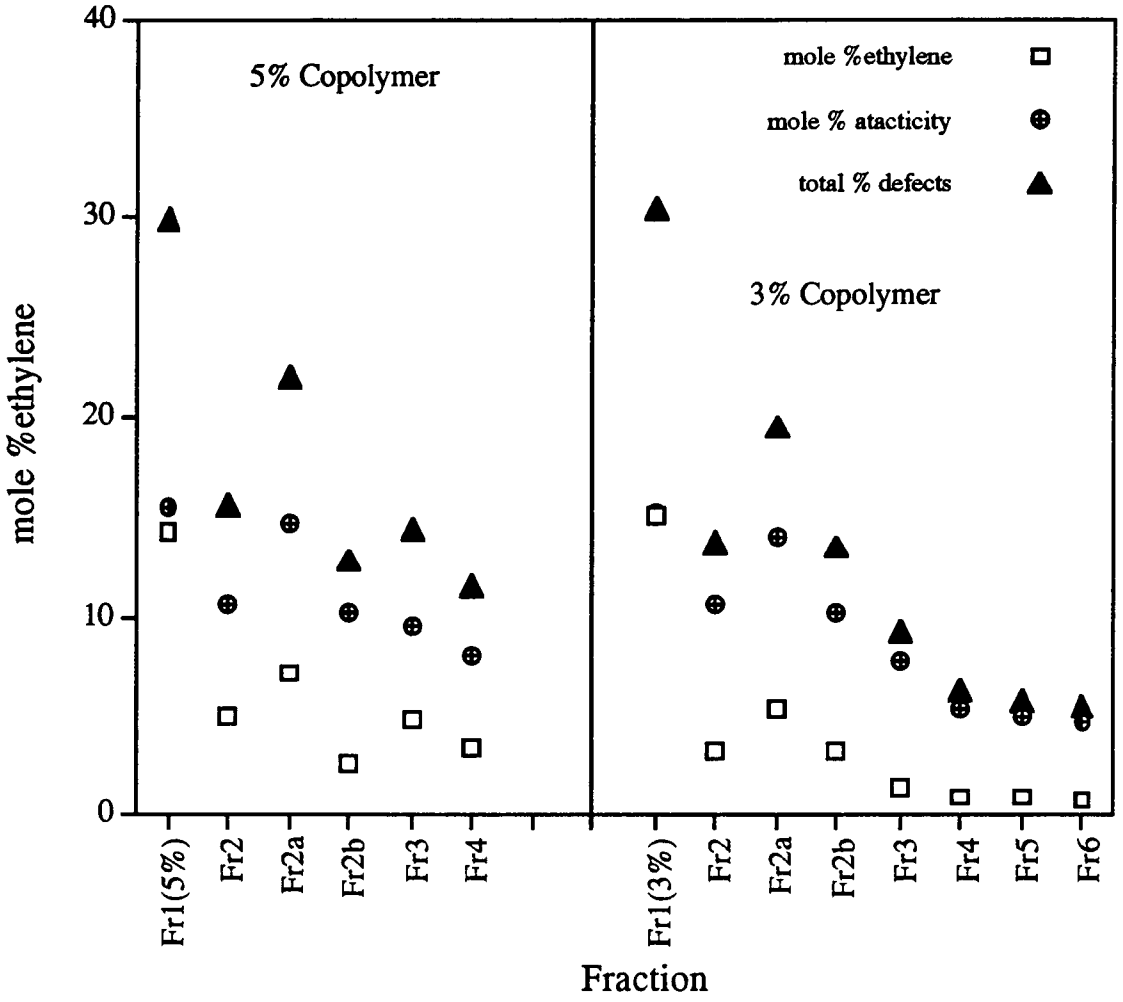


Fig. 5.1 Effect of fractionation on comonomer content and stereoregularity.

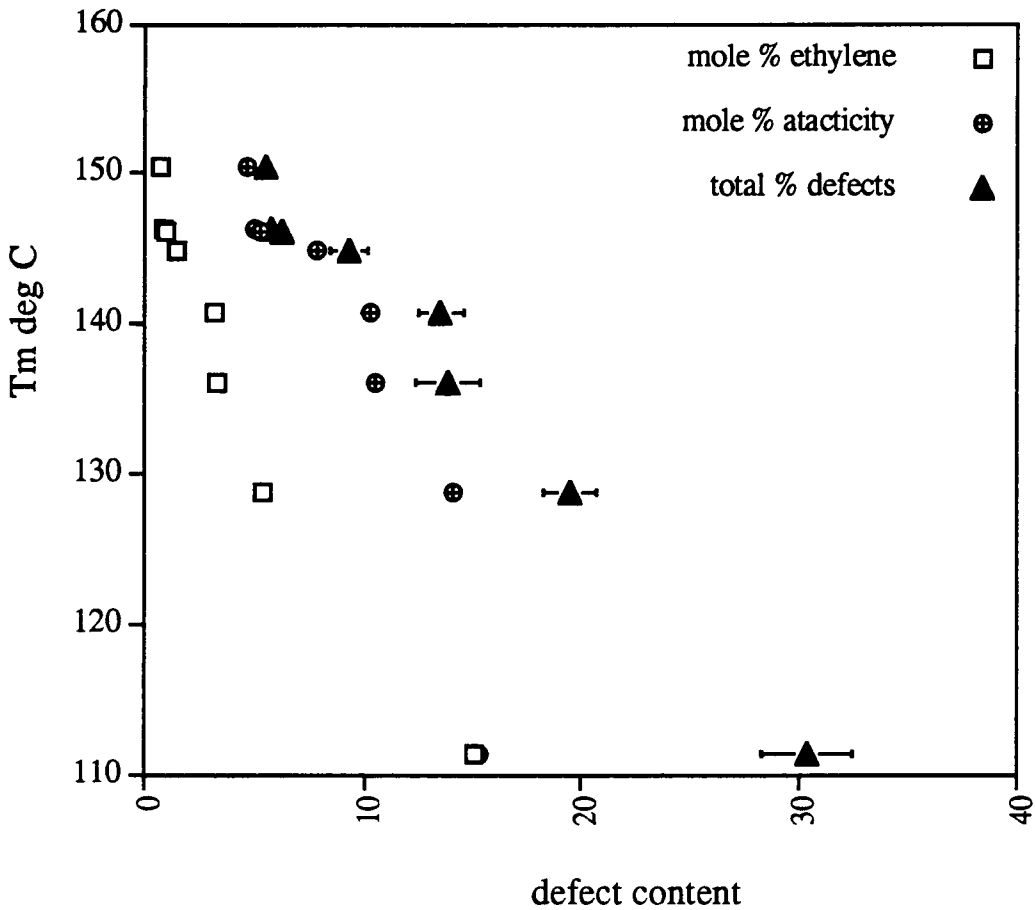


Fig. 5.2 Effect of defects on the melting of copolymer fractions.

5.2 Equilibrium Melting Temperature

The equilibrium melting temperature (T_m^o) of a polymer coincides with the melting of an infinite crystal. The T_m^o of a polymer can sometimes be.obtained by the Hoffman-Weeks plot (Hoffman and Weeks, 1966) where a simple extrapolation is done on the T_m Vs T_c plot. It is obvious that the T_m can never be less than T_c, thus the line $T_m = T_c$ will represent the lower limit of the melting behavior. The intersection of the experimental data with this line will give T_m^o. This point represents the melting temperature of a polymer crystallized infinitely slowly, and for which crystallization and melting would take place at the same temperature. A better approach to determine this is by using SAXS. Mezghani and Phillips (1994) have recently studied these methods in detail for polypropylene. They have also elucidated the overestimation of T_m^o due to lamellar thickening at low supercoolingsThe current experiments were conducted using the procedure detailed by Mezghani and Phillips (1995) and peak-temperature extrapolations were taken for calculation rather than the return-to-baseline method The equilibrium melting points for the copolymers iPP3, iPP5 and iPP 0.5 (not used in this study) have already been reported by the same group (Fig. 5.3). In extension to the previous study the extracted samples and the fractions have been studied here. The extracted samples xiPP3 and xiPP5 gave similar T_m^o values though slightly higher. Fig. 5.4 shows a plot of Tm Vs Tc for the copolymer fractions. It is important to note that the γ content in the copolymers increased with comonomer content and decreased with supercooling. Since all the experiments for extrapolation of T_m^o were done at considerably lower supercoolings, it is more logical to relate the slope to that of the γ form. This is in agreement with the interpretations of Mezghani

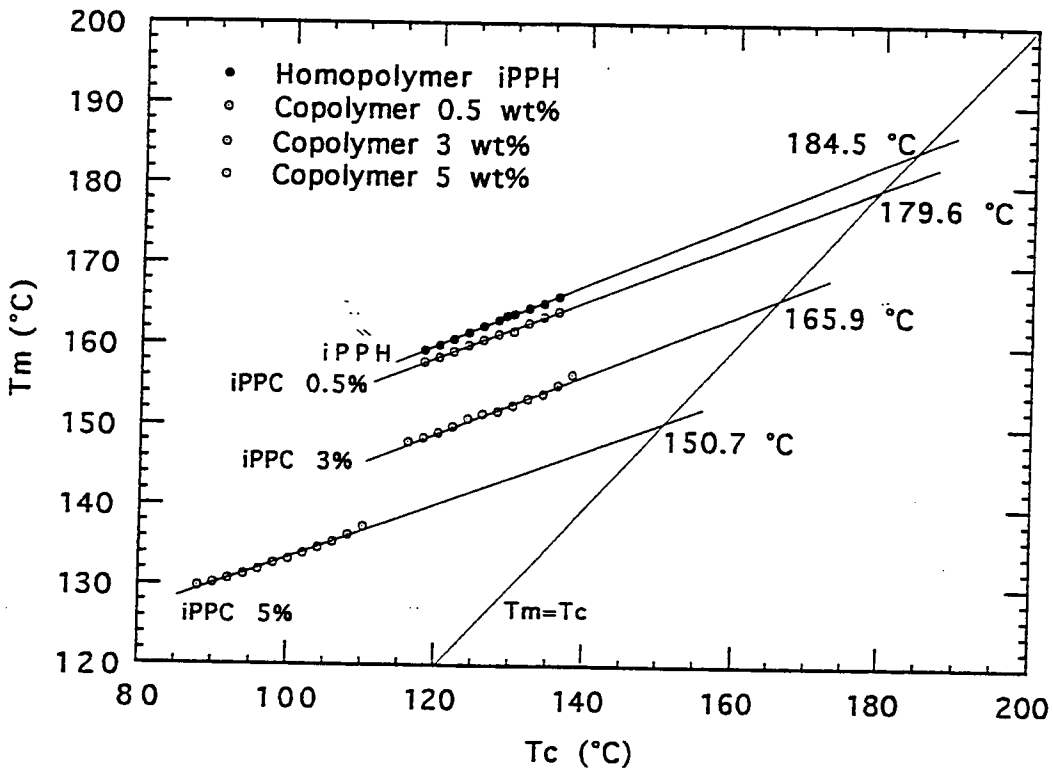


Fig 5.3 Equilibrium melting points of unfractionated copolymers obtained from DSC.(data obtained from Khaled Mezghani)

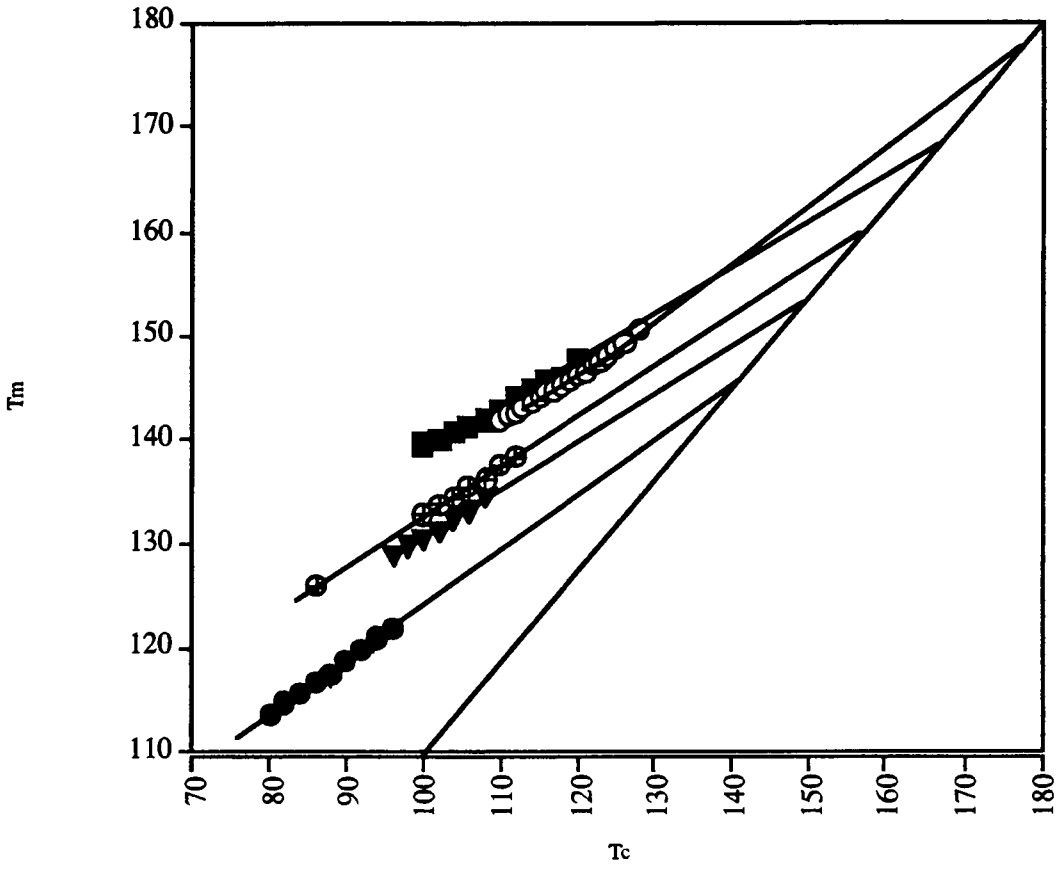


Fig. 5.4 Equilibrium melting points of fractionated copolymers from Hoffman-Weeks plots

and Phillips (1995) on unfractionated samples. There was a strong decrease in the equilibrium melting point with increase in comonomer content except for the 10 % fraction. The applicability of Flory's copolymer equation for the prediction of the equilibrium melting points has been compared with the experimental results to check its validity (Fig. 5.5). For the fractions studied, there is not much deviation from the Flory T_m^o for zero comonomer content. The values obtained are clearly well below the predictions of the Flory estimation of the equilibrium melting point depression, if the comonomer effect is only taken into account. When the combined effects of comonomer content and atacticity are used, it fits perfectly to the Flory's predicted model of total exclusion. Interpretations of this particular system show that the depression in melting is not totally governed by the comonomer effects but by the total impurity content. In order to understand the effect of defects on the equilibrium melting point, total defects was compared to a homopolymer with varying tacticities (Janimak 1991) Fig. 5.6. When these are compared to the. Flory's model, the tacticity effect on the melting depression of the homopolymer is similar to the effect of total defects in the copolymer.

5.3 Gamma phase in Copolymer fractions

The complicated polymorphism of the α and the γ phase of polypropylenes at elevated pressures and in the presence of comonomer content is quite evident from previous studies (Turner-Jones 1971 and Phillips *et al.*, 1992, 1995). From the present studies on copolymer fractions, it is seen that not only the comonomer content but also the comonomer distribution plays an important role in the formation of the gamma form. It can be clearly seen from Table 4.9, that between the 5% fraction and the

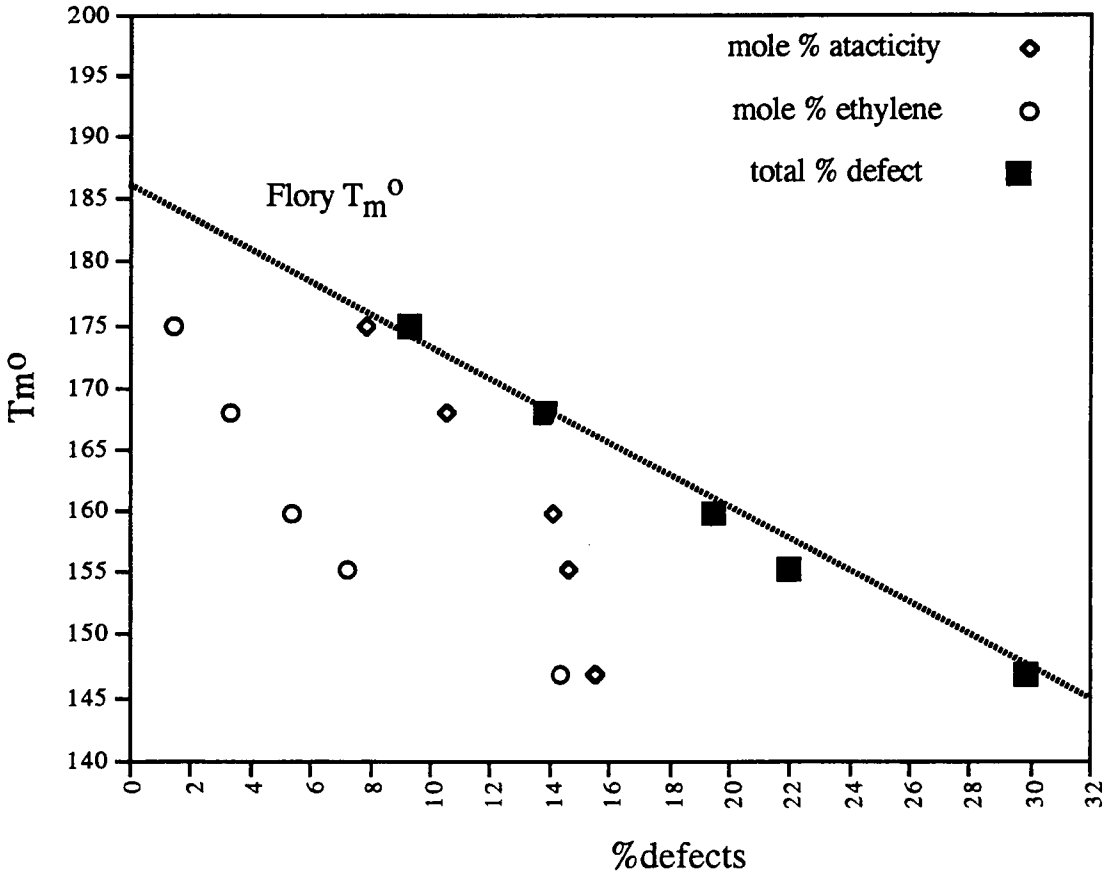


Fig 5.5 Comparison of Flory's predicted T_m^o to the calculated T_m^o Phillips (1995) on unfractionated samples.

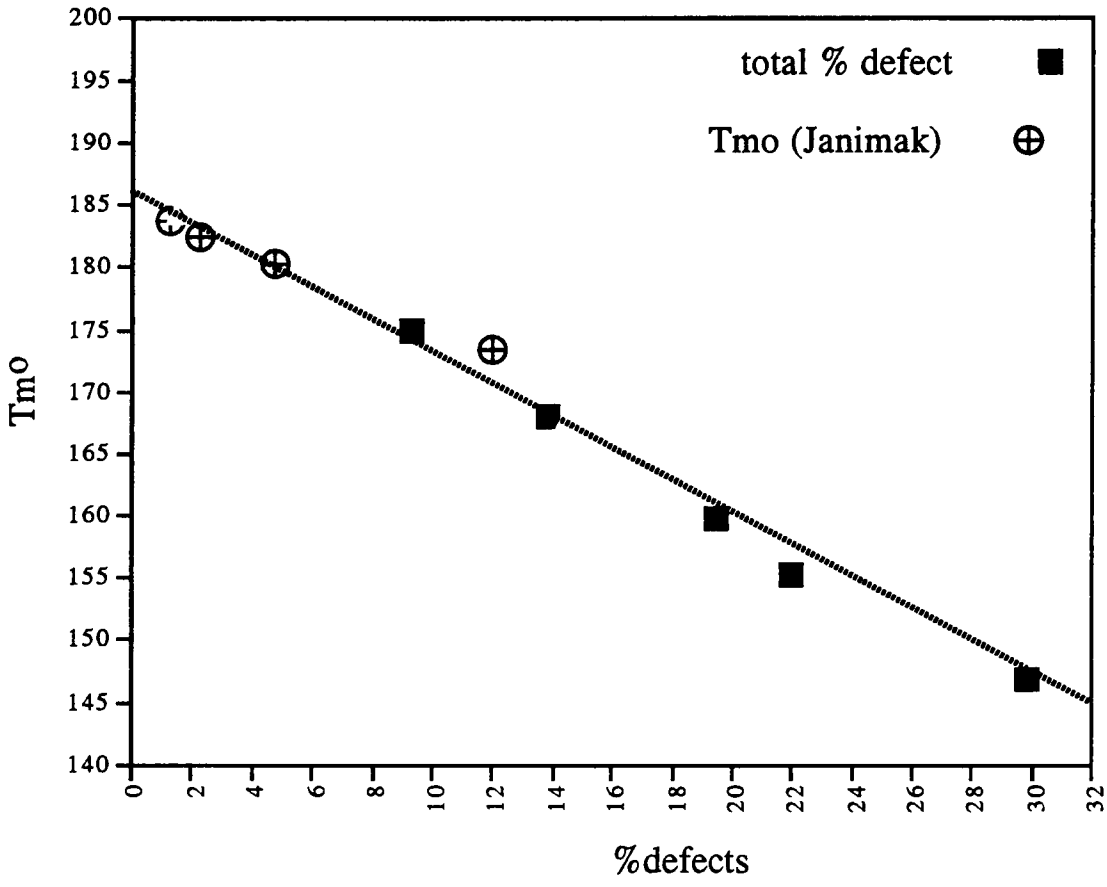


Fig. 5.6 Effect of tacticity on the equilibrium melting of polypropylene homopolymer compared with the total defect content in the copolymer fraction.

unfractionated (iPP5) there is a difference of 30-40 % gamma content at each supercooling. It can also be inferred that the γ content decreases with supercooling for each sample, which has been shown by Mezghani *et al.* for polypropylene at atmospheric and elevated temperatures.

The amount of γ content obtained in the 5 % fraction at 100° C were above 90%, which has not been reported to date on copolymers. The closest to this value was on copolymers (10% copolymer) with 83% gamma content achieved in controlled thermal conditions by Corradini *et al.* (1985).

5.4 Crystallization

Linear Growth Rates

Linear growth rates for various copolymers were obtained by measuring their spherulite diameter from the video monitor as a function of time. This resulted in a relationship of radius and time. Least squares method on these plots was used to determine the linear growth rates. Plots of linear growth rates Vs crystallization time for various copolymer fractions are shown in Fig. 5.7. The morphology at low supercoolings for copolymers was either sheaf like or open spherulites, tending to a spherulitic morphology. A very interesting behavior of the growth of copolymer fractions can be observed from Fig. 5.7. At low supercooling, the low ethylene fractions tend to have growth rates similar to those of high ethylene fractions.

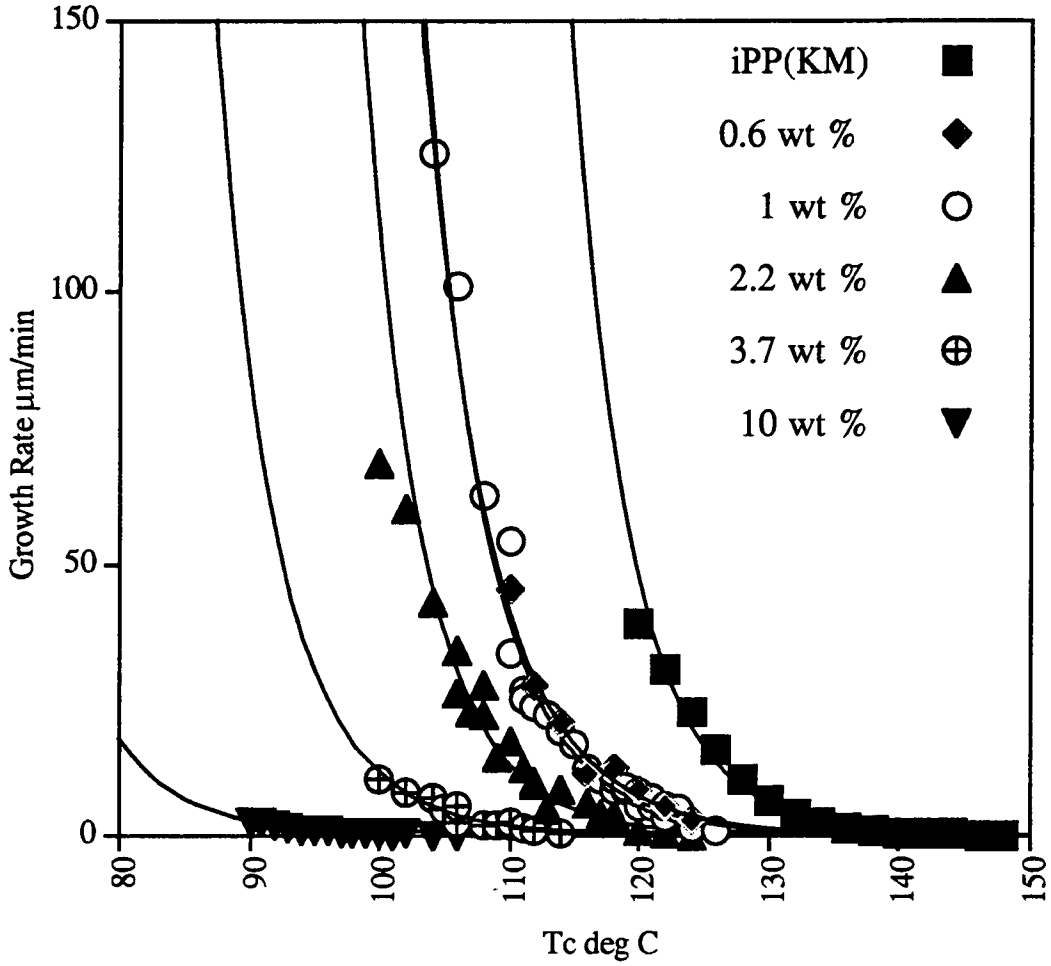


Fig.5.7 Growth rate as a function of crystallization temperatures for fractions of varying ethylene contents

thought to be random, the most important point from the growth data is the difference in growth rates of the unfractionated and fractionated samples Fig. 5.8. It can be observed from the growth rates that the 2.2 % fraction has a lower growth rate than the u3% and the 3.7% fraction lower than the u5%. This clearly indicates that the comonomer distribution not only plays an important role in the formation of the gamma phase but also in its spherulitic growth. This is a further indication that the fractionation has been successful in separating fractions of closer comonomer distributions.

Molecular weight has a reasonable effect on the growth of polymers, the lower the molecular weight the easier to crystallize or faster growth. From the present morphological study and fractionation literature published by other authors mentioned earlier, the reduction of molecular weight with increase in solvent power is quite possible. From the growth studies it is very obvious that the amount of reduction of molecular weight, if any, was not considerable to affect the growth.

Secondary Nucleation Analysis

Lauritzen-Hoffman analysis was used on the growth data to determine the regime transitions in the copolymers. For this analysis, data obtained by Mezghani on iPP was used as a standard for understanding the copolymer kinetics. The value for T_m^o = 186.1 °C, that for T_g = -12 and for U* = 1500 cal/mol. Based on these standard values, the regime transitions for the copolymers are illustrated in Fig. 5.9. It can be seen from these plots that the unfractionated copolymer u5%, like the homopolymer, shows only two transitions. In the fractionated copolymers, the presence of three regimes is

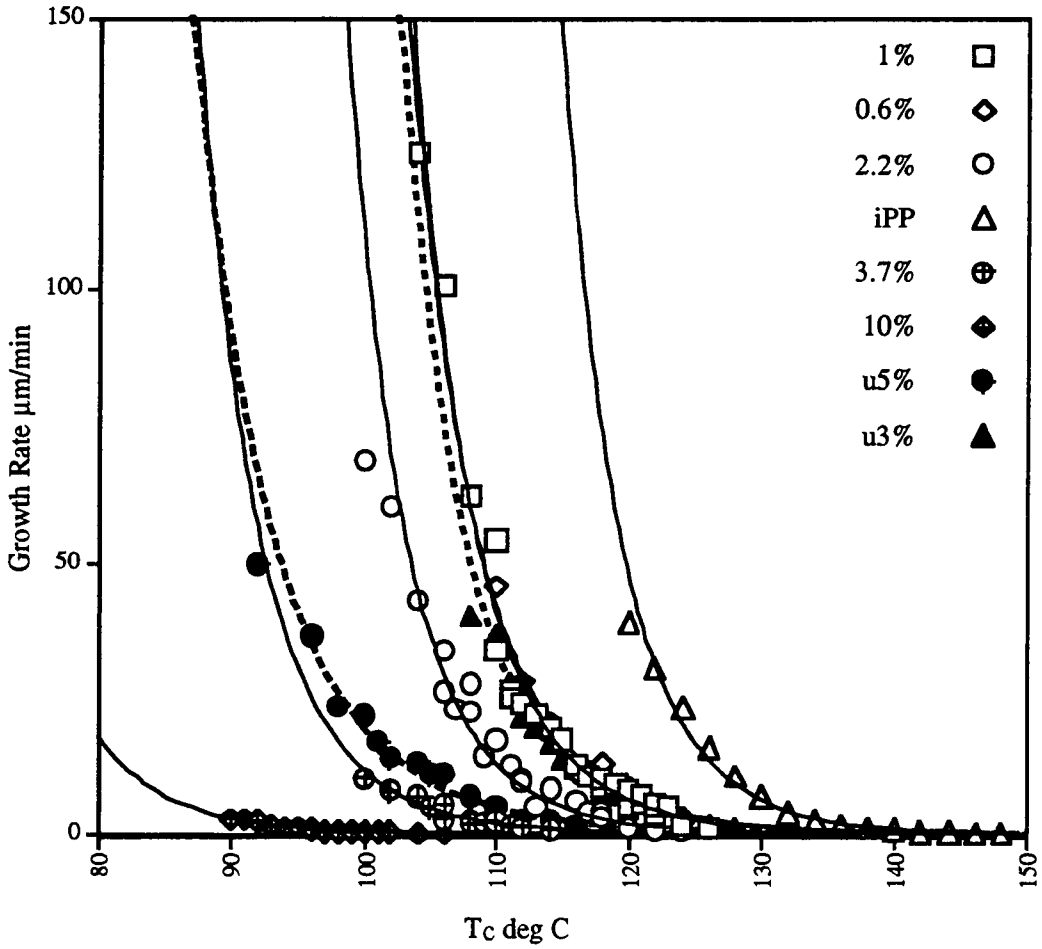


Fig 5.8 Growth rate vs. Crystallization temperatures for Copolymers, iPP data obtained from Khaled Mezghani

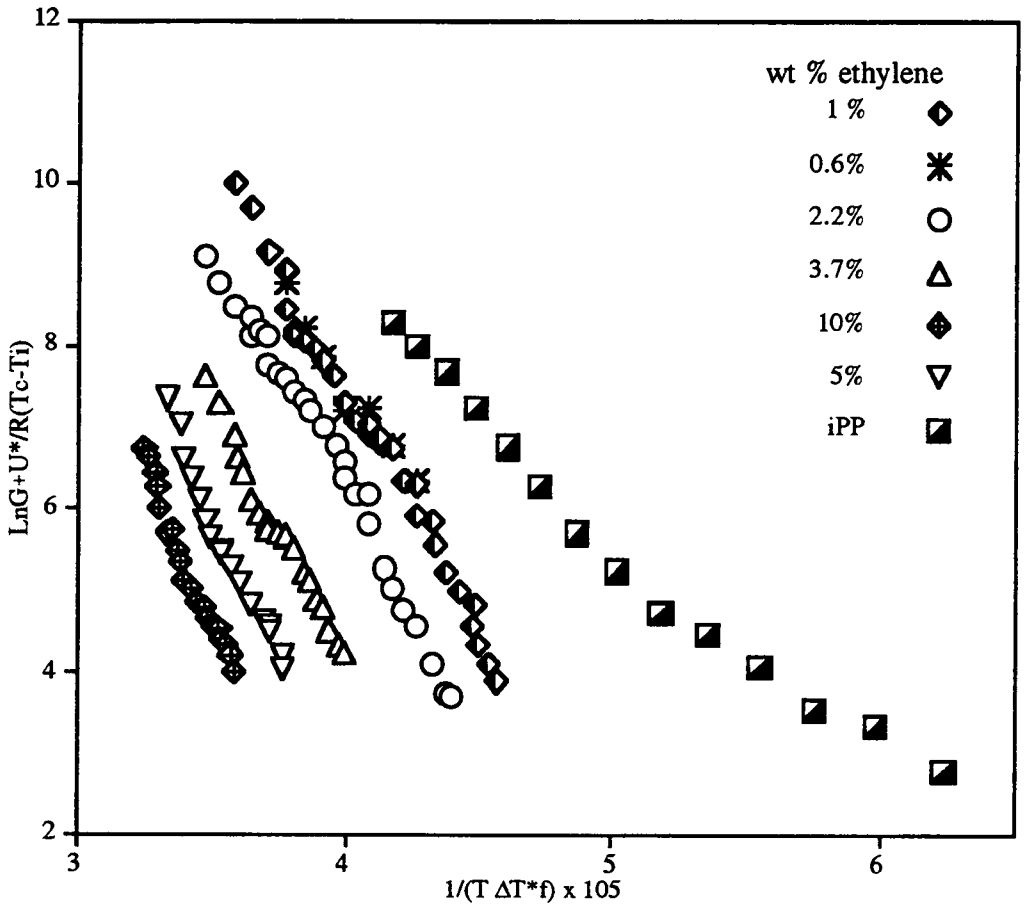


Fig. 5.9 Regime Transitions in Fractions of propylene Copolymers

noticed at lower ethylene contents and as the ethylene content increases, the Regime II region becomes smaller. Further increase in comonomer content beyond 5% ethylene results in only Regime II and Regime III.

The effect of the thermodynamic variables is very critical for regime analysis. Effect of changes in T_m^o, T_g and U* have been studied by Campbell (1992) and Mezghani (1995). The change in T_m^o has a significant effect in changing the slope but does not affect the temperature of the transition. The effect of Tg and U* is observed by a relative shift in regime lines along the X and Y axes. In order to account for these critical thermodynamic changes in the copolymers, the values of the T_m^o as calculated from Hoffman-Weeks plot (Fig. 5.3) were used. Since the T_g of the copolymers also varies significantly, these values were also incorporated in the regime analysis. Fig 5.10-5.16 clearly shows the change in the slopes for each sample compared to the standard analysis which was done previously. The super coolings of the I-II transitions for all the samples were in the range of 52-54. The supercoolings in the II-III transition were 60 in the low ethylene copolymers (1 and 2.2%), were in the range of 50-52 for the (3.7, 5 and 10%) fractions and were 53 and 56 for the u3% and u5% copolymers.

From this, it can be inferred that the II-III transition is not dependent on the supercooling, but only on a temperature characteristic of the material. This is unlike what is observed for Regime I-II transition where the transition is very much dependent on the supercooling irrespective of the material characteristics. K_g, the slopes of the plots, were calculated to aid in the determination of the fold surface free energy σ_e. The calculations were based on equation 2.2. T_m^o and Δh_f have been previously estimated. It is to be noted

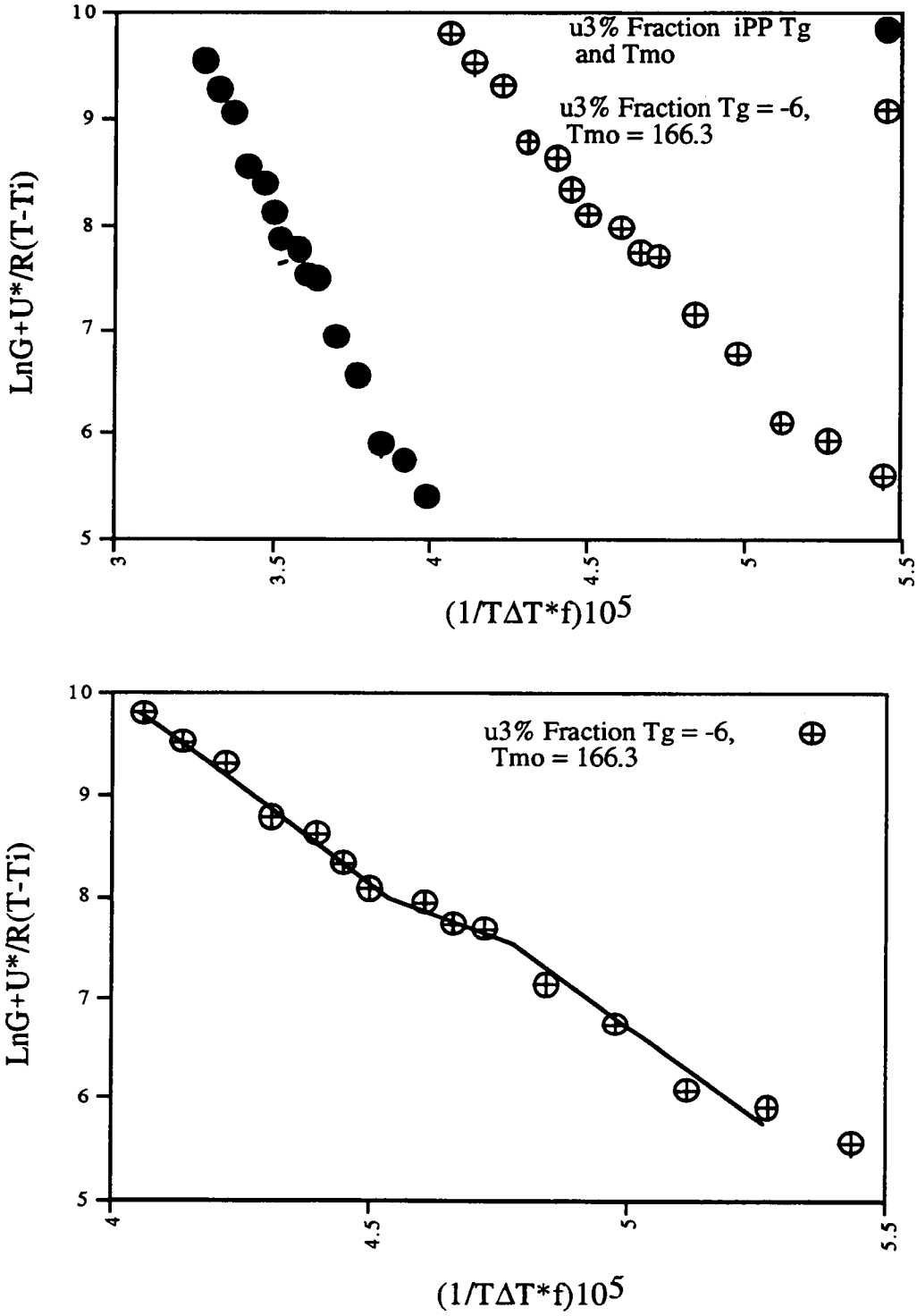


Fig. 5.10 Effect of T_g and T_{mo} on regimes of u3% copolymer fraction.

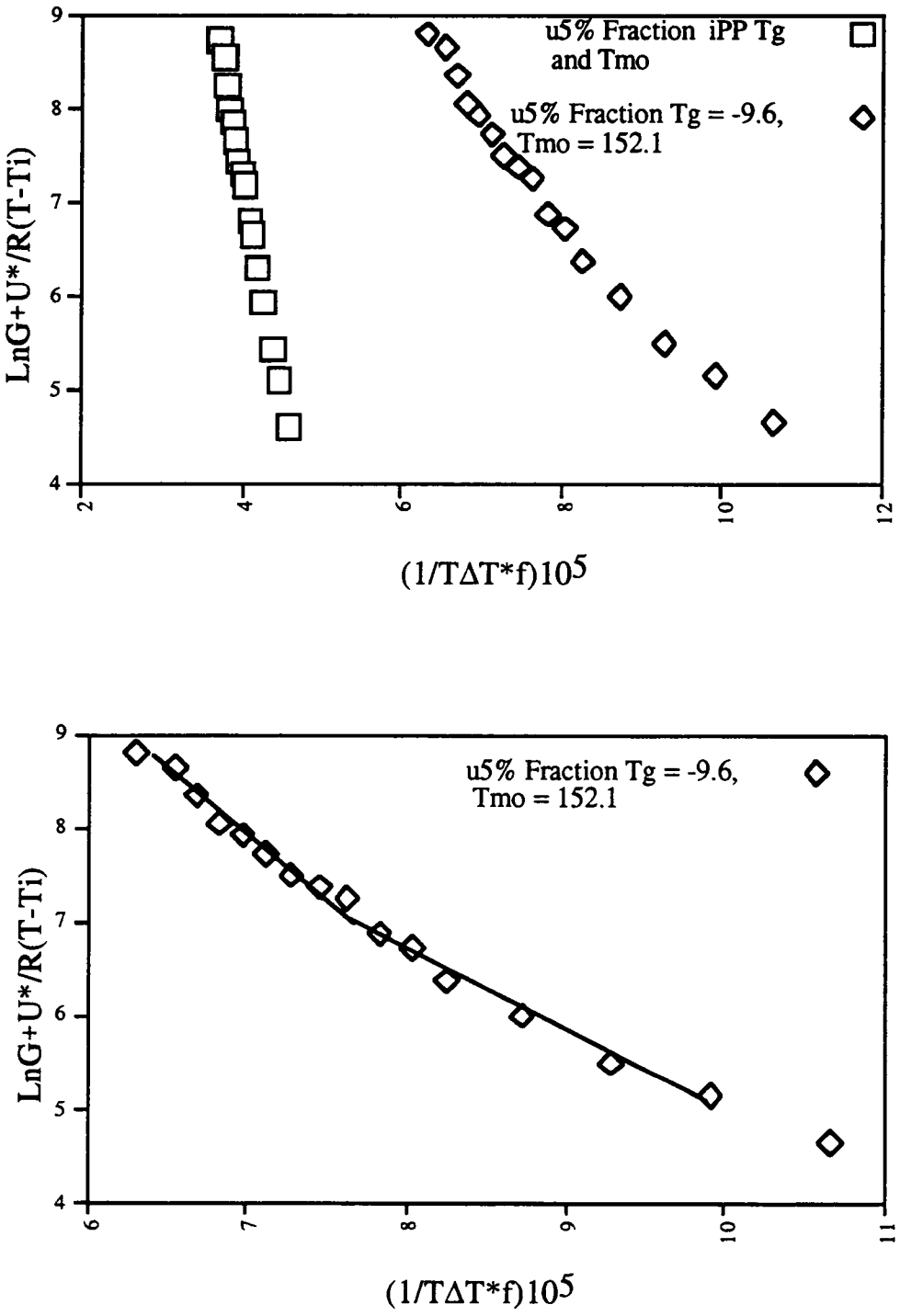


Fig. 5.11 Effect of T_g and T_{mo} on regimes of u5% copolymer fraction.

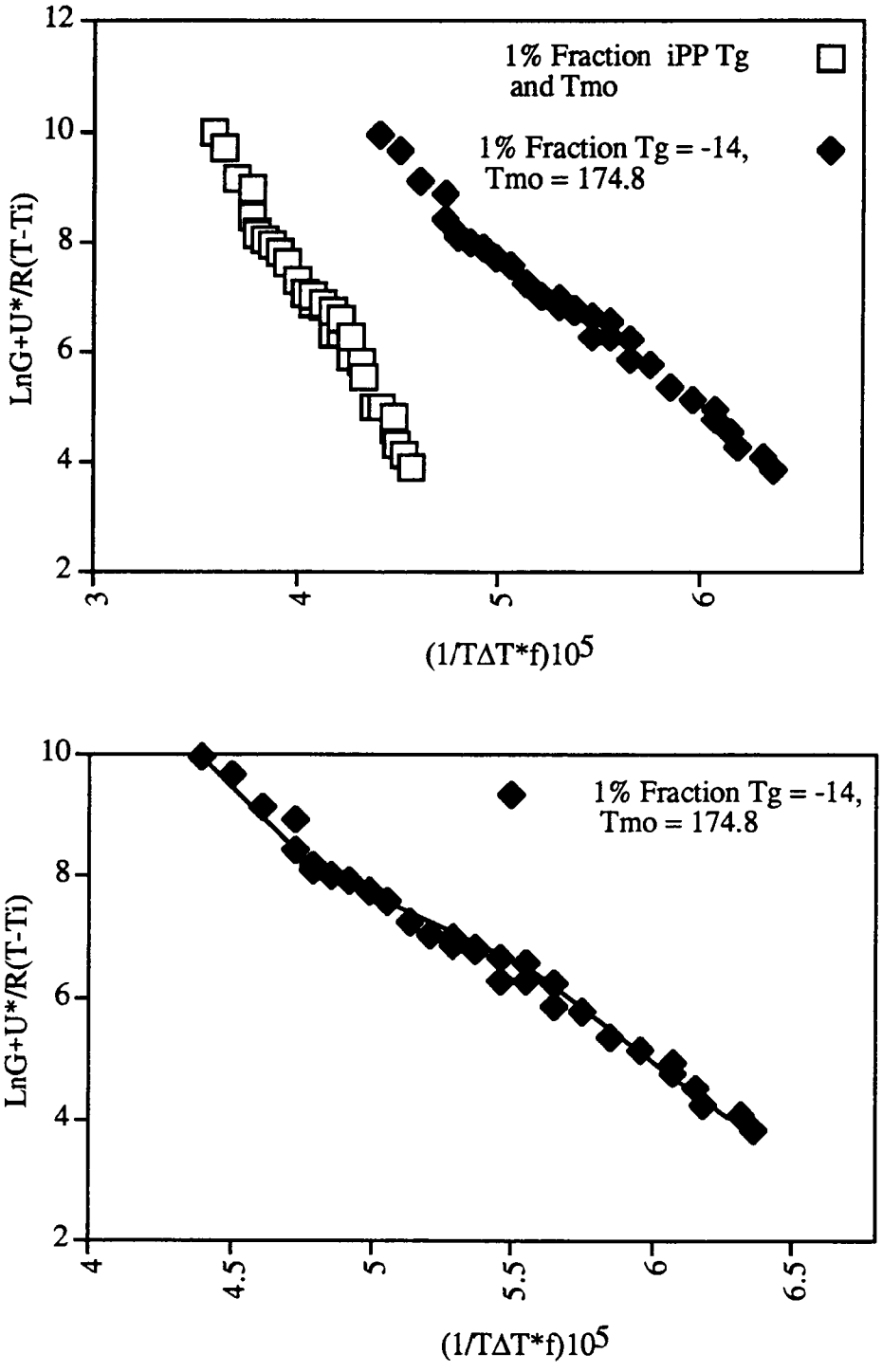
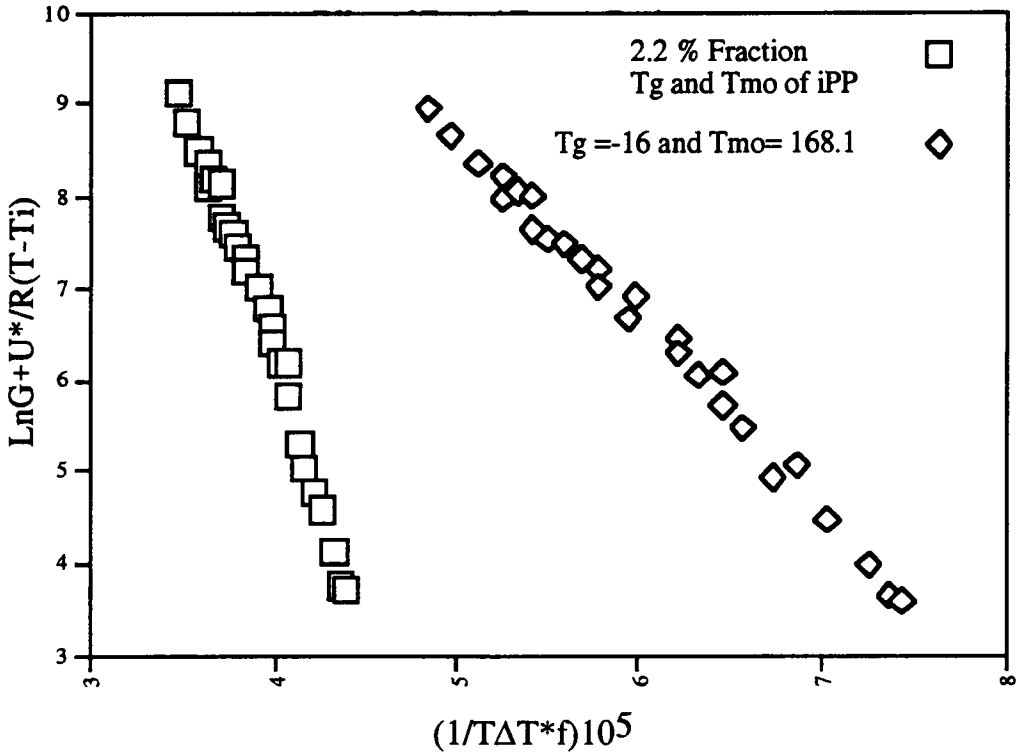


Fig. 5.12 Effect of T_g and T_{mo} on regimes of 1% copolymer fraction.



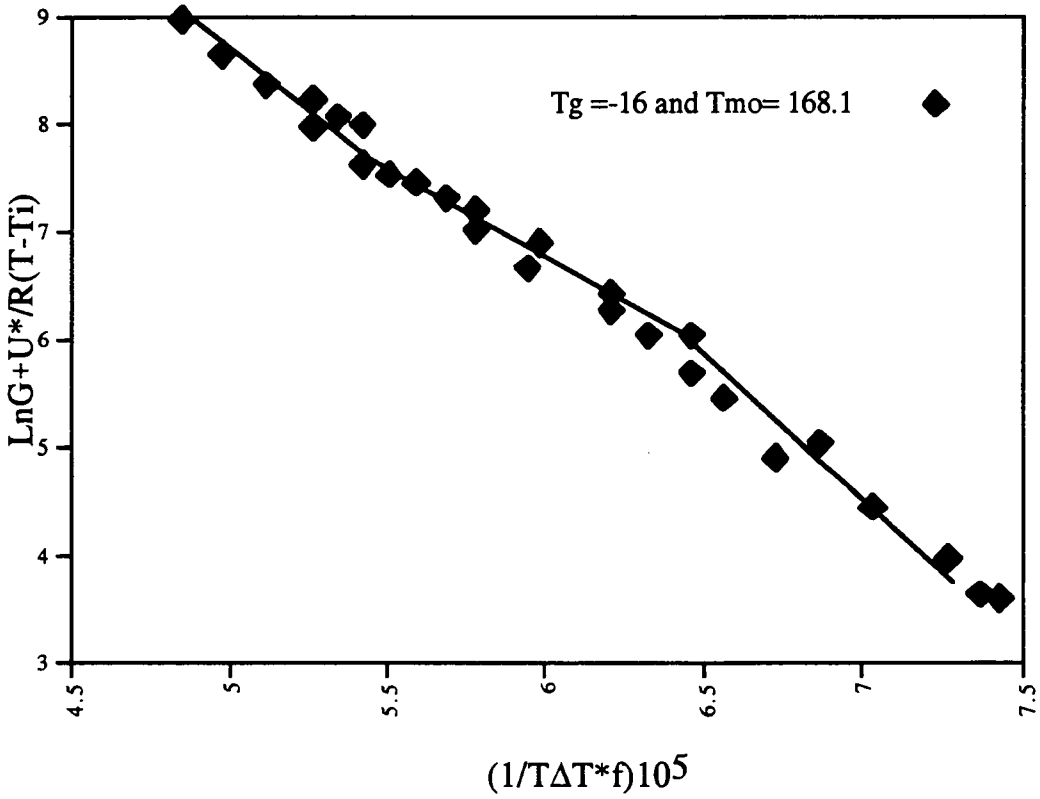


Fig. 5.13 Effect of T_g and T_{mo} on regimes of 2.2% copolymer fraction

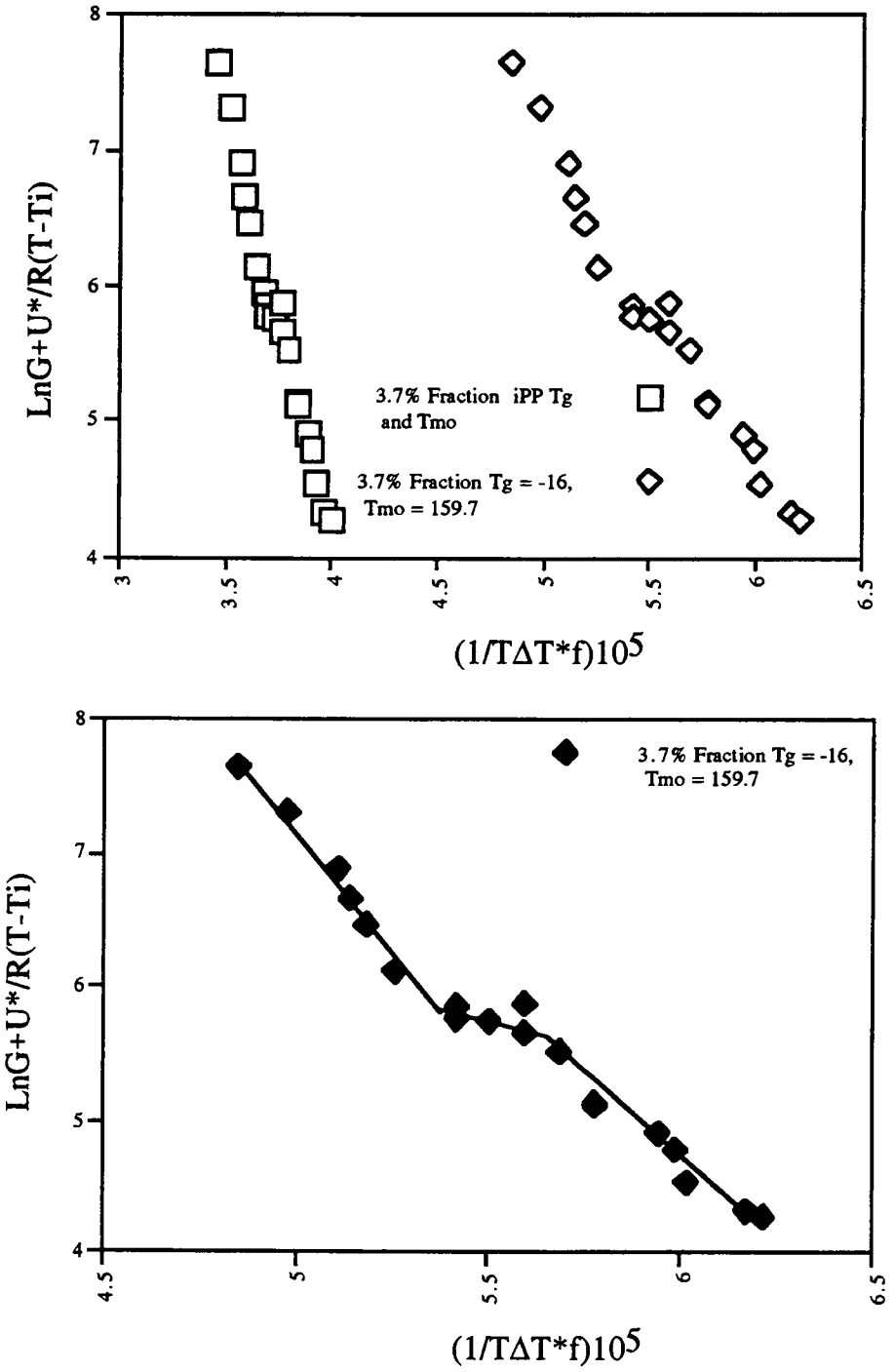


Fig. 5.14 Effect of T_g and T_{mo} on regimes of 3.7% copolymer fraction

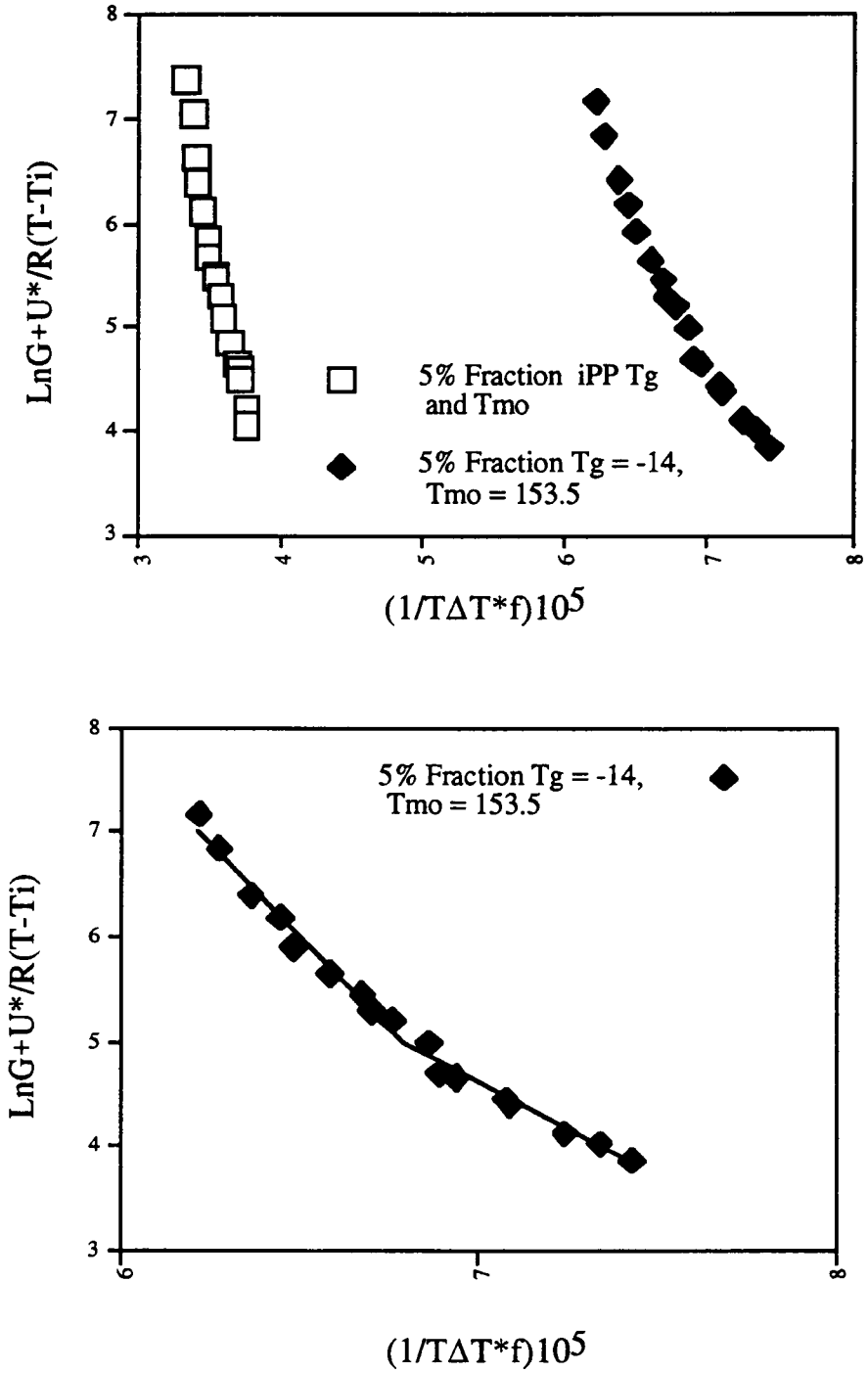
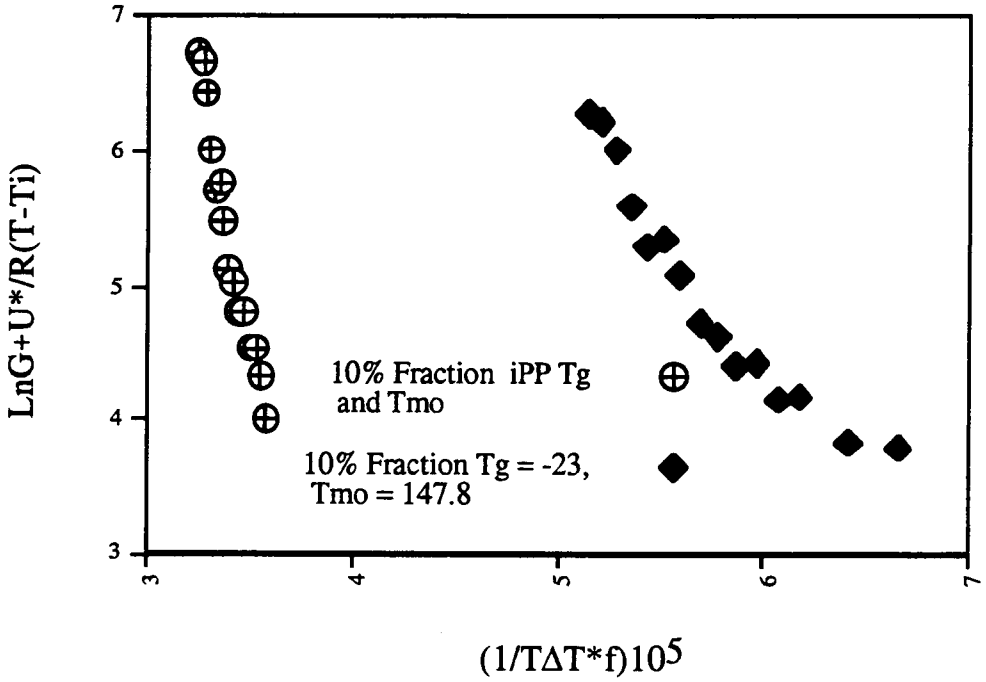


Fig. 5.15 Effect of T_g and T_{mo} on regimes of 5% copolymer fraction



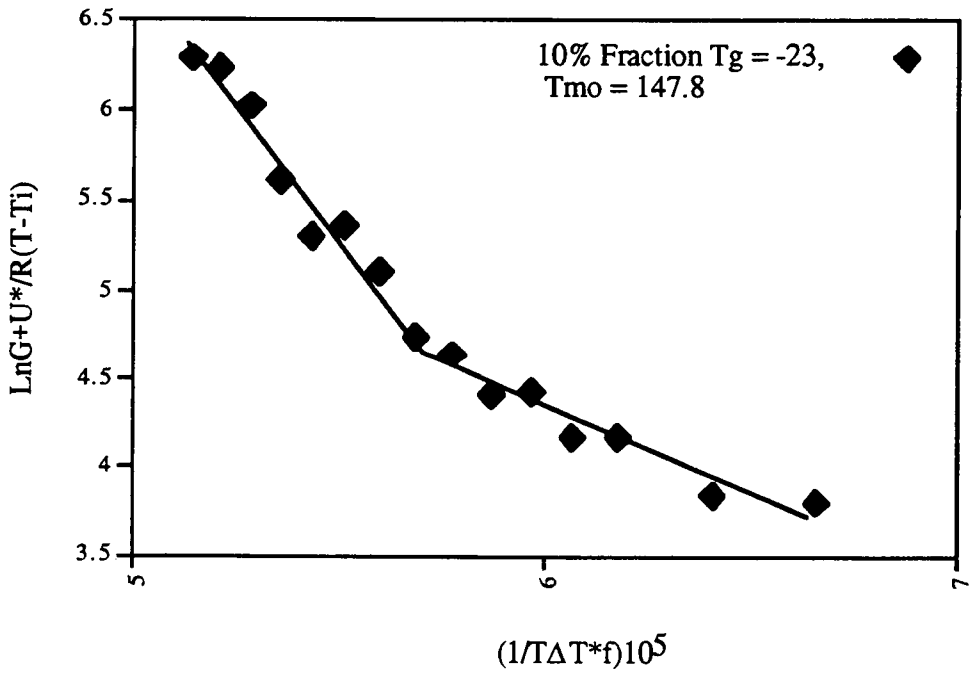


Fig. 5.16 Effect of T_g and T_{mo} on regimes of 10% copolymer fraction

The values of the $\sigma\sigma_e$ at different regimes for various copolymers are listed in Table 5.1. In order to determine the value σ, the Thomas-Stavely equation was used based on Hoffman modification;

$$\sigma = 0.1\ \Delta h_f \sqrt{a_o\ b_o}$$

The value of σ estimated from the above equation is applicable in all the regimes. The value of the lateral surface free energy was further used to determine the σ_e values for different copolymers in different regimes. This is illustrated in Table 5.1. that the Δh_f values calculated were not corrected for the heat of fusion of polypropylene (210 J/g), since melting behavior of the copolymers were far different than the melting of the homopolymers. The a_o(5.49Å) and b_o (6.26 Å) values of the [110] growth plane of polypropylene were used for the determination of $\sigma\sigma_e$.The work done in chain folding is then determined from the relation;

$$q = 2\sigma_e a_o b_o$$

From the calculated $\sigma\sigma_e$ values, it can be observed that the work needed for a chain to fold decreases with increase in the comonomer content. There seems to be a decrease in the fold surface free energy value with increase in comonomer content but not consistently, this might lead to incorporation of ethylene segments in the folds. The reduction of lateral surface free energy is due to the decrease in latent heat of fusion, and that of the fold surface free energy is dependent both on heat of fusion and the slopes of the regime transitions. Since the decrease in fold surface free energy favors exclusion of

Table 5.1 Crystal Growth kinetic data for copolymer fractions

Table 5.1									
Fraction	Heat of Fusion	Kg I	kgII	kgIII	σ	Tmo			
	J/g	10^5	10^5	10^5	$ergs^2/cm^4$	deg.C	er		
u3	159.31	4.03	2.14	4.15	9.34	166.30	77.73	82.55	80.05
u5	148.63		1.53	2.88	8.71	152.10		60.59	57.03
1.0	194.25	3.88	2.20	4.38	11.39	174.80	73.69	83.57	83.15
2.2	181.36	3.18	1.76	3.72	10.63	168.10	60.82	67.51	71.17
3.7	144.36	3.43	1.83	3.75	8.46	159.70	67.05	71.44	73.35
5.0	139.48		1.79	3.04	8.18	153.50		70.78	60.24
10.0	108.72		1.56	3.18	6.37	146.80		61.58	62.64

the comonomer from the crystal, the possibility of inclusion cannot be ruled out.

The effect of microstructural impurities on the regimes of crystallization has been recently reviewed by Phillips (1993). The effect of crosslinking and branching on polyethylenes, and a generalized regime behavior for the exclusion of comonomer from the crystal has been discussed.

The presence of three regimes in iPP has been reported by Janimak (1991) in low molecular weight fractions. The presence of the first regime in polymers has been observed either due to low molecular mass or broad molecular mass distribution (Janimak 1991). In the copolymers analyzed, the u3% showed three regimes while the u5% did show only two. These unfractionated samples were high molecular weight samples, and thus the effect of comonomer content on the crystallization regimes is critical.

6 CONCLUSIONS

Fractionation of copolymers helped in better understanding of the effect of stereoregularity and comonomer content on the crystallization behavior of random copolymers. The fractionation of the copolymers by solvent extraction was achieved based on tacticity and comonomer content. The comonomer distribution of the fractions were found to be random in nature, based on comonomer sequencing information obtained by FTIR. The results obtained from NMR for the high tacticity and low tacticity homopolymers used here for calibration shows that tacticity determination by xylene insoluble index is more useful than the tacticity obtained from heptane insoluble index.

The effect of stereoirregularities combined with that of comonomer contact had a synergistic effect in depressing the melting of the copolymer crystals. Glass transition temperature of the copolymers decreased with addition of comonomer content.

The gamma phase formation increased with incorporation of ethylene comonomer. In the 10% weight copolymer fraction more than 90 % gamma content was achieved at crystallization temperature of 100 °C. The amount of gamma phase present in the 10% sample crystallized at 10 °/min was close to 75%. The comonomer distribution has a distinct effect on the formation of the gamma phase, as there is a tendency to form higher gamma contents if the distribution is narrower.

Based on linear growth kinetics the tendency to move to a lower regime with comonomer incorporation might be due to reduction in secondary nucleation relative to the surface spreading. As the comonomer content increases, the crystallinity drops and the possibility of finding continuous propylene sequences of appropriate stem length reduces. There is a distinct change in morphology from the 1% ethylene containing fraction to the 10% ethylene containing copolymer. The development of spherulites at lower ethylene content corresponds to that of iPP, but as the comonomer content increases there are more distortions seen in the spherulites due to inclusion of chain irregularities. There is a tendency for crystals to grow axialites at the 3.7% - 5% weight ethylene content fractions, and as stacks in the 10 % copolymer. From the observations during the secondary growth analysis it is seen that the subtle change in morphology with supercooling does not correlate to the regime transitions. The growth rate significantly changed with comonomer distribution; this can be seen when the unfractionated and fractionated samples are compared. Based on equilibrium melting point comparisons with Flory's model and work done on homopolymers with different tacticities by Janimak it is evident that the effect of the total impurities is more critical than the separate effects of tacticity and comonomer contents.

Recommendation for Future work

Cross fractionation of copolymers might give more homogeneity based on molecular weight, tacticity and comonomer content. Detailed NMR studies to determine the comonomer sequencing, the impurity content / mole, and tacticity will be very useful in differentiating the effects of various defects on the crystallization behavior. Studies using SAXS to determine the lamellar thickness and equilibrium melting point are recommended for better understanding of the crystallization of these random copolymers. Computer simulations of ethylene incorporation in the propylene backbone will be interesting and can give more understanding on the sequencing of these random copolymers.

REFERENCES

REFERENCES

Addlink and Beinten Polymer, 2, 185, (1961)

Awaya Polym. lett. 4, 127, (1966)

Barham PJ., Chivers RA, Keller A and Organ SJ J. Matl, Sci. 19, 2781 (1984)

Bassett Principles of Polymer Morphology, Cambridge Univ. Press, London

Bennett C Huttiker M and Thomas H J. Stat. Phys. 24, 419, (1981)

Bevis Polymer Vol 35 No 12 (1994)

Bly RM, Kiener PE and Fries BAAnal. Chem. Vol 38 No. 2 (1966)

Brucner S and Meillle SV Prog. Polym. Sci., Vol 16, 361, (1991)

Bunn and Alcock Trans. Faraday Soc. 41, 317 (1945)

Bunn CW, Trans. Faraday Soc. 35, 482, 1939

Burdfield DR and Loi PST, J. Appl. Polym. Sci., Vol36,279 (1988)

Buterlov AM and Goryainov, J. Russ. Chem. Soc. 302, (1873)

Campbell R and Phillips PJ, Polymer, 32, 2902, (1992)

Cantow MJR, Polymer Fractionation, Academic Press (1967)

Cheng HN Makrom. Chem.188, 2665 (1987)

Cheng HN, Macromolecules, 17, 1950 (1984)

Clark EJ and Hoffman JD, Macromolecules 17, 878, (1984)

CorishPJ and Tunnicliffe ME J. Poly. Sci. Part C, No. 7, 187 (1964)

Cozewith C and VerStarate G Macromolecules, 4, 481 (1971)

Cozewith, C Macromolecules, 20, 1237, (1987)

De Rosa G, Gruerra, Petraccone Eu. Poly. Journal, Ed. 20, 937, (1984)

Di Marzio EA and Passaglia E, J. Chem. Phys. 87, 4908, (1987)

Di Marzio EA, J. Chem. Phys. 47, 3451, (1967)

Di Marzio EA. and Passaglia E, J. Chem. Phys. 87, 4901, (1987)

Disc. Faraday Soc. 68, (1979)

Doi Yand Soga K Macromolecules, 20, 616 (1987)

Doi Y Koyama and Soga K Polymer Vol 25, 1640 (1984)

Dosiere, Hand Book of Polymer Sci. and Technology, Vol2 P 367 (1989)

Encyclipedia of Polymer Science and Engineering, Mc GrawHill, (1988)

Fatou JG, and Mandelkern L. J. Phys. Chem. 69, 417, (1965)

Fatou JG, Eur. Poly., 7, 1057 (1971)

Fischer, Z. Naturf. 12a 173 (1957)

Flory P J, Trans. Faraday Soc., 51 848, (1955)

Galeski A. J Poly. Sci. Part C, 38, 23 (1972)

Galli P. Milani, F and Simonazzi, T Polymer Journal, Vol 17, No 1, 37, (1985)

Goldbeck-Wood Polymer Crystallization Theories, Advances in Polymer Science Vol 100, (1992)

Greco, R *et al.* Makrom. Chem. 188, 2231 (1987)

Gruerra, Petraccone J. Poly. Sci., Ed 22,1029, (1984)

Hayashi *et al.* Polymer 20, 107, (1988)

Hefland E. and Lauritzen JI. Macromolecules, 6, 631, (1973)

Higgins, ML. J. Poly. Sci., C.4, 445, (1963)

Hikosaka M, J. Makro. Sci. B 1991; Japan J. Appl. Phys. 21& 23 L 332 & 956, (1982/84)

Hikosaka M Polymer 31 458, (1990)

Hikosaka M. Polymer 28, 1257, (1987)

Hock CW, J. Polymer Sci. B-3, 573 (1965)

Hoffman JD and Weeks J J, J. Res. Natl. Bur. Stand, 66(A) 13, (1962)

Hoffman JD and Miller RL. Macromolecules 21, 3028 (1988)

Hoffman JD and Lauritzen JI, J. Res. NBS 65 A, 297 (1961)

Hoffman JD and Lauritzen JI, J. Res. NBS 79A, 671 (1975)

Huggins ML Polymer Fractionation, Academic Press, NY ,p.1 (1967)

Inoue Y, Asakura Tand Hayashi T Polymer Vol 29, 138 (1988)

Jackson KA J. of Crystal Growth 24 130 (1974)

Jacodine Nature, 176, 305 (1955)

Janimak J J. Ph.D. Dissertation, Univ. of Akron, (1991)

KakugoM , Naito Y and Mizunuma K Macromolecules, 21, 2309 (1988)

Kamide K and Yamaguchi K, Makromol. Chem, 162, 219 (1972)

Kawamura H, Inoue Y and Hayashi T Macromolecules, 22, 2121-9, (1989)

Ke B , J. Polym. Sci. 52, 15, (1960)

Keith and Padden J. Poly. Sci. 39, 101 & 123 (1959)

Keith and Padden, J. Poly. Sci. Polym. Phys. Ed 25 229, 2265, (1987)

Keith and Padden, Polymer 27, 1463 (1986)

Keith H. D, Padden FJ, Kissel WJ, and Wyckoff HW, J. Appl. Phys. 30, 1485, (1959)

Keller A and Norton DR, Polymer 26, 704 (1985)

Keller A and Sawada S. Makromol. Chem. 74,190 (1964)

Keller A J. Poly. Sci. A-2 10, 221 & 239 (1971)

Keller A J. Poly. Sci. 39, 151 (1959)

Keller A Phil. Mag. 2 1171 (1957)

Keller A Rep. Prog. Phys. 31 623 (1966)

Kojima M J. Polym. Sci., A-2(6), 1255, (1968)

Koningsveld Adv. Poly. Sci., 7,1 (1970)

Kossel W, Nachr. Ges. Wiss. Gottingen: 135 (1927)

Lauritzen JI Jr., Di Marzio E. A. and Passaglia E., J. Chem. Phys. 45, 4444, (1966)

Lautitzen JI Jr., J Appl. Phys. 44, 4353, (1973)

Lovinger A, J. *et al.* Polymer, 1595, (1985)

Lovinger AJ, Meille SV, Padden FJ, Bruckner S and Ferro, DR, Macromolecules, 27,2615, (1994)

Mandelkern L Macromolecules, 10 1224 (1977)

Mandelkern L, Acc. Chem. Res. 9,81 (1976)

Mandelkern L, Macromolecules 5, 147 (1972)

Mandelkern L, J. Phys. Chem. 75, 3909, (1971)

Mandelkern L, Polymer Bull. 17, 473,(1987)

Mansfield M L, Polymer, 29, 1755, (1988)

Mansfield M N, Macromolecules 16 914 (1983)

Martuscelli E, Simonazzi T, Rossi E, Segre A and Avella M Makrom. Chem. 187, 1927 (1986)

Martuscelli E and Simonazzi T Makrom. Chem.185, 1041 (1984)

Mehta A and Wunderlich B, J. Poly. Sci. Poly. Phys. Ed. 12, 225 (1974)

Meille S V and Bruckner, V. 340, 455 Nature (1989)

Meille S V and Bruckner, V16, 361 Prog. in Poly. Sci. (1991)

Mezghani K and Phillips PJ, Macromolecules, 27, 997 (1994)

Mezghani K. and Phillips, P. J, Polymer, 36, 2407 (1995)

Mezghani K., and Campbell R. A., Phillips P J, Macromolecules, 27, 997 (1994)

Mezghani K. Proposal PhD, (1995)

Milani Fand Abis L Makrom. Chem.187, 1877 (1986)

Miller R L and Seeley E. G., J. Polym. Sci., Poly. Phys. Ed., 20, 2297 (1982)

Morrow and Newman, J. Appl. Phys., 39, 4944 (1968)

Morrow D. R. and Newman B A, J. of Appl. Phys. 39, 4944 (1968)

Natta G, Atti. Acc. Naz. Lincei, Mermorie, 4, 61, (1955)

Natta G, Peraldo M and Corradini P, Rend. Accad. Naz. Lincei. 26, 14 (1959)

Natta G. and Corradinni, P, Nuovo Cimento. Suppl. 15, 40 (1960)

Palmer R P and A J Cobbold, Makromol. Chem. 74,174 (1964)

Papaptrou A, Z Kryst. 92, 89 (1936)

Paukkeri R and Lihtinen A , Makromol. Chem. Phys. 195, 1539 (1994)

Pek Choo Ng *et al.* Polymer Comm,, Vol 25, 250 (1984),

Phillips PJ., Handbook of crystal growth (1992)

Phillips PJ Rep. Prog. Phys. 53 549 (1990)

Point JJ and Dosiere M, Polymer 23, 256, (1989)

Price J. Poly. Sci. 39, 139 (1959)

Randall A and Hsieh T, Macromolecules, 15, 1584 (1982)

Randall A, Macromolecules, 11,592 (1978)

Randall JC J. Poly. Sci, Polym. Phys. Vol 14, 2083 (1976)

Ray GJ, Jhonson and Knox PR Macromolecules, 10, 773 (1977)

Sadler DM Polymer 24, 1401 (1983)

Sadler DM, J. Chem. Phys. 87,1771 (1987)

Sadler DM, J. Poly. Sci. Poly. Phys. Ed. 23, 205 (1982)

Sadler DM, Polymer, 28, 1440(1987)

Sadler DM Structure of Crystalline Polymers, Elsivier, Barking, 125 (1984)

Sanchez IC and Di Marzio EA., J. Chem. Phys. 55, 893 (1971)

Sanchez IC and Di Marzio EA., J. Res. Nat. Bur. Std., 76A, 213 (1972)

Sanchez IC and Eby R. K., Macromolecules, 8, 639 (1975)

Sanchez IC and Eby RK., J. Res. Natl. Bur. Stand. 77(A) 353, 1973

Ser van der Ven, Polypropylene and other Olefins, pg. 220, Elsevier, 1990

Seymour RB and Cheng Tai, Advances in Polyolefins, Plenum Press Ney York, 1988.

Skaare LE, Klaeboe P and Nielsen C Vibrational Spectroscopy, 3, 23 (1992)

Slichter and Mandell J. Appl. Phys., 29,1438, (1958)

Smith WV J. Poly Sci. Polym. Phys. Ed. 18, 1573, (1980)

Spells SJ and Sadler D M Polymer 25, 739, (1984)

Stranski I, N Z Phys Chem. 136, 259 (1928)

Suzzane WM, Masters Thesis, Univ. of Tenn. (1995)

Till, J. Polymer Sc. 24 30 (1957)

Tonneli AE and Schilling FC. Acc.Chem. Res. 14, 233 (1981)

Tonneli AE, Macromolecules, 11, 565 (1977)

Topchiev Dokl. Acad. NaukSSSR, 147,1389, (1962)

Tung LH Fractionation of Synthetic Polymers Marcel Dekker, Inc , (1977)

Turner-Jones A, Aizlewood JM and Beckett DR Makromol. Chem. 75, 134, (1964)

van SchootenJ and Duck EW Polymer 2, 357 (1961)

van SchootenJ and Mostert S Polymer 4, 135, (1963)

Vasanthakumari R. and Pennings A. J. Polymer 24, 175, (1983)

Wei E Peter, Anal. Chem. Vol 33 No. 2 (1961),

Wilkes C J *et al.* J. Poly. Sci. C 43, 237, (1973)

Wuderlich B Moakromol. Chem. 9, 76, (1988)

Wunderlich B Macromolecular Physics, Vol1, Academic Press, (1976)

Zambelli A, Bovey. Macromolecules, 8, 687 (1975)

Zanneti R, Busi P and Guidetti GP Eu. Poly. J, Vol 19, No 9, 757. (1983)

Zhu S-N Polymer J., 16, 859 (1984)

Vita

Rajesh Ramamurthy was born in Kottayam, India on July 7, 1971. After finishing his high school at Vana Vani he joined S.J.College of Engineering to do his Bachelor of Science in Polymer Science and Technology (1988-1992). He then entered University of Tennessee to earn his Masters in Polymer Engineering. (1993-1995). Soon after his completion he has started working with MRC Polymers, Inc. Chicago as a Product Development Engineer for recycled plastics.